PPPL--2401

DE87 004047

THEORY OF CURRENT-DRIVE IN PLASMAS

Nathaniel J. Fisch
Princeton University, Plasma Physics Laboratory
P.O. Box 451, Princeton, NJ 08544

Abstract

The continuous operation of a tokamak fusion reactor requires, among other things, a means of providing continuous toroidal current. Such operation is preferred to the conventional pulsed operation, where the plasma current is induced by a time-varying magnetic field. A variety of methods has been proposed to provide continuous current, including methods which utilize particle beams or radio frequency waves in any of several frequency regimes. Currents as large as half a mega-amp have now been produced in the laboratory by such means, and experimentation in these techniques has now involved major tokamak facilities worldwide.

CONTENTS

I. Preliminaries

A. Introduction

The theory of current-drive relies upon a number of other concepts: the tokamak, plasma waves, wave-particle interactions, and other elementary notions. In this first chapter, we briefly review these notions, outline the scope of our problem, and try to give a feel for the parameter regime which we are concerned about in this paper. Here, we try to acquaint the non-tokamak specialist with the motivation behind driving current. Subsequent chapters are written with a less casual reader in mind.

B. The Tokamak

Current-drive refers to the production of toroidal electric current in a plasma torus - that is, current that encircles the torus hole. We review here a number of methods that have been invented to drive such a current. The intended use of this current is the enabling of a tokamak fusion reactor to operate continuously. This is an exciting prospect. Current generation is a fundamental process, and may enjoy broader applications than just to tokamaks, but the focus here will be on tokamaks, where these techniques can be assessed with one particular goal in mind.

The tokamak, a toroidal magnetic trap, has emerged today as the leading approach to controlling nuclear fusion for the purpose of electrical power generation. The central problem of controlled nuclear fusion is the confinement of the charged constituents of the fusile fuel. These particles are so hot that they form a completely ionized plasma. Since a large magnetic field inhibits charged particle motion perpendicular to it, the confinement problem may be reduced from three dimensions to one dimension by immersing the plasma in a strong magnetic field; unbounded charged particle motion is then permitted only along the field lines, except for a much slower diffusion of particles across field lines when particles collide. Confinement in the third dimension is achieved by bending the field lines into a circle, hence, the toroidal geometry.

Unfortunately, however, bending the magnetic field introduces other forces on the plasma which tend to destroy the confinement. The effect of these forces can be neutralized by twisting the magnetic lines of force while they are being bent into the toroidal shape. The resultant, twisted field is

the sum of two fields, a toroidal field encircling the torus hole and a poloidal field encircling the center of the minor cross section of the torus (see Fig. 1.1). In a tokamak, the toroidal field component is large compared to the poloidal field component.

How does a twist in the field lines stabilize particle motion? The stabilization here is somewhat analogous to the stabilization against gravity of coal particles in a coal slurry in a long pipe by superposing on the longitudinal flow a swirling (poloidal) motion around the pipe axis. The coal particles are always falling relative to the liquid, but because of their entrainment in the swirling motion, they spend the same amount of time falling towards the pipe axis as away from it. The particles are then entrained in nested, somewhat off-center, surfaces. In a tokamak, the magnetic field plays the role of the liquid flow lines, and charged particles do not stray far from what are called magnetic surfaces.

The toroidal magnetic field is easily produced by poloidal electric currents flowing in coils outside the plasma that encircle the mirror cross section and thread the torus hole. The poloidal magnetic field is more difficult to produce -- it may be produced by a toroidal current, but this current must flow inside the plasma. The natural way to produce this current is by inducing a constant toroidal electric field in the plasma. This may be done by treating the plasma as a secondary in a transformer circuit. Placed outside the plasma is a primary coil whose axis threads the hole of the plasma torus. This is the basic tokamak design. In fact, the word tokamak, coined by Golovin, is a Russian acronym for "toroidalnaya kamara i magnitnaya katushka," meaning "toroidal chamber and magnetic coil," after its salient features. Note, however, a fundamental limitation: a toroidal electric field has curl, so by Maxwell's equation ($\nabla \times \vec{E} = -\partial\vec{B}/\partial t$), a constant toroidal electric field can be sustained only by a monotonically changing magnetic field, hence only temporarily, limited by the magnetic flux available from the primary circuit. In a tokamak reactor, the required electric field is small, so each pulse might last as long as an hour.

There is a considerable technological advantage in building a tokamak that could operate in a continuous rather than in a pulsed mode. For steady-state operation, a method of continuously driving the toroidal current is essential. This paper reports on methods of providing such a current.

C. Current-Drive Apparatus - Brief Overview

To provide a toroidal current continuously, some toroidal asymmetry must be introduced into the tokamak. We shall consider several means of tampering with a toroidal plasma to distinguish one toroidal direction over the other.

For example, traveling waves may be induced in the tokamak. These waves may be injected via a phased array of waveguides or coil arrays at the periphery of the tokamak or, at higher frequencies, a horn waveguide may be pointed at the tokamak tilted with respect to one toroidal direction. In such a manner, an asymmetry is produced; we shall examine shortly the physical basis for the current generation. One may imagine, for now, that the traveling wave could carry toroidal momentum which might be transmitted to either the plasma electrons or ions, but not both. Figure 1.2 gives a feel for apparatus that might be used to provide asymmetry by injecting waves in various frequency regions.

Alternatively, one might direct neutral beams into the tokamak. These beams penetrate the magnetic fields as neutrals, but are quickly ionized when in contact with the hot plasma. The ionized beams are then confined by the magnetic fields. Directing the beams with a component in one toroidal direction may provide the required asymmetry. Figure 1.3 depicts a neutral beam injector designed for the TFTR tokamak at Princeton.

Other roads to asymmetry are available as well. The tokamak walls might be asymmetric reflectors of radiation or particles. Frozen pellets of hydrogen might be injected, in some way, asymmetrically.

Thus, particle beams, traveling waves, and reflectors all exemplify tools for current generation. Not every asymmetry leads to useful current production. The goal of this review is to identify the most promising possibilities.

D. Early Principles

That waves could be employed in generating toroidal electric current in a plasma torus was recognized as early as 1952, when Thonemann et al. produced a current in a small cold plasma confined in a toroidal glass tube. A traveling wave was induced around the device so that electrons were pushed relative to ions. The wave itself was evanescent in the device, but that mattered little because the device was so small.

The challenge to apply this technique to larger devices did not come till much later. The tokamak approach had been formulated in 1950 by Tamm and Sakharov, but it was not until a series of successful tokamak experiments, headed by Artsimovich of the Kurchatov Institute, was conducted in the 1960's that the concept gained serious acceptance. In 1968, a very hot plasma with a long confinement time was reported on the Russian T-3 tokamak.

It was recognized then that the basic tokamak design might be improved considerably if the toroidal current could be produced continuously. The leading suggestions at the time were to do so by means of neutral beams (Ohkawa, 1970) or by means of Alfvén waves (Wort, 1971), the latter method being somewhat reminiscent of Thonemann's experiment. These methods were both motivated by the two principles that guided early current-drive research:

1. An external source that deposits toroidal momentum into electrons is necessary for current generation.
2. It is most efficient to push slow electrons.

It is worthwhile to explore these early principles, although, as it turned out, neither is exactly correct.

The first principle is exemplified by each of these early suggestions, neutral beams and Alfvén waves. Neutral beams (discussed in more detail later) enter the plasma, ionize, and then collide primarily with the electrons, resulting in a drift of electrons relative to ions. Alfvén waves similarly push the electrons: the Alfvén wave is somewhat like a moving magnetic mirror and, as envisioned by Wort, pushes electrons in a peristaltic fashion. Exemplifying the second principle, in both cases, is the fact that thermal electrons (as opposed to superthermal, $v > v_T$, electrons, where v_T is the electron thermal velocity) are pushed. In the case of neutral beams, this occurs because, while all electrons contribute to slowing down the beams, most electrons are thermal. In the case of Alfvén waves, this occurs because the wave phase velocity is picked so that only slow electrons are pushed by the wave.

Let us digress for a moment to review the basics of the wave-particle interaction. Momentum and energy can be exchanged between waves and particles obeying a resonance condition: either the so-called Landau resonance $\omega-\vec{k}\cdot\vec{v}$

$= 0$, or, in the case of a strong magnetic field, the cyclotron resonance, $\omega - k_\parallel v_\parallel - n\Omega = 0$, where ω and $\vec{k}$ are the wave frequency and wave number, Ω is the particle cyclotron frequency, $\vec{v}$ is the particle velocity and n is an integer. Vector quantities may be decomposed into projections parallel and perpendicular to the magnetic field - thus, $v_\parallel$ and $v_\perp$ are the particle speeds, respectively, parallel and perpendicular to the strong dc magnetic field $\vec{B}$. (The problem, of course, is to generate current in the parallel, which is roughly the toroidal, direction.) The sense of the wave-particle interaction is dictated by the sense of a diffusion process: particles near equilibrium generally occupy lower energy states rather than high energy states; hence, it is the wave which transfers its energy (a positive quantity) and momentum to the resonant particles. In the case of Alfvén waves, the Landau resonance condition $\omega - k_\parallel v_\parallel = 0$ pertains, and the wave frequency and wave number are picked so that $v_\parallel$ is subthermal, i.e., $v_\parallel < v_T$, while the perpendicular velocity of resonant electrons is, on average, $v_\perp \approx v_T$.

The first early principle is merely an intuition; the second principle rests on the notion that it is easier to push a slow electron than a fast electron (slow and fast refer here to motion in the direction parallel to the push). Suppose an electron with mass m and charge q ($q \equiv -e$), in interacting with a wave or other source of momentum, is accelerated from velocity $\vec{v} = v_\parallel \hat{i}_\parallel + \vec{v}_\perp$ to velocity $\vec{v} + \Delta v_\parallel \hat{i}_\parallel$, where $\hat{i}_\parallel$ is the unit vector in the parallel direction. The parallel momentum absorbed by this electron is $m\Delta v_\parallel$; the incremental current carried by this electron is $\Delta j = q\Delta v_\parallel$; and the incremental increase in the electron kinetic energy is $\Delta\varepsilon = mv_\parallel \Delta v_\parallel$. The fact that the ratio of absorbed energy to incremental current, $\Delta\varepsilon/\Delta j$, is proportional to the velocity projection $v_\parallel$ indicates that it is energetically favorable to accelerate a slower, rather than faster, electron. Thus, Ohkawa's neutral beams push thermal electrons and Wort's Alfvén waves are designed to push low-$v_\parallel$ electrons.

E. Fast Electrons

Although it may be easier to push slow electrons, it may actually be more effective to push fast electrons. In practice, this would be done by injecting waves with faster parallel phase velocities to deposit momentum in faster resonant electrons.

The Coulomb collision cross section becomes smaller with increasing relative speed between the colliding particles. Thus, fast, superthermal electrons collide less often than slower thermal electrons, since the average relative speed between superthermal electrons and most other electrons and ions is far greater than the relative speed between thermal electrons and most other electrons and ions. In fact, the ratio of these speeds is roughly v/v_T, where v is the superthermal electron velocity.

Although it may be energetically expensive to accelerate fast electrons in the first place, this energy deposition need occur less often. Current lasts longer when carried by relatively less collisional electrons, so the power requirements to sustain a given current against collisions can be small. To derive this, assume that the velocity $\vec{v}$ of an electron is randomized by collisions in a momentum destruction time $1/\nu(v)$. An incremental energy input $\Delta\varepsilon$ then produces an incremental current Δj that persists for time $1/\nu$. From the preceding section, we have the relationship

$$\Delta j = \Delta\varepsilon \frac{q}{mv_\parallel} \quad . \tag{1.1}$$

The power requirement to refresh this current at time intervals $1/\nu$ is

$$P_d = \nu\Delta\varepsilon \quad . \tag{1.2}$$

Combining Eqs. (1.1) and (1.2) and adapting the notation $J=\Delta j$ (the only current is the driven current), we have the steady-state efficiency

$$\frac{J}{P_d} = \frac{q}{mv_\parallel \nu(v)} \quad . \tag{1.3}$$

Evidently, the efficiency (or current per power dissipated) is maximized when the expression $v_\parallel \nu(v)$ is minimized. There are two important limits; for $v_\parallel \to 0$, but $v_\perp \approx v_T$, we have $\nu \sim$ constant; for $v_\parallel >> v_T$, however, we have $\nu \sim 1/v_\parallel^3$. The first limit, which characterizes the case of Alfvén waves, results in a high efficiency since $J/P_d \sim 1/v_\parallel$ and $v_\parallel$ is small. The second limit, which characterizes the case of waves with high parallel phase velocity, also results in a high efficiency since $J/P_d \sim v_\parallel^2$, with $v_\parallel$ large. The second case, identified by Fisch (1978), argues for the utilization of the so-called lower-hybrid wave which can easily be excited in a plasma with high parallel phase

velocity. These two regimes in which high efficiency might be attained are depicted in Fig. 1.4.

Although, in principle, high current-drive efficiency can be realized in either of these limits, the low-phase-velocity approach suffers from a serious drawback. In tokamaks, it is just the low-$v_\parallel$ average-$v_\perp$ electrons that are trapped in magnetic wells and prevented from flowing freely along the field lines. As pointed out by Bickerton (1972), these electrons cannot then carry current as required for Alfvén wave current-drive. This objection is both fundamental and serious and may be responsible for the absence of serious experimental effort in this otherwise hopeful regime for current-drive (but see Sec. III.B).

The problem of trapped electrons does not, luckily, touch on the opposite high efficiency limit, i.e., that of lower-hybrid waves. Electrons with high $v_\parallel$ and average $v_\perp$ would be just those electrons that are not trapped. The most intense effort in current-drive has, in fact, been directed at this limit, and lower-hybrid current-drive experiments have now been performed at major tokamak facilities worldwide.

To illustrate the effect on the electron distribution function f caused by the injection of high-phase-velocity waves, we reproduce in Fig. 1.5 the results of a numerical calculation (Karney and Fisch, 1979). The details of this calculation are reserved for Sec. 2.8; note, however, that the joint action of both interparticle collisions and unidirectional waves results in an asymmetric distribution function, indicating the presence of current. Note also that electrons slower than the phase velocity of the injected waves tend to be Maxwellian; in the resonant region, however, there exists a plateau of electrons with high perpendicular temperature.

The asymmetry, it turns out, is large enough to signify very large currents, in the vicinity of what would be needed for a tokamak reactor. Progress in the laboratory since 1978 has proceeded at a quick pace as shown in Fig. 1.6. Currents in excess of 500 kA have now been generated by this method.

F. The Cyclotron Resonance

In the previous section, it was shown that pushing fast electrons may be efficient, something contrary to early thinking on current-drive. Here, following Fisch and Boozer (1980), we show, in contrast to the other principle of early current-drive theory, that an outside source of parallel momentum is not a necessity for efficient current generation. The falsification of the principle means that waves such as electron-cyclotron waves may be useful for driving current.

To see that momentum input is not necessary, consider pushing in the perpendicular direction (say from velocity space position 1 to position 2 as depicted in Fig. 1.7a) an electron that is moving to the right in the parallel direction. The probability that current is retained by an electron decays with time, though this decay is quicker for slower, more collisional electrons. Thus, the current carried by the electron at later times, depicted in Fig. 1.7b, is a function of its initial velocity space coordinates. Although the initial dislocation of the electron does not impart to it parallel momentum, or equivalently there is no instantaneous production of current, there is net production of current that appears, with delay, subsequent to the push; essentially, this current is the difference between the two curves of Fig. 1.7b. One may imagine that, at first, the electron velocity distribution is symmetric, with equal numbers of electrons going to the left and to the right. If, as a result of our pushing in the perpendicular direction electrons going to the right, the right-going current persists longer, then an imbalance will appear at some later time in the form of a current. The repeated pushing of electrons in this manner results then in a steady current.

Note that current has been produced in the absence of momentum input. Lest this appear to violate the conservation of momentum, observe that if electrons moving to the right are heated perpendicularly and hence are less collisional, they will drag less on the ion population than do the unheated electrons moving to the left. Ions, therefore, on balance are dragged to the left, conserving the total momentum of both species.

The electron-cyclotron wave interacts with electrons in just the way envisioned here, by pushing resonant electrons largely in the perpendicular direction. Electrons with $v_\parallel = (\omega-\Omega_e)/k_\parallel$ are resonant with the wave, and by

pointing a horn antenna tangentially into the plasma (so that the $k_\parallel$ spectrum is not symmetric), electrons moving in one toroidal direction are selected over counter-streaming electrons.

The cyclotron resonance would have been of little use for current-drive were momentum input required. This is because these waves are nearly free-space waves with superluminous parallel phase velocities ($\omega/k_\parallel > c$). Since wave energy is proportional to $\hbar\omega$, while wave momentum is proportional to $\hbar\vec{k}$, these waves have relatively negligible parallel momentum. Consequently, when they do interact with electrons, they impart their energy in such a way as to push the electrons largely in the perpendicular direction. There is a hierachy of sorts in the waves so far discussed: Alfvén waves have a high content of parallel momentum, lower-hybrid waves have a low content, and electron-cyclotron waves are almost absent in parallel momentum.

G. Application to Reactors

The preceding sections introduced already a number of steady-state current-drive techniques. Here we remark upon the utility of these schemes for the application of interest, the steady-state tokamak reactor.

At present, the parameters of what will eventually be a successful tokamak reactor are purely speculative. In the 1970's, the UWMAK reactor studies (e.g., Badger et al., 1973) offered a reactor with a major radius, R, of 13 meters and a minor radius, a, of 5 meters. This is now considered to be too large to be attractive to commercial utility interests. Designs now tend to be smaller, say R = 8 and a = 3. Something like 10 MA will be the required toroidal current.

Two rough formulas illustrate the quantities and parameters with which we are concerned. One quantity is the ratio of current I generated to power dissipated P, which may be written, in the case of lower-hybrid waves as

$$\frac{I}{P} \approx \frac{(v_{ph}/v_T)^2}{30} \left(\frac{T_{10}}{R_1 n_{14}}\right) \frac{\text{Amps}}{\text{Watt}} \quad , \tag{1.4}$$

where T_{10} is the temperature normalized to 10 keV, n_{14} is the density normalized to 10^{14}cm^{-3}, and R_1 is the major radius in meters. Note that the right-hand side of Eq. (1.4) is strictly independent of temperature; the thermal velocity was introduced to accentuate the importance of the parameter

v_{ph}/v_T, which governs wave damping. Typically, one might expect $(v_{ph}/v_T)^2 \simeq 20$. For $T_{10} = 0.1$, $R_1 = 1$, and $n_{14} = 0.1$, typical of present-day experiments, it would take about 3 watts absorbed by the proper electrons to drive 2 amps of current. Typical needs might be several hundred kA and up to several MW of rf power might be available. The power P, referred to in Eq. (1.4), indicates wave power that is absorbed by targeted resonant electrons. Not included in the measure of efficiency, I/P, is the efficiency of producing and delivering this power to the targeted electrons. Our concern in this review will focus on the ratio I/P, with the understanding that further sources of inefficiency need be considered too.

A quantity of interest for reactor applications is the ratio of rf power needed to sustain the current required for confinement to the fusion power P_f generated by the reactor. The ratio P_{rf}/P_f gives a rough estimate of the circulating power requirements, once the inefficiencies of producing the rf power and delivering it to the targeted electrons are taken into account. A rough estimate of P_{rf}/P_f in terms of macroscopic plasma parameters may be written as

$$\frac{P_{rf}}{P_f} \simeq \frac{15}{J/P_d} \frac{1}{(n_{14}T_{10}a_1R_1)^{1/2}(3\ T_{10}-2)} , \qquad (1.5)$$

where a_1 is the minor radius in meters and J/P_d is a dimensionless efficiency parameter; for lower-hybrid waves with $(v_{ph}/v_T)^2 \simeq 20$, we have $J/P_d \simeq 30$. Equation (1.5) is a reasonable approximation in the regime $1 < T_{10} < 3$, which is the contemplated regime for D-T tokamak fusion reactors.

Two designs are considered in Table 1. For the small and cold design, $P_{rf}/P_f \simeq 0.1$; considering then other inefficiencies, which might waste as much as twice the absorbed power, a circulating power of about 30% of the fusion output is required to drive the current. It would be debatable as to whether the large circulating power requirement is worth the trouble. On the other hand, for the large and hot design, $P_{rf}/P_f \lesssim 0.02$, which implies that were such a reactor desirable, the current-drive power requirements to make it steady state would be easily met.

The desire for tokamak reactors that are both small and continuously operating forces us to take factors of two in power requirements very seriously. At present, contemplated current-drive mechanisms are neither so

power intensive that they could be dismissed out of hand, nor are they such meager consumers of power that the exact power requirement is not of interest. As a result, it has been necessary to evaluate carefully the power requirements of schemes for generating current. In part, because different schemes work better in different tokamak parameter regimes and because the ultimate reactor regime is still a matter of great debate, it is still worthwhile to consider, at present, a large number of possibilities.

Design 1 (small and cold)	Design 2 (large and hot)
$T_{10} = 1$	$T_{10} = 2$
$n_{14} = 1$	$n_{14} = 1/3$
$a_1 = 3$	$a_1 = 5$
$R_1 = 8$	$R_1 = 13$
$P_f = 1.8$ GW	$P_f \approx 3.3$ GW
$H_p \approx 1.5$ MW/m^2	$H_p \approx 1$ MW/m^2
$\frac{P_{rf}}{P_f} \approx \left(\frac{15}{J/P_d}\right)$ 20%	$\frac{P_{rf}}{P_f} \approx \left(\frac{15}{J/P_d}\right)$ 3%

Table 1. Paradigmatic Reactor Designs

(H is the wall loading and P_{rf} is the rf power that is absorbed by targeted electrons.)

H. Advantages of Steady-State Operation

Steady-state operation is desirable for a number of very different reasons. It is very difficult, at present, in the absence of working reactors, to assess exactly how important these advantages are. Here we very briefly enumerate some of the chief attractive features of steady-state operation.

Structural components of the pulsed tokamak will be subjected to large temperature variations, resulting in heat stresses that may significantly

shorten their lifetime. The continuously operating tokamak presents a constant temperature environment, which should increase component lifetime and allow a wider choice of materials. Additionally, the pulsed tokamak presents fluctuating magnetic forces to the large magnets, incurring mechanical fatigue. As a result of these forces, which occur both in and out of the coil plane, extensive and expensive structural reinforcement may be necessary.

Tokamaks are subject to disruptions, unpredictable sudden losses of confinement. Presumably, some parameter regimes are less prone to disruption than others, and with steady-state operation, the steady-state tokamak parameters can be chosen to lie in a favorable regime. A frequently pulsed tokamak, on the other hand, must negotiate often through many parameter regimes, some of which are no doubt perilous. Disruptions are taken, at present, quite seriously; as much as a kilogram of material might be ablated from the tokamak walls as the result of one disruption and only several hundred might be tolerated in a reactor lifetime.

The apparatus that produces the steady-state current is less cumbersome than the transformer coils that produce the ohmic, pulsed current. Replacing the transformer coils frees up valuable space in the tokamak hole, which could instead be used, e.g., for shielding material or energy extraction means. Alternatively, it might be geometrically favorable to build a low aspect ratio tokamak (a/R large) and shrink the hole.

The toroidal magnetic field in tokamak reactors is likely to be provided by superconducting coils. The refrigeration requirements for these coils are likely to be greater in a pulsed reactor where time-varying magnetic fields could produce inductive losses in the coils.

The continuously operating tokamak also has the economic advantage of less down time. The down time in pulsed reactors is utilized to reset the transformer coils. Shortening this dwell period requires more expensive electric power supplies, and some form of temporary storage of the plasma thermal energy may be required.

Against these and other benefits must be weighed the liabilities associated with the capital cost, the circulating power requirements, and the reliability of the current-drive apparatus.

I. Intent, Scope, and Additional Resources

The intent of this work is to acquaint the nonspecialist with an exciting area of plasma physics, as well as to direct the active researcher towards what this author considers to be the present frontier in the field. Accordingly, the material here is in part tutorial, in part advanced, and in part fairly opinionated. Sections can be omitted on a first reading, although this is not directly indicated. This work is also intended to be a compilation of the relevant resources on the topic of current-drive.

Insufficient attention in this review is paid to the topic of wave propagation. Here, we focus on the wave-particle interaction that occurs after the waves have been injected at the plasma boundary, have possibly tunneled through a small region of wave evanescence, have possibly propagated through a region of plasma turbulence, and have arrived at the plasma center where they may be absorbed by the plasma. Figure 1.8 schematically illustrates these regimes for the case of lower-hybrid waves. The lower-hybrid wave grill, an endfire waveguide array pioneered by Lallia (1974) and by Brambilla (1976), optimizes the coupling of the wave to the plasma vessel. Different waves, however, propagate differently, and it is a separate project to explore, in detail and for each wave, the theory of wave propagation. Of the waves we consider here, the electron-cyclotron wave is a free space wave, whi › the lower-hybrid wave exists only in the plasma, but can be described, using an eikonal approximation, in terms of rays. Other waves, such as low-frequency magnetosonic waves, are global eigenmodes of the plasma torus.

There has been, of course, much work devoted to tracing waves from the plasma periphery to the plasma center, the details of which are but touched on here. For a review of recent work of ray tracing, one may consult Bonoli (1984), and Santini (1985) recently reviewed the theory of lower-hybrid waves. The theory of plasma waves is presented in the classic work of Stix (1962).

Other general sources may be useful. Recent tokamak developments towards a working fusion reactor are described by Furth (1979). Engineering considerations are given by Conn (1983). A fine set of course notes on the topic of current-drive has been prepared by Uckan (1985), including, among other things, more emphasis than here on the propagation characteristics of

different waves. For a more elementary review of wave-driven currents, see Fisch (1983). A classic text on plasma physics and controlled nuclear fusion is Rose and Clark (1961). Its still relevant preface contains precious passages from Ben Johnson's "The Alchemist."

J. Outline of Succeeding Chapters

In Chapter II we present the theory of generating current by methods which exploit the small collisionality of superthermal resonant electrons. The most useful approximations and precise numerical and analytical results are available in this regime, which has enjoyed particular experimental attention, too.

In Chapter III we consider, in less detail, a wide range of current drive effects. Some of these methods are quite promising, such as by injecting netural beams. Other methods are included to emphasize the diversity of possible effects and the room in this problem for imaginative solutions. In Chapter IV we review the experimental effort to date. Of particular interest is the very substantial convergence now of our experimental capability and theoretical understanding of the lower-hybrid current-drive effect.

In Chapter V we consider methods of driving current in which not all plasma parameters are held constant. Such so-called "quasi-steady-state operation" leads to some interesting effects, but it is not favored over completely steady-state operation.

In Chapter VI, we review the leading current-drive methods in light of application to first generation D-T tokamak reactors. The reader, more interested in the possibility of steady-state tokamak operation than in the description and mathematical quantification of current-drive methods, might skip immediately to Chapter VI and then skim the intervening chapters as necessary.

II. Current-Drive with Fast Electrons

A. Introduction

For electron-based current-drive schemes, it is always necessary to calculate the balance between effects due to collisions, which tend to drive

the electrons to thermal equilibrium, i.e., to a Maxwellian distribution, and effects due to injected waves, which tend to produce the asymmetry that is necessary for the current-drive. The equation at the heart of the matter is the Fokker-Planck equation, which describes mathematically the evolution of the electron distribution function in the presence of these competing effects.

Solutions to this equation have dominated the work on current-drive. At first, research centered on the nature of momentum transfer in a wave-particle interaction and the possibility for current-drive in the first place (Wort, 1971; Klima, 1973; Midzuno, 1975). The first solutions to the Fokker-Planck equation were crude one-dimensional approximations (Fisch, 1978; Klima and Longinov, 1979) which purported to capture the important effects. To a surprisingly large extent, one-dimensional approximations were backed up by numerical solutions (Karney and Fisch, 1979; Harvey, Marx, and Rawls, 1980) to the Fokker-Planck equation.

Numerical solutions to the Fokker-Planck equation have been valuable for several reasons. First, they provide a check on analytically derived quantities, such as the current-drive efficiency. Second, they provide a revealing picture of the solution of a model equation for a specific set of wave data and boundary conditions. Numerical solutions alone, do not, however, fully satisfy us. First, there are many permutations of the parameters, and what we need is an idea of what is possible, say, as we vary our wave or plasma data, rather than the solution in one instance. Second, the full unapproximated equations are too difficult to solve even numerically, and guidance is necessary to decide which approximations should be attempted. Finally, plasmas are now described by very complicated numerical codes that incorporate far more than the effects that we desire to isolate here. What is needed is a succinct expression for the wave-induced effects that can then be included in the more complicated picture that might contain, for example, the effects of wave propagation, fusion production, and particle and heat transport. The numerical solutions offered at present would be too time-consuming to be included in such a larger calculation.

To remedy this deficiency, researchers have focused their attention on linearizing the Fokker-Planck equation, and reformulating the problem in order to find useful Green's functions for various plasma responses, including the current-drive effect. It is then possible to pose very general problems that,

in some cases, even have useful analytic solutions. These techniques involve solving Langevin or adjoint equations, rather than solving directly the Fokker-Planck equation.

At present, the field makes use of all the techniques described here in dealing with the Fokker-Planck equation. This chapter reviews these techniques and useful approximations for describing the major current-drive effects involving fast electrons.

B. Fokker-Planck Equation

The evolution of the electron distribution function f is described by the Fokker-Planck equation (see, e.g., Montgomery and Tidman, 1964),

$$\frac{df}{dt} = C(f,f) + C(f,f_i) - \frac{\partial}{\partial \vec{v}} \cdot \vec{S}_w \quad , \tag{2.1}$$

where $C(f,f)$ represents the self-collisions of electrons, $C(f,f_i)$ represents the scattering of electrons off ion distribution f_i, and the wave-induced flux $\vec{S}_w$ depends, in general, on both the nature of the wave-particle interaction and the velocity-space gradient of the electron distribution function, i.e.,

$$\vec{S}_w \equiv -\bar{D}_{QL} \cdot \partial f/\partial \vec{v} \quad . \tag{2.2}$$

We refer to $\bar{D}_{QL}$ as the quasilinear diffusion coefficient. (The unusual nomenclature arises from its derivation in connection with the propagation and damping of small amplitude waves. Deviations of f from a Maxwellian depend on the wave amplitude, the small parameter in this derivation. Diffusion depends both on the wave spectral energy density and the gradient of the wave-perturbed distribution function, so, in this sense, is a nonlinear effect in the wave amplitude - hence, the nomenclature. For our purposes here, however, $\vec{S}_w$ is linear in f; the nonlinearities in the Fokker-Planck equation are associated with the collision terms.) For the case of lower-hybrid waves, for example, $\bar{D}_{QL} \sim \hat{i}_\parallel \hat{i}_\parallel$, indicating parallel diffusion by parallel gradients only. Representing the wave effect as an induced diffusion of electrons in velocity space is an excellent approximation. Alternative, more complicated, representations produce the same effect (Gell and Nakach 1984; 1985).

The total time derivative for the guiding center motion of electrons in a strong magnetic field is most directly written for $f(\mu,\varepsilon,\vec{r})$, i.e., using for independent variables the magnetic moment $\mu = mv_\perp^2/2B$ and the energy $\varepsilon = mv^2/2$. The total time derivative can then be put in the form

$$\frac{d}{dt} = \frac{\partial}{\partial t} + (\vec{v}_{dr} + v_\parallel \hat{b}) \cdot \frac{\partial}{\partial \vec{r}} + \frac{\partial \varepsilon}{\partial t}\frac{\partial}{\partial \varepsilon} \quad , \tag{2.3a}$$

where $\partial\mu/\partial t = 0$ and

$$\frac{\partial \varepsilon}{\partial t} = qv_\parallel E_\parallel - \mu B \vec{\nabla} \cdot \vec{v}_E + (mv_\parallel^2 - \mu B)\, \vec{v}_E \cdot (\hat{b} \cdot \vec{\nabla})\hat{b} \quad , \tag{2.3b}$$

where $\vec{v}_{dr}$ is the drift velocity perpendicular to magnetic field $\vec{B}$ (with unit direction $\hat{b}$ and $\vec{v}_E \equiv \vec{E} \times \vec{B}/B^2$.

For describing the homogeneous plasma, $\partial/\partial\vec{r} \to 0$, and it is then convenient to write f as $f(v_\parallel, v_\perp)$, and solve Eq. (2.1) with

$$\frac{d}{dt} = \frac{\partial}{\partial t} + \frac{qE_\parallel}{m}\frac{\partial}{\partial v_\parallel} \quad . \tag{2.3c}$$

The homogeneous plasma approximation is generally adequate to describe well the most efficient current-drive methods. Except for Sec. 3.3, where trapped electron effects are considered explicitly, the approximation $\partial/\partial\vec{r} \to 0$ will be assumed and d/dt will be defined as in Eq. (2.3c).

The collision operator is given by (Landau, 1936)

$$C(f_a, f_b) = -\frac{\partial}{\partial \vec{v}} \cdot \vec{S}^{a/b} \tag{2.4a}$$

with

$$\vec{S}^{a/b} = \frac{q_a^2 q_b^2}{8\pi \varepsilon_o^2 m_a} \ln\Lambda^{a/b} \int \bar{U}(\vec{y}) \cdot \left[\frac{f_a(\vec{v})}{m_b}\frac{\partial}{\partial \vec{v}'} f_b(\vec{v}') - \frac{f_b(\vec{v}')}{m_a}\frac{\partial}{\partial \vec{v}} f_a(\vec{v})\right] d^3\vec{v}' \tag{2.4b}$$

where

$$\bar{U}(\vec{y}) \equiv \frac{y^2\bar{I} - \vec{y}\vec{y}}{y^3} \quad , \qquad \vec{y} \equiv \vec{v} - \vec{v}' \quad . \tag{2.4c}$$

Thus, we intend to solve Eq. (2.1) under a set of simplified circumstances: namely, we assume that f possesses azimuthal symmetry [$(f = f(v_\parallel, v_\perp)$] and we generally consider the homogeneous case $\partial/\partial\vec{r} \to 0$ only.

C. Linearized Fokker-Planck Equation

There are several powerful simplifications that may be employed now in order to extract information from the rather complicated Fokker-Planck equation.

First, for electron-based current-drive problems it is always a superb approximation to treat the ions as infinitely massive. The only role that ions then play is to scatter electrons in direction, not in energy. The justification for this approximation is that the electron-ion energy equilibration time is orders of magnitude longer than other times of interest. For ion-based current-drive schemes, for example, when more than one species of ions are present, this approximation can still be made with respect to electron-ion collisions, but not with respect to ion-ion collisions.

Second, as discussed above often we restrict ourselves to the case of homogeneous plasmas, i.e., $\partial/\partial\vec{r} \to 0$ in Eq. (2.3). This assumption represents a large simplification and isolates the effects we wish to calculate. It is an excellent assumption for current-drive using fast electrons, because trapped-electron effects are small. For current-drive using marginally trapped electrons, this assumption cannot be made. Other approximations might then be employed (see Sec. 3.3).

Third, it is always an excellent approximation to linearize the collision operator, even when the rf power is intense. This is because the main effect of even intense rf waves is to distort the distribution function f only in some resonant region of velocity space, while the bulk of the distribution remains Maxwellian. An example was shown in Fig. 1.5. Therefore, even though the distortion in $f(\vec{v})$ may be large for some $\vec{v}$, e.g., the "plateau" in Fig. 1.5 is a large distortion in the tail of the electron distribution, all electrons collide most frequently with the bulk electrons which are still more numerous than the plateau electrons. Accordingly, we let $f = f_m + \tilde{f}$, and approximate

$$C(f,f) \approx C(f_m,\tilde{f}) + C(\tilde{f},f_m) \quad , \tag{2.5}$$

where the zeroth-order term, $C(f_m,f_m)$ vanishes since a Maxwellian distribution has no further to relax via collisions. The distribution f_m is defined by

$$f_m \equiv n(2\pi T/m)^{-3/2} \exp(-\varepsilon/T) \quad , \tag{2.6}$$

where particle kinetic energy ε is defined by $\varepsilon \equiv mv^2/2$.

For notational convenience, we group

$$C(\tilde{f}) \equiv C(\tilde{f},f_m) + C(f_m,\tilde{f}) + C(\tilde{f},f_i) \quad , \tag{2.7}$$

so that the linearized Fokker-Planck equation that will occupy our attention may be written as

$$\frac{\partial}{\partial t}\tilde{f} + \frac{q\vec{E}}{m}\cdot\frac{\partial}{\partial \vec{v}}\tilde{f} - C(\tilde{f}) = -\frac{\partial}{\partial \vec{v}}\cdot\vec{S}_w - \frac{q\vec{E}}{m}\cdot\frac{\partial}{\partial \vec{v}} f_m$$
$$-\left[\frac{\dot{n}}{n} + \left(\frac{\varepsilon}{T} - \frac{3}{2}\right)\frac{\dot{T}}{T}\right] f_m \quad , \tag{2.8}$$

where we neglect spatial derivatives, and use

$$\frac{\partial f_m}{\partial t} = \frac{\partial n}{\partial t}\frac{\partial f_m}{\partial n} + \frac{\partial T}{\partial t}\frac{\partial f_m}{\partial T} \equiv \frac{\dot{n}}{n} f_m + \left(\frac{\varepsilon}{T} - \frac{3}{2}\right)\frac{\dot{T}}{T} f_m \quad , \tag{2.9}$$

with f_m assumed to evolve on a slow time scale compared to $\tilde{f}$.

Boundary and initial conditions must be specified on the distribution $\tilde{f}$. The initial condition is usually taken to be that f is Maxwellian, i.e., that $\tilde{f}(v,t=0) = 0$, although this need not be so. Boundary conditions will be discussed in greater detail as specific problems are solved, but we note here that the linearization $f = \tilde{f} + f_m$ is unique only if the density and energy contained in the distribution $\tilde{f}$ is specified. It is natural and easiest to allow f_m to evolve slowly according to Eq. (2.9), while demanding that $\tilde{f}$ contain no particles and no energy, i.e., its zeroth and second moments in v vanish. The Maxwellian background then evolves uniquely and compatibly; for example, integrating Eq. (2.8) over all velocity space, we find $\dot{n} = 0$, since all terms conserve particles. Multiplying Eq. (2.8) by ε and then integrating gives us the evolution equation for the temperature

$$\frac{3}{2} n \frac{\partial T}{\partial t} = \int \vec{S}_w \cdot \partial \varepsilon / \partial \vec{v} \, d^3\vec{v} \quad + \quad \vec{E} \cdot \vec{J} \quad , \tag{2.10}$$

where

$$\vec{J} \equiv - \int e\vec{v} \, \vec{f} \, d^3\vec{v} \quad . \tag{2.11}$$

The first term on the right-hand side of Eq. (2.10) accounts for heating by injected waves and the second term represents the Joule heating due to an electric field.

The linearized Fokker-Planck electron-electron collision operator shares many of the "nice" mathematical properties of the original operator. In particular, we have the relations

$$\int C(f_a, f_b) d^3v = 0 \tag{2.12a}$$

$$\int \left[m_a \vec{v} \, C(f_a, f_b) + m_b \vec{v} \, C(f_b, f_a) \right] d^3v = 0 \tag{2.12b}$$

$$\frac{1}{2} \int \left[m_a v^2 \, C(f_a, f_b) + m_b v^2 C(f_b, f_a) \right] d^3v = 0 \quad , \tag{2.12c}$$

which correspond to conservation of number density, momentum and energy in collisions between distributions a and b. Both the linearized and original Fokker-Planck equations exploit these properties to conserve these quantities, so long as both distributions, a and b, are evolved. In practice, in the limit $m_i/m_e \to \infty$, the ion distribution is presumed to be a nonevolving momentum sink, while the electrons conserve number and energy.

The linearized Fokker-Planck equation does not, however, in the presence of joule or wave heating, guarantee the non-negative nature of f, a guarantee which is a property of the original equation. Also lost is a strict H-theorem. On the other hand, in the calculation of all quantities of interest, the linearization is an excellent approximation, and it produces an equation that may be exploited using Green's function techniques.

D. High-Velocity Limit

Much that we wish to describe involves only the dynamics of fast electrons. Thermal electrons, i.e., $v \lesssim v_T$, are all, in velocity space, roughly a speed v_T distant from most other electrons; hence they all experience about the same electron-electron collisionality with collision rate $\nu \sim v_T^{-3}$. Fast electrons are defined by $v \gg v_T$. These electrons are, in velocity space, roughly a speed v distant from most other electrons; hence the collision frequency of these electrons will be $(v_T/v)^3$ smaller than for other electrons. In practice, even an electron with $v/v_T \approx 3$ may be considered fast, and hence relatively collisionless, and amenable to the approximations employed in this section.

The picture we have then (see Fig. 1.7) is that a fast electron slows down in energy in collisions with slower electrons; as it loses energy it collides also more frequently with ions; and, eventually, it becomes a thermalized electron, frequently colliding with ions, and having no longer any directed motion. For our purposes here, where we are interested in the current carried by an electron, the details of an electron's trajectory as it slows down to subthermal speeds no longer interest us. Initially, at high speed, it does carry substantial current; when it slows down it carries a much smaller current and, because by then it is colliding frequently, even this small current persists only for a very short time. Therefore, it is a very good approximation to assume in Eq. (2.4) that collisions always take place in the high-velocity limit, meaning $v \gg v_T$, where we can simplify,

$$C(f,f) \approx C_H(f,f) \equiv \Gamma \left[\frac{1}{v^2} \frac{\partial}{\partial v} \left(\frac{v_T^2}{v} \frac{\partial f}{\partial v} + f \right) + \frac{1 - v_T^2/2v^2}{2v^3} \frac{\partial}{\partial \mu} (1-\mu^2) \frac{\partial}{\partial \mu} f \right], \quad (2.13)$$

where $\mu \equiv v_\parallel/v$ and $\Gamma \equiv nq^4 \ln\Lambda / 4\pi\epsilon_0^2 m^2$. (Note that the direction cosine μ defined here is not to be identified with the magnetic moment.) The first term describes energy diffusion and frictional deceleration, while the second term describes diffusion in direction or "pitch-angle" scattering. Electron-ion collisions, with $m_i/m_e \to \infty$, are automatically in the high-velocity limit (even for thermal electrons) since only $v > v_{Ti}$ need be satisfied, so we have

$$C(f,f_i) = \frac{\Gamma Z_i}{2v^3} \frac{\partial}{\partial \mu} (1-\mu^2) \frac{\partial}{\partial \mu} f \quad . \quad (2.14)$$

The high-velocity limit equation is then

$$\frac{\partial f}{\partial t} + \frac{qE}{m}\frac{\partial f}{\partial v_{\parallel}} = C_H(f,f) + C(f,f_\perp) - \frac{\partial}{\partial \vec{v}} \cdot \vec{S}_w \quad . \tag{2.15}$$

Note that in the presence of collisions only, i.e., $\vec{E}$, $\vec{S}_w \to 0$, the steady-state solution to Eq. (2.15) is a Maxwellian with thermal velocity v_T. The high-velocity limit equation corresponds physically to immersing test electrons in a Maxwellian background of electrons with temperature T. The test distribution then tends to equilibrate to this temperature.

In the limit $v >> v_T$, *the first term in* Eq. (2.13) is order $(v_T/v)^2$ smaller than the other terms; strictly speaking, it should not appear, and $C_H(f,f)$ should be temperature independent to lowest order in v_T/v. However, the retention of this somewhat higher-order term leads to correct behavior of the equation for $v \to 0$, namely, that the distribution tends to a Maxwellian. The rate, according to Eq. (2.15), at which f tends to a Maxwellian near $v \to 0$ is grossly inaccurate; however, that turns out to be inconsequential for applications of interest. Competition between wave and collisional effects, in the case of lower-hybrid current-drive, occurs only for v large, so that f tends quickly to a Maxwellian in any event as $v \to 0$. *The precise rate is not* important since events associated with v large occur on such a longer time scale. Note, however, that effects associated with the electric field, such as Spitzer conductivity, will be incorrectly described by Eq. (2.15).

In addition to the above desirable properties, the high-velocity limit equation does also preserve both number density and the non-negative nature of f, *although, as discussed above, neither momentum nor energy is conserved.* Examples in which the high-velocity limit equations cannot be used are Spitzer conductivity (Spitzer and Härm, 1953; Coher, Spitzer and Routly, 1950) and current-drive with low phase velocity waves (Fisch and Karney, 1981).

E. Langevin Equations

The Boltzmann equation written in the strict high-velocity limit (i.e., diffusion in energy is neglected) is a linear equation corresponding to fast electrons acted upon by drag (dynamical friction) by background electrons, by acceleration by an electric field, and by pitch-angle scattering due to collisions with both electrons and ions. These effects can be captured in a

set of Langevin equations (Chandrasekhar, 1943 and Wang and Uhlenbeck, 1945), which are a set of ordinary differential equations that track the trajectory of a single electron, i.e.,

$$\frac{dv}{dt} = -\left(\frac{\Gamma}{v^3}\right)v + \left(\frac{qE}{m}\right)\mu \tag{2.16a}$$

$$\frac{d\mu}{dt} = B(t) + \frac{(qE/m)(1-\mu^2)}{v} \quad , \tag{2.16b}$$

where the stochastic term B(t) is responsible for pitch-angle scattering and is itself described by the statistical properties

$$\langle B(t)\rangle = -\left(\frac{\Gamma}{v^3}\right)(1 + Z)\mu \tag{2.17a}$$

$$\langle B(t)B(t')\rangle = \left(\frac{\Gamma}{v^3}\right)(1 + Z)(1 - \mu^2)\delta(t - t') \quad , \tag{2.17b}$$

where the angle brackets denote averaging over the ensemble defined by all realizations. In practice, the Langevin equations may be advanced numerically from time t to time t + Δt by picking the integral of B in this interval from an ensemble with mean $-\Delta t(1 + Z)$ and with variance $\Delta t(1 + Z)$, with μ and v evaluated at time t.

Solving the Langevin equations gives the trajectory defined by $\mu(t)$ and v(t). The ensemble average of these trajectories, weighted by various functions of μ and v, gives us quantities of interest. For example, the ensemble-averaged current, $\langle qv_\parallel\rangle$, carried by an electron as a function of time, as sketched in Fig. 1.7b, is a quantity of interest. Our notation is that an electron has elementary charge q = -e. Note that $v_\parallel = v_\parallel(t,\vec{v})$, where $\vec{v}$ is the initial velocity of the electron at time t = 0.

Suppose that we expend energy $\varepsilon_2 - \varepsilon_1$, in pushing an electron from velocity space location 1 to location 2, as depicted in Fig. 1.7a. The ensemble averaged current difference at time t as a result of such a push at time τ is

$$\Delta j(t) = q\langle v_\parallel(t - \tau, \vec{v}_2)\rangle - q\langle v_\parallel(t - \tau, \vec{v}_1)\rangle \quad . \tag{2.18}$$

The rate of pushing a density of electrons is simply $P/(\varepsilon_2 - \varepsilon_1)$, where P is the power density expended. The current density J that appears at time t can then be written as

$$J(t) = \int_0^t d\tau \, \frac{P(\tau)}{\varepsilon_2 - \varepsilon_1} \langle q v_\parallel(t-\tau, \vec{v}_2) - q v_\parallel(t-\tau, \vec{v}_1) \rangle$$

$$\xrightarrow[\lim \vec{v}_2 \to \vec{v}_1]{} \int_0^t d\tau \, P(\tau) \, \frac{\vec{S}_w \cdot (\partial/\partial \vec{v}_1) \langle q v_\parallel(t-\tau, \vec{v}_1) \rangle}{\vec{S}_w \cdot (\partial/\partial \vec{v}_1) \, \varepsilon(\vec{v}_1)} \quad , \tag{2.19}$$

where, for notational convenience, we set $\vec{v}_2 = \vec{v}_1$ in the limit, and where the limit was taken for incremental displacement along the displacement direction, which for electrons pushed by waves is, by definition, in the direction of $\vec{S}_w$, the wave-induced flux.

A special case of Eq. (2.19) occurs for constant power input density, $P(\tau) = P_d$. Here, for $t \to \infty$, the integral may converge, in which case a steady-state current-drive efficiency may be defined by

$$\frac{J}{P_d} = \frac{\vec{S}_w \cdot (\partial/\partial \vec{v}_1) \int_0^\infty \langle q v_\parallel(t, \vec{v}_1) \rangle dt}{\vec{S}_w \cdot \partial \varepsilon / \partial \vec{v}_1} \quad . \tag{2.20}$$

It remains, of course, to find the integral of $\langle q v_\parallel \rangle$, and this can be done by tracking the Langevin equations.

The Langevin approach becomes particularly simple when there is no dc electric field, i.e., E = 0. Taking the ensemble averages of Eqs. (2.16), we find that v is nonstochastic, i.e., $\langle v \rangle = v$, which satisfies

$$\frac{dv}{dt} = -\left(\frac{\Gamma}{v^3}\right) v \quad , \tag{2.21a}$$

while the average pitch-angle evolves according to

$$\frac{d\langle \mu \rangle}{dt} = -\left(\frac{\Gamma}{v^3}\right)(1+Z)\langle \mu \rangle = (1+Z)\langle \mu \rangle d(\ln v)/dt \quad , \tag{2.21b}$$

where we substituted for Γ/v^3 from Eq. (2.21a) to write the second equality in Eq. (2.21b). We can then integrate Eq. (2.21b) to get

$$\frac{\langle \mu \rangle}{\mu_1} = \left(\frac{v}{v_1}\right)^{1+Z} \quad , \tag{2.22}$$

where $\mu(t=0) = \mu_1$ and $v(t=0) = v_1$ are initial conditions. Note that Eq. (2.22) expresses a parameterization of the likely pitch angle in terms of the electron speed and the initial coordinate.

The quantity we wish to calculate is $\langle qv_\parallel \rangle = \langle qv\mu \rangle = qv\langle\mu\rangle$, or more precisely, its integral over time. Using then Eq. (2.22), we have

$$\int_0^\infty \langle qv_\parallel \rangle dt = q\mu_1 v_1 \int_0^\infty \left[\frac{v(t)}{v_1}\right]^{2+Z} dt \quad . \tag{2.23}$$

The integral may be evaluated by parameterizing t by v using Eq. (2.21a), i.e., $dt = -v^2 dv/\Gamma$ with $v(t = \infty) = 0$, with the result

$$\int_0^\infty \langle qv_\parallel \rangle dt = \frac{q\mu_1 v_1^3}{\Gamma} \int_0^{v_1} \left(\frac{v}{v_1}\right)^{4+Z} dv = \frac{q\mu_1 v_1^4}{(5+Z)\Gamma} \quad . \tag{2.24}$$

The efficiency for steady-state current-drive by pushing fast electrons at velocity space location $\vec{v}$ (i.e., for notational convenience we now define $\vec{v}_1 \to \vec{v}$) is

$$\frac{J}{P_d} = \left(\frac{q}{\Gamma(5+Z)}\right) \frac{\hat{S}_w \cdot (\partial/\partial\vec{v})\ (v^3 v_\parallel)}{\hat{S}_w \cdot (\partial/\partial\vec{v})(mv^2/2)} \quad . \tag{2.25a}$$

The steady-state current drive is often expressed in normalized quantities; J is normalized to $-env_T$ and P_d is normalized to νnmv_T^2, where $\nu \equiv \Gamma/v_T^3$. Our convention is that an electron carries charge $q = -e$, where e is the elementary charge unit. Additionally, velocities may be normalized by $\vec{u} = \vec{v}/v_T$, with the further convention $w \equiv v_\parallel/v_T$ and $x \equiv v_\perp/v_T$. The convention we employ is that the thermal velocity v_T is $(T_e/m_e)^{1/2}$. (The reader is cautioned that some authors adopt a convention wherein the thermal velocity is defined larger than ours by a factor of $\sqrt{2}$.) The normalized efficiency is then written as

$$\frac{J}{P_d} = \left[\frac{1}{5+Z}\right] \frac{\hat{S}_w \cdot (\partial/\partial\vec{u})(wu^3)}{\hat{S}_w \cdot (\partial/\partial u)(u^2/2)} \quad . \tag{2.25b}$$

The normalized quantities will generally be distinguished here by context, rather than by a separate notation.

This result (Fisch and Boozer, 1980) indicates that it is efficient not only to push electrons in the parallel direction ($\hat{S}_w \sim \hat{i}_\parallel$) as in the case of

lower-hybrid current-drive, but it is almost as efficient to push them in the perpendicular direction ($\vec{S}_w \sim \hat{i}_\perp$). The precise ratio of these efficiencies is 4:3. This result is quite precise; it has been verified numerically to be accurate for $v \gtrsim v_T$ (see Fig. 2.1 reproduced from Karney and Fisch, 1981). Ignored here are relativistic effects, but they may be handled similarly using relativistic Langevin equations (Fisch, 1981). A more important limitation, however, is that while the efficiency is accurately given in terms of the wave-induced flux, that quantity is only surmised, not found, in this calculation. In the case of finite electric field, the Langevin equations cannot be solved analytically and numerical integration is necessary (Fisch and Karney, 1985). Further calculations of the electron-cyclotron wave current-drive effect were carried out by Eldridge (1980) (neglecting electron-electron collisions) and by Parail and Pereverzev (1982).

The Langevin equations are useful because the physical interpretation at every step is transparent. An entirely equivalent formalism, the adjoint method, exploits outright of the linearity of Eq. (2.8) and derives directly the Green's function (see Sec. II.I). The adjoint method makes use of more powerful and more easily implementable mathematical techniques, and it is usually the preferred method of solution now.

F. One-Dimensional Theory

A very crude, but very useful, simplification in solving the Fokker-Planck equation is the so-called 1-D (one-dimensional) approximation (Vedenov, 1967). Both the Langevin equations and the adjoint formalism (which we discuss later) are suitable for solving for plasma responses once the wave-induced flux $\vec{S}_w$ is known. Neither formalism, however, is capable of easily solving for f, which may be necessary if one is to know $\vec{S}_w$. (Note, however, that sufficient information concerning the flux may often be deduced as described in Sec. II.G.) To find f precisely, there is generally no recourse other than to solve numerically the Fokker-Planck equation. Even linearized, this equation still demands considerable numerical computation (see Sec. 2.H). Often, however, 1-D theory provides a suitable solution, and it is used for the important special case of lower-hybrid current-drive, where $\vec{D}_{QL} \sim \hat{i}_\parallel \hat{i}_\parallel$.

In 1-D theory, it is argued ad hoc that the most important velocity space dynamics is in the parallel rather than perpendicular direction. Moreover, it is arbitrarily assumed that the distribution function f is a Maxwellian in the perpendicular direction with the same temperature that characterizes the bulk of the electrons. Thus, one substitutes into the high-velocity limit equation the ansatz

$$f = f_m(v_\perp)\, F(w), \tag{2.26}$$

where $w = v_\parallel/v_T$, and then one integrates both sides of the resulting equation over $v_\perp$. The result is an equation to be obeyed by F at large w, namely

$$\frac{\partial F(w)}{\partial \tau} = \frac{\partial}{\partial w} D_{LH} \frac{\partial}{\partial w} F + (2 + Z_i) \frac{\partial}{\partial w} \left(\frac{1}{w^3} \frac{\partial}{\partial w} + \frac{1}{w^2}\right) F - \frac{qE}{m\nu} \frac{\partial F}{\partial w} \quad , \tag{2.27}$$

where we normalized $\tau = \nu t$ and $D(w) = D_{QL}/\nu v_T^2$. For $E \to 0$, and with constant wave excitation $D(w,t) = D(w)$, this 1-D equation has a steady-state solution

$$F(w, \tau \to \infty) = C \exp\left[\int_0^w \frac{-w\, dw}{1+w^3 D(w)/(2+Z)}\right] \quad , \tag{2.28}$$

where C is a constant that may be determined by a normalization condition. Note that Eq. (2.27), however arbitrary its derivation, still conserves both particles and the non-negative nature of f.

Note that where D(w) vanishes, F is locally Maxwellian, and where $D(w)w^3 \gg 1$, F is locally flat. A useful model for lower-hybrid waves is to take

$$D(w) = \begin{cases} D, & w_1 < w < w_2 \\ 0, & \text{elsewhere} \end{cases} \tag{2.29}$$

where $D \to \infty$. It is remarkable that this very crude, reasonable, but ultimately unjustifiable, method gives very good answers to questions of interest. For example, f in Fig. 1.5 corresponds to $w_1 = 3$ and $w_2 = 5$; integrating that 2-D numerical solution over $v_\perp$ gives F(w) (numerically) as shown in Fig. 2.2. Note that the 1-D derivation of F(w), Eq. (2.28), captures the salient features of the numerical solution, except for the regime $w > w_2$ where F falls off too rapidly with w. For $w \to 0$, F is Maxwellian as it should be, even though Eq. (2.27) is derived, albeit ad hoc, in the high-velocity limit.

The most important use of the 1-D theory has been to predict the high efficiency of current-drive by using high phase velocity waves and to give reasonable estimates for the current and power dissipated (Fisch, 1978). From Eq. (2.28) we find the current density for $D \to \infty$.

$$J = -env_t \int dw\, w\, F(w) = -env_T F_m(w_1)(w_2^2 - w_1^2)/2 \quad ,$$

$$= 6.5 \times 10^8\, n_{14} T_{10}^{1/2}\, F_m(w_1) w_1 \Delta \frac{A}{m^2} \quad , \tag{2.30}$$

where in the last approximate equality we used $\Delta = w_2 - w_1 \ll w_1$ and normalized quantities. Similarly, the power dissipated may be calculated as

$$P_d = \nu n m v_T^2 \int dw \frac{w^2}{2} \frac{\partial}{\partial w} D \frac{\partial}{\partial w} F = \nu n m v_T^2 \,(2 + Z)\, F_m(w) \ln\left(\frac{w_2}{w_1}\right) \quad .$$

$$= 5 \times 10^9\, n_{14}^2\, T_{10}^{-1/2} (2 + Z_i) F_m(w_1) w_1 \Delta \frac{W}{m^3} \quad . \tag{2.31}$$

The quantity J/P_d gives the 1-D steady-state efficiency which (for $Z = 1$) is about a factor 2.5 smaller than the correct numerically derived 2-D result (Karney and Fisch, 1979).

The 1-D equations have been elaborated upon in several ways. Justification for the model has been sought by Wegrove and Englemann (1985). Better agreement with the 2-D results has been achieved by Fuchs et al. (1985) by formulating 1-D equations taking into account two perpendicular moments of the Fokker-Planck equation. Note, however, that both the current and power dissipated are extremely sensitive functions of w_1, although their ratio is not. Since the spectrum location, experimentally, is not in any event accurately determinable, it is not necessary to demand a more accurate calculation of the current or power dissipated. What is important is to give correctly the relationship between these quantities. Therefore, an entirely adequate and time-efficient approach is to accept the 1-D estimate for the power dissipated, and to use the Fisch-Boozer efficiency, Eq. (2.25), to calculate the current. Of course, if a very accurate calculation of f is required, which is generally not the case, a fully 2-D numerical treatment would be necessary.

The 1-D theory has also been employed to good effect in the case of a small electric field (Borass and Noncentini, 1984) and for more complicated wave models. A similar model has been employed by Liu et al. (1985). Of course, in some cases, the 1-D theory is hopelessly inadequate. For example, the 1-D theory is incapable of uncovering the current-drive effect associated with electron-cyclotron-wave current-drive, where $\vec{S}_W \sim \hat{i}_\perp$. A second example is the impossibility of describing the physics of backward runaway electrons, a topic which perhaps deserves a short digression.

Runaway electrons occur in the presence of a dc electric field; electrons fast enough to overcome the dynamical friction of Coulomb collisions with background electrons may be accelerated indefinitely by the dc field, with collisional effects growing fainter and fainter as the field accelerates the essentially free-streaming electrons (Dreicer, 1960). In contrast to these "forward" runaways, for which the collisional effect is monotonically decreasing, there exists also what might be called "backward" runaways. These electrons initially travel counter to the force exerted by the dc electric field. As the field decelerates these electrons to lower kinetic energy, collisional effects first increase. If, however, these collisional effects are too small to thermalize these electrons (this can happen if $v_\perp$ is large when an electron nears $v_\parallel = 0$), then the electric field succeeds also in subsequently accelerating these electrons to higher energy, just as for the forward runaways. These runaways, born backward-streaming, are distinguished as backward runaways, and, in contrast to the forward runaways, the 1-D theory is incapable of describing them, because all electrons, in 1-D, emerging from the backward direction, possess the same properties as they pass through the singularly collisional region $v_\parallel = 0$.

A final note to correct a misperception concerning 1-D theory: it is not a physically 1-D model in the sense that electrons are modeled as if living in a 1-D world, like beads on a string. Certainly, in such a world there could not even be like-particle collisions, since to conserve energy and momentum in 1-D colliding like particles could only exchange positions in phase space. Rather, by 1-D theory we merely refer to a sometimes very useful, rather arbitrarily posited, partial differential equation with one independent velocity variable.

G. Calculating the Wave-Induced Flux

Quantities of interest, such as the current, may be calculated with precision using the Langevin formalism if only the wave-induced flux, $\vec{S}_w$, were itself known precisely. Unfortunately, since $\vec{S}_w = \overline{\overline{D}}_{QL} \cdot (\partial/\partial \vec{v})f$, and f is unavailable, this luxury is not generally to be had. It is often possible, however, to deduce $\vec{S}_w$, or at least a great deal about $\vec{S}_w$, without solving for f. When this is possible, it renders the Langevin and the equivalent adjoint approach quite powerful.

Information about $\vec{S}_w$ might be divided into three parts: its direction, its location in velocity space, and its magnitude. The direction of $\vec{S}_w$ is available immediately as a consequence of the nature of the wave-particle interaction. Resonant electrons obey the resonance condition $\omega - k_\parallel v_\parallel - n\Omega_e = 0$. For lower-hybrid waves, e.g., we have n=0, the Landau resonance, and we deduce that $\vec{S}_w$ must be in the parallel direction. This is a consequence of energy and momentum conservation between wave and particle. For $n \neq 0$, such as for the cyclotron resonance, the direction of $\vec{S}$ is such as to be along velocity-space contours of constant energy in the wave frame of reference, i.e., moving with $\vec{v} = \omega/k_\parallel$. This conclusion, again, is a consequence of energy and momentum conservation between wave and particle. (Consider that in the wave frame, $\omega = 0$, so a particle is caught in a static potential well, able to exchange unlimited momentum, but not energy, with the well.) For current-drive applications of interest, in the case of cyclotron waves, the wave-induced flux $\vec{S}_w$ is very nearly in the perpendicular direction.

It is often the case, particularly for current-drive in reactor-grade tokamaks, that the spectrum of the injected waves is narrow in $k_\parallel$, or, equivalently, in parallel phase velocity $\omega/k_\parallel$. Consequently, only electrons with $v_\parallel \approx v_{res}$ would be resonant with the wave, where the parallel resonant velocity v_{res} is found from the wave dispersion relation. If this resonant region is not only narrow, but also fast, i.e., $v_{res} >> v_T$, then one may surmise that unless the distribution function is grossly distorted, most resonant electrons satisfy $v_\parallel \approx v_{res} >> v_T$, and $v_\perp \approx v_T$, which very nearly pinpoints the region in velocity space in which $\vec{S}_w$ is finite. The exact slope of f, of course, would be required to deduce exactly $\vec{S}_w$, but even if f is not known, for an important class of problems $\vec{S}_w$ may be surmised except for magnitude, i.e., up to a multiplicative constant.

Knowledge of all but magnitude of $\vec{S}_w$, together with the fact that $\vec{S}_w$ drives a linear system, means that, with no further information, statements can be made about current-drive efficiency, J/P_d, since it is formed by the ratio of two linear responses to $\vec{S}_w$, i.e., the current and the power dissipated. Similarly, ratios of other responses, such as incremental radiation per power absorbed, can be computed. The result is that without knowledge of f, a great deal can be inferred about how the plasma responds to injected rf waves.

Of course, the magnitude of $\vec{S}_w$ indicates the amount of power absorbed and the extent of all other wave-induced effects, and so it too is needed. Here, also, there may be adequate approximations. For low levels of rf power, linear damping theory is appropriate, i.e., calculate $\vec{S}_w$ on the basis of an unperturbed $f = f_m$. For the important problem of the injection of intense lower-hybrid waves at high parallel phase velocity, the linear theory is no longer adequate, but the 1-D quasilinear theory gives a reasonable estimate. The extent here to which one strives for precision in deducing $\vec{S}_w$ given the wave excitation is limited by the accuracy with which one can ever produce or detect w_1 and w_2 in any event. Since the power absorbed or current generated is so sensitive to the location of the spectrum, it is not often worthwhile to seek a much more accurate account of $\vec{S}_w$ than afforded by these estimates.

H. Numerical Characterizations of f

Before turning our attention to the equation adjoint to the linearized Fokker-Planck equation, we present some numerical solutions of the Fokker-Planck equation. Our aim here is merely to outline the major characteristics of these solutions in the case of current-drive by fast electrons. For a thorough treatment of numerical solutions to the Fokker-Planck equation, an excellent review is provided by Karney (1986).

The first numerical studies to check the assertions of the 1-D theory concerning lower-hybrid current-drive were performed by Karney and Fisch (1979) and Harvey et al. (1981). The model used by Harvey et al. was to solve the nonlinear Fokker-Planck equation together with an ad hoc loss term modeling heat transport across field lines. A somewhat simpler approach was adopted by Karney and Fisch, who solved an approximate linearized Fokker-Planck equation, approximating $C(f,f) \approx C(f,f_m)$. The background Maxwellian

electron distribution then acts as a heat sink, and the test distribution function f evolves then to a steady state. Both approaches, however appear to be in agreement on the most important elements of the problem.

In either model, there are three dimensionless parameters that characterize collisions: m_i/m_e, T_i/T_e, and Z. Taking $m_i/m_e \to \infty$ also renders the problem insensitive to the ratio T_i/T_e, as the ions are so much slower than electrons so that in electron-ion collisions the ion velocity is unimportant. The ion charge state Z does remain as an important parameter; it indicates the relative importance of pitch-angle scattering collisions to electron-electron collisions that induce energy diffusion and slowing down.

It is important also to minimize the number of parameters used to describe the wave spectrum. For waves resonant with high-velocity electrons, even a small amount of wave power tends to dominate collisional effects and tends to plateau the distribution function in the resonant region. Therefore, an adequate characterization of wave spectra is to take $D \to \infty$ in Eq. (2.29), reducing to two the number of spectrum parameters, i.e., the spectrum edges (in phase-velocity space) w_1 and w_2.

In the model considered by Karney and Fisch (1979), over fifty cases, varying w_1, and w_2 with Z = 1 (hydrogen plasma), were examined. An example of the resulting steady-state distribution $f(\vec{v}, t\to\infty)$ was shown in Fig. 1.5, and its integral over $v_\perp$, giving F(w), was shown in Fig. 2.2. In comparing the collection of cases to what would be predicted by 1-D theory, the expectations expressed in the last section were confirmed. As shown in Fig. 2.3, the 1-D prediction of the current is eminently adequate. More significant deviation from 1-D theory occurred in the calculation of the steady-state efficiency, J/P_d. The numerical efficiency was found to be greater than in 1-D theory with a different dependence on Z, and the spectrum width. A rule of thumb, for Z = 1 and not too large a resonant region, was an increase in efficiency by a factor of about 2.5. The 1-D theory is inaccurate here for two main reasons: it fails to take into account that pitch-angle scattering dissipates no energy and it does not take into account the larger perpendicular speeds of resonant electrons during wide spectra excitation. It should be emphasized however, that the theoretical efficiency predicted by the Langevin analysis is, for narrow spectra, accurate and supported by other numerical studies. (e.g., see Fig. 2.1).

One other area in which there is some discrepancy between the 1-D theory and the numerical results is the question of turn-on time, τ_{t-o}, of the current, i.e., the time it takes the current to reach about half its steady-state value. The prediction of 1-D theory (Fisch, 1978) is

$$\tau_{t-o} \approx \left(\frac{2}{Z+2} w_1^2 \Delta\right) \frac{1}{\nu} \quad , \tag{2.32}$$

where $\Delta \equiv w_2 - w_1$, whereas the numerical 2-D result is (for $Z = 1$)

$$\tau_{t-o} \approx \left[6\Delta^{1/2} w_1^2\right]/\nu \quad , \tag{2.33}$$

which is substantially longer than the 1-D result. Note, however, that in either of these analyses the turn-on time is short (typically about 1 second in a reactor), so that, in fact, the calculations are likely to be invalidated by the presence of a large counter-induced electric field. The question of current increase is, therefore, more complicated than the models here describe; instead, we address this question with a fresh approach in Sec. 2.9, when we consider adjoint methods.

Although the numerical solutions evolve to a steady state, they do not prove the existence of a steady state to the original equations. The computational solution is too crude at high energies, where collisional time scales are exceedingly long and the numerical mesh grows coarse, to resolve the question of steady state in an unbounded velocity domain. Note that the heat sink provided by the background Maxwellian is a necessary but not a sufficient condition for the existence of a steady state in the presence of the rf-induced quasilinear diffusion.

An asymptotic analysis (Fisch and Karney, 1985), however, shows that a normalizable steady-state solution does, in fact, exist. This solution treats with rigor the simultaneous limits $D_{QL} \to \infty$, $v \to \infty$, and $w_1 \gg 1$. The utility of the details of this solution in describing $f(v \to \infty)$ is probably greater with respect to the problem of plasma radiation, which is sensitive to $f(v \to \infty)$ rather than with respect to current-drive, for which the distribution of the more numerous intermediate energy electrons tends to be more important. In Fig. 2.4a, we show a comparison between numerical and analytical estimates of bremsstrahlung emission. The analytic estimate may be helpful in using

bremsstrahlung data taken from lower-hybrid current-drive experiments (von Goeler et al., 1985; Stevens et al., 1985) in order to deduce the lower-hybrid spectrum (see Fig. 2.4b). Other analytical attempts (e.g., Krapchev et al.) at describing f in 2-D have been more ambitious in scope than is the asymptotic analysis, but cannot be shown to be rigorously correct in any particular limit.

For the case of electron-cyclotron waves, the diffusion is very nearly in the perpendicular direction, i.e., $\bar{D}_{QL} \sim D\hat{i}_\perp\hat{i}_\perp$. Here, the waves, for $D \to \infty$, *present a far greater distortion to the distribution function than do lower-*hybrid waves. The exact perpendicular dependence of D becomes critical. An example (Karney and Fisch, 1981) contrasting the lower-hybrid with the extraordinary wave is shown in Fig. 2.5. Here, the perpendicular extent of D was limited only by the region of integration ($v/v_T < 10$). In practice, the finite perpendicular wavelength of electron-cyclotron waves cause $D(v_\perp)$ to decrease at high $v_\perp$ with a $1/v_\perp$ dependence (Kennel and Engelmann, 1966). One interesting result of these numerical studies is that despite the large distortions here in f, the damping rate of the wave is nearly independent of the wave power, so linear damping theory, i.e., based on $f \to f_m$, can be used. In contrast, note that for lower-hybrid waves, the damping rate vanishes at high power, because of the parallel flattening in the resonant region. Numerical studies were also performed by Alikaev and Vdovin (1983).

A useful and revealing depiction of velocity-space dynamics in steady-state current-drive problems is afforded by a flux plot of streamlines of $\vec{S}$, where the flux $\vec{S}$ is defined through

$$\partial f/\partial t = -(\partial/\partial\vec{v}) \cdot \vec{S} \quad . \tag{2.34}$$

In the steady-state $\vec{S}$ is divergence-free and may be expressed as the curl of a stream function, i.e.,

$$\vec{S}(\vec{v}) = \vec{\nabla} \times \left[\frac{A(v_\parallel, v_\perp)}{2\pi v \sin\theta}\,\hat{\phi}\right] \quad , \tag{2.35}$$

where in the cylindrical coordinate system ($v_\parallel$, $v_\perp$, ϕ), ϕ is the azimuthal coordinate and $\cos\theta = v_\parallel/v$. Contours of A represent streamlines of $\vec{S}$, projected onto the $v_\parallel - v_\perp$ plane; the difference between the values of A on

two contours equals the flux flowing between those contours. For the case of Fig. 2.5, i.e., $w_1 = 3$ and $w_2 = 5$, the flux plot (from Karney and Fisch, 1979) is shown in Fig. 2.6.

A second numerical technique in analyzing rf-driven currents is to simulate directly many particles (Abe, 1984; Decyk, 1985; Decyk and Abe, 1986). Such particle simulations are not yet advanced enough, however, to uncover new phenomena, and researchers are, in the present developmental state of the art, content merely with exhibiting in the simulation what is perceived by other techniques to be the relevant dynamics.

I. Adjoint Techniques

Adjoint techniques for solving the Fokker-Planck equation were employed in the problem of neoclassical transport theory (Robinson and Bernstein, 1962; Grad, 1963; Rosenbluth, Hazeltine and Hinton, 1972: Ware, 1973; Hinton and Hazeltine, 1976) and were first introduced into the problem of steady-state current-drive by Hirshman (1980). Hirshman (1980) and Taguchi (1982) studied adjoint equations for neutral-beam-driven currents. The technique was presented particularly clearly by Antonsen and Chu (1982), who formulated the problem of current-drive with fast electrons in toroidal geometry. Taguchi (1983) considered the same problem, and demonstrated agreement with a calculation by Cordey et al. (1982). Antonsen and Yoshioka (1986) generalized the method to calculate rf-induced radial transport.

The advantage of the adjoint technique is its directness. One recognizes at the outset the linearity of the governing equations and solves them by Green's function techniques. Researchers using this technique also identified new problems of interest. Pursuing this technique, and including a small electric field, Fisch (1985) found the so-called "hot conductivity," the enhanced conductivity of a plasma due to its contact with an outside source of heat. Ehst (1985) formulates plasma equilibria. A relativistic adjoint equation was written by Karney and Fisch (1985).

The method was further generalized by Fisch (1986), who wrote down an adjoint equation suitable for dynamic ($\partial/\partial t \neq 0$) problems with possibly large electric fields. Also in this work, quantities of interest such as the rf-induced runaway rate, in addition to the current, were identified and shown to be amenable to calculation by adjoint techniques.

Key response functions were calculated numerically by Karney and Fisch (1986), and were put into a form that allowed both easy comparison with experiments and easy implementation in transport codes describing more completely the plasma. In this work, also shown was the equivalence of the adjoint technique to the physically transparent, but more cumbersome, Langevin approach.

The idea behind the adjoint techniques is to separate out the wave-induced flux as though it were a known quantity. Thus, one writes the Boltzmann equation in the form

$$\left(\frac{\partial}{\partial t} + M\right) f = -\frac{\partial}{\partial \vec{v}} \cdot \vec{S}_w \quad , \tag{2.36a}$$

where M is a linear operator that depends on the particular approximation to the collision operation that we employ. Associated with Eq. (2.36a) is a Green's function g, which solves

$$\left(\frac{\partial}{\partial t} + M\right) g(\vec{v},t;v') = 0 \quad , \tag{2.36b}$$

with initial condition $g(\vec{v},t;v') = \delta(v - v')$. Then f is found by

$$f = \int_0^t d\tau \int d^3v' \, \vec{S}_w(\vec{v}',\tau) \cdot \frac{\partial}{\partial \vec{v}'} g(\vec{v}, t-\tau; v') \quad , \tag{2.37}$$

and moments of f may be obtained from moments of g.

The advantage here, of course, is that Eq.(2.36b) need not be solved separately for each excitation $\vec{S}_w$. The method is useful only when $\vec{S}_w$ can be reasonably surmised or hypothesized.

The Green's function g has the following physical interpretation (Karney and Fisch, 1986). Suppose an electron is observed to travel with velocity v' at time t = 0. Then $g(v,t;v')d^3v$ is the probability, conditional on the observation at t = 0, that the velocity of that electron is located at time t in the velocity space element d^3v centered at $\vec{v}$. Thus, the Green's function g in Eq. (2.37) can be determined by following the Langevin equations for an ensemble of electrons, as shown by Karney and Fisch (1986). This, in fact, was the approach first taken in numerically finding the Green's function for conversion of wave energy to magnetic energy (Fisch and Karney, 1985). The

adjoint approach we now describe is equivalent, but computationally more easily achieved than this Langevin, or Monte Carlo, approach.

Following Fisch (1986), consider the two linear operators L and D_t, where D is parameterized by subscript t,

$$L\phi(\vec{v},t') \equiv \frac{\partial}{\partial t'} f_m\phi + \frac{eE(t')}{m} \frac{\partial}{\partial v_\parallel} f_m\phi - C(f_m\phi) \tag{2.38}$$

$$D_t\psi(\vec{v},t') \equiv f_m \frac{\partial}{\partial t'} \psi - \frac{eE(t-t')}{m} f_m \frac{\partial}{\partial v_\parallel} \psi - C(f_m\psi) \quad . \tag{2.39}$$

Define a commutative operation on two functions $\phi(\vec{v},t')$ and $\psi(\vec{v},t')$ by

$$[\phi,\psi]_t \equiv \int_V d^3v \int_0^t \phi(\vec{v},t-\tau)\, \psi(\vec{v},\tau)d\tau \quad , \tag{2.40}$$

where V is a possibly finite velocity space domain, and where the operation [ ] is parameterized by t. It can then be shown that for operands ϕ and ψ obeying homogeneous boundary and initial conditions, the operator D_t is adjoint to the operator L with respect to the inner product $[\ ]_t$, i.e.,

$$(\phi,D_t\psi)_t = (L\phi,\psi)_t \quad , \tag{2.41}$$

where, in writing Eq.(2.41), we made use of the self-adjoint property of the collision operator in the event of homogeneous boundary conditions, or, equivalently, in the limit $V \to \infty$. Actually, for problems of interest to us, especially in the presence of a nonzero dc electric field or for problems to be solved numerically in a finite domain, the boundary terms are significant. Therefore, we employ a more general property for the collision operator

$$\int_V [\phi C(f_m\psi) - \psi C(f_m\phi)]d^3v = -\int_\Sigma [\phi\vec{S}_c(f_m\psi) - \psi\vec{S}_c(f_m\phi)]\cdot d\vec{a} \quad , \tag{2.42}$$

where Σ is the bounding surface in velocity space to the domain V and $\vec{S}_c$ is defined by $C = -(\partial/\partial\vec{v})\cdot\vec{S}_c$. For $V \to \infty$, the surface terms vanish, and the well-known property of the collision operator results. For our needs here, however, we keep the boundary terms.

Consider functions ϕ and ψ which are orthogonal both to f_m and to εf_m over the finite velocity domain V, e.g., for ψ we have

$$\int_V d^3v\, f_m\, \psi(\vec{v},t) = \int_V d^3v\, \varepsilon f_m\, \psi(\vec{v},t) = 0 \quad . \tag{2.43}$$

Suppose, further, that ψ obeys the evolution equation

$$D_t\psi(\vec{v},t') = q_1 f_m + q_2 \varepsilon f_m \quad , \tag{2.44}$$

where the constants (of $\vec{v}$) $q_1(t')$ and $q_2(t')$ are chosen to assure that the orthogonality conditions on ψ are obeyed subsequently given that they are obeyed initially. These constants are independent of $\vec{v}$, but are linear functionals of ψ, obtained by taking the appropriate moments of Eq. (2.44). Initial and boundary conditions on ψ must be specified; we take

$$\psi(\vec{v},t' = 0) = \psi_o(\vec{v}) \tag{2.45a}$$

$$\vec{S}(\psi) = \vec{S}_b(\vec{v},t') \text{ on } \Sigma \quad , \tag{2.45b}$$

where $\vec{S}$ is the total flux, i.e.,

$$\vec{S}(\psi) \equiv \vec{S}_c(\psi) - \frac{eE(t-t')}{m} f_m \hat{i}_{\parallel} \quad , \tag{2.46}$$

where ψ_o and $\vec{S}_b$ are arbitrary functions to be chosen, as we shall see, to give us the Green's functions that we seek.

The linearized, dynamic, spatially homogeneous Boltzmann equation may be written as

$$L\phi = -\frac{eE(t)}{m}\frac{\partial}{\partial v_{\parallel}} f_m + \left(\frac{\varepsilon}{T} - \frac{3}{2}\right)\frac{\dot{T}}{T} f_m - \frac{\partial}{\partial \vec{v}} \cdot \vec{S}_w \quad , \tag{2.47}$$

where $\dot{T}/T$ is chosen to assure that ϕ remain orthogonal to εf_m in the finite domain V given that the orthogonality holds initially. Additionally, ϕ is orthogonal to f_m because there are no particle sources in Eq. (2.47). Taking the indicated inner product of ϕ and $D_t\psi$, and using the orthogonality properties, one finds

$$\int_V d^3v\, f_m\, \phi(\vec{v},t)\psi_o(\vec{v}) + \int_o^t d\tau\, \phi(\vec{v},t)\vec{S}_B(\vec{v},t-\tau)\cdot d\vec{a}$$

$$= \int_V d^3v \int_o^t d\tau\, \vec{S}_*(\vec{v},t-\tau)\cdot \frac{\partial}{\partial \vec{v}}\, \psi(\vec{v},\tau) + \int_o^t d\tau \int_\Sigma \psi(\vec{v},t-\tau)[\vec{S}(\phi)+\vec{S}_w]\cdot d\vec{a}\ , \quad (2.48)$$

where

$$\vec{S}_*(\vec{v},t) = \vec{S}_w(\vec{v},t) + \frac{eE(t)}{m}\, f_m\, \hat{i}_\parallel \quad (2.49)$$

is the sum of the wave-induced flux $\vec{S}_w$ and the flux induced by the dc electric field accelerating the background Maxwellian electron distribution. This last flux leads to the ohmic current and to the runaway electron current.

By choosing $\psi_o(\vec{v})$ and $\vec{S}_B(\vec{v},t)$, it is possible to construct Green's functions for either arbitrary moments of f or arbitrary functions of f on the boundary. For example, to find the current, we choose $\psi_o(\vec{v}) = v_\parallel$ and $\vec{S}_B = 0$ in solving Eq. (2.44) for the Green's function ψ. Once ψ is determined, then, of course, the right-hand side of Eq. (2.48) gives the contribution to the current in the domain V for arbitrary wave excitation $\vec{S}_w$. The problem now is to recognize interesting quantities for which we would want these Green's functions.

J. Response Functions

Using Eq. (2.48), various Green's functions, or response functions, may be calculated. Here we consider several important examples.

First, we calculate the rf-induced runaway rate in the presence of a dc constant electric field. Let us cast the relatively old question of runaway production (Dreicer, 1960; Bernstein and Kruskal, 1962; Kulsrud et al. 1972) in conceptually new terms. Rather than calculate directly runaway rates from solutions to the evolution equation for f (see e.g., Chan and McClain, 1983), we follow Fisch and Karney (1985) and associate a runaway probability $R(\vec{v})$ with electrons of velocity $\vec{v}$. The question of runaway production is then cast as an incremental problem: how does an rf-induced flux affect incrementally the number of runaways? Again, the linearity of the equations means that this question is sensible so long as the rf-induced flux can be determined or reasonably surmised. The runaway probability function $R(\vec{v})$ then captures the necessary response information.

Suppose that the velocity domain boundary Σ is placed at sufficiently high velocity that collisional effects are negligible so that any electron appearing on Σ may be safely defined as a runaway, i.e., $R(\vec{v}) = 1$, for $\vec{v}$ on Σ. The number of runaway electrons appearing on Σ between time $\tau = 0$ and time $\tau = t$ may be written as

$$N_R(t) = \int_0^t d\tau \int_\Sigma \vec{S} \cdot d\vec{a} \quad , \tag{2.50}$$

where, in the high-velocity limit which by assumption is valid on Σ, we have

$$\vec{S} \simeq \left(\frac{eE}{m}\hat{i}_\parallel - \frac{\Gamma\vec{v}}{v^3}\right)\phi\, f_m \quad , \tag{2.51}$$

where $\Gamma\vec{v}/v^3$, just as in the Langevin equations, represents the dynamic friction due to collisions. Thus, solving Eq. (2.44) for ψ with conditions

$$\psi(\vec{v}, t = 0) = 0 \tag{2.52}$$

$$\vec{S}(\vec{v}, t - t') = \frac{eE}{m}\hat{i}_\parallel - \frac{\Gamma\vec{v}}{v^3} \quad , \qquad \text{on } \Sigma \tag{2.52b}$$

and then substituting into Eq. (2.48), gives

$$N_R = \int_V d^3v \int_0^t d\tau\, \vec{S}_*(\vec{v}, t - \tau) \cdot \frac{\partial}{\partial\vec{v}}\, \psi(\vec{v}, t), \tag{2.53}$$

where, had we written $\vec{S}_w$ above rather than $\vec{S}_*$, we would have included only the rf-induced contribution to the runaway number.

Note that $\psi(\vec{v}, t)$ may be interpreted as the probability with which an electron appears on the boundary Σ by time t given that it had velocity $\vec{v}$ at time τ. In the presence of finite temperature, all electrons eventually run away, i.e., appear on the boundary Σ. A useful definition is to consider as runaway electrons only those that appear on Σ without first becoming bulk electrons, i.e., without first having speed $v < v_T$. Bulk electrons also appear on Σ, but only after spending considerable time dominated by collisions with other electrons and ions; the time for bulk electrons to run away will be exponential in $(v_R/v_T)^2$, where v_R, defined later in Eq. (2.56), is the runaway velocity (the velocity at which collisional drag equals the field force). Typically, $v_R >> v_T$, and the time scale for bulk runaway is long compared to other times of interest, such as the particle confinement time.

To distinguish runaways originating in the bulk from what we have defined now as true runaways, one can tabulate N_R only for times short compared to the bulk runaway time. Alternatively, one could introduce into the electron evolution model a particle sink or an artificially large collision frequency near $v \to 0$, thus preventing bulk electrons from running away at all. This, in fact, occurs when using the high-velocity limit of the collision integral. Then the probability of an electron running away in the sense that we define here may be written as

$$R(\vec{v}) = \psi(\vec{v}, t \to \infty) \quad . \tag{2.54}$$

The operator adjoint to the strict ($v_T \to 0$) high-velocity limit Coulomb collision operator C_H, defined by Eq. (2.13) with $v_T \to 0$, may be written as

$$C_H^*(f_m\psi) = \frac{f_m \Gamma}{v^3}\left[-v\frac{\partial}{\partial v} + (1+Z)\frac{\partial}{\partial \mu}(1-\mu^2)\frac{\partial}{\partial \mu}\right] \quad . \tag{2.55}$$

The operator C_H^* may be substituted for C in Eq. (2.39) in order to get the high-velocity limit adjoint operator. Karney and Fisch (1986) solved numerically the high-velocity limit adjoint equation, i.e., by using C_H in Eq. (2.39) and solving $D_t\psi = 0$, with initial and boundary conditions given by Eqs. (2.52). Note, however, that employing the collision operator of Eq. (2.55) reduces the equation from elliptic to parabolic; hence, boundary conditions are imposed only where the total flux $\vec{S}$ points into the domain V. A convenient normalization in this work is $\vec{u} = \vec{v}/v_R$, where

$$v_R \equiv -\text{sign}(qE)\left(\frac{m\Gamma}{|qE|}\right)^{1/2} \quad , \tag{2.56}$$

where the magnitude of the runaway velocity v_R is the speed at which the collisional dynamic frictional force (for electrons with $v_\perp = 0$) equals the acceleration due to the electric field. The more familiar Dreicer velocity (Dreicer, 1960) is given by $-(2+Z)^{1/2}\, v_R$. The convention here is that where electrons run away to the right, v_R is negative. The result for the response function $R(\vec{v}/v_R)$ is reproduced in Fig. 2.7.

Note that for $|\vec{v}/v_R| < 1$, R vanishes, indicating that frictional retarding forces are larger than the electrical forces that accelerate the runaways. In Fig. 2.7, the force of the electric field carries electrons to

the left, so the runaway probability of left-going electrons tends to be greater than the runaway probability of right-going electrons. Note, however, the finite probability of right-going electrons; this is the "backward" runaway probability, a quantity that is not available in a 1-D formulation of the problem.

The runaway probability R is a distinguishing property of electrons. It is often helpful to use such a property to distinguish the contributions of distinct groups of electrons to a given effect. It would then be possible to see at a glance what the effect might be, for example, if one group, such as the runaways, were not confined.

For example, it is possible to write the current density as

$$J = J_R + J_S \quad , \tag{2.57}$$

where J_R is the runaway electron contribution to the current and J_S is the contribution of stopped electrons, i.e., electrons that do not run away in the sense that we defined here. Having the runaway probability function $R(\vec{v})$ now allows us to write

$$J_S(t) = \int_V d^3v \; f_m \phi(\vec{v},t) \left[v_\parallel \left(1 - R(\vec{v})\right) + C_1 + \varepsilon C_2 \right] \quad , \tag{2.58}$$

where C_1 and C_2 are constants to be determined, but, in view of the orthogonality properties of ϕ, the terms multiplied by these constants do not affect directly the current J_S. By inspection of Eq. (2.58), it is readily apparent that ψ_S, the appropriate Green's function for J_S, solves Eq. (2.44) with

$$\hat{S}(\psi_S) = 0 \quad , \text{ on } \Sigma \tag{2.59a}$$

$$\psi_S(\vec{v}, t = 0) = v_\parallel \left[1 - R(\vec{v})\right] + C_1 + \varepsilon C_2 \quad , \tag{2.59b}$$

where we now exploit our freedom to choose C_1 and C_2 to do so in a way that gives the required orthogonality properties for $\psi_S(\vec{v}, t = 0)$. The subsequent orthogonality properties of $\psi_S(\vec{v}, t > 0)$ is, of course, guaranteed by choosing appropriate constants q_1 and q_2 in Eq. (2.44). Solving then for ψ_S, we determine the wave-induced contribution to the current carried by stopped electrons,

$$J_s = -[\psi_s, (\partial/\partial\vec{v}) \cdot \vec{\mathbb{S}}_w] \quad . \tag{2.60}$$

As an electron decelerates, it contributes part of its kinetic energy to the bulk electrons with which it collides, and the remainder of its kinetic energy it contributes to the electromagnetic field that decelerates it. The latter energy contribution appears as magnetic energy storage, while the former contribution appears merely as heat. The problem of current "ramp-up" refers to using current-drive to increase the toroidal current and thereby to increase the inductive energy stored in the poloidal magnetic fields (i.e., $LI^2/2$, where L is the tokamak inductance and I is the toroidal current). For current ramp-up, an important efficiency criterion is the fraction of rf energy that is converted to magnetic field energy. This fraction will depend on the nature of the wave-induced flux $\vec{\mathbb{S}}_w$.

The power (electric) delivered to the field by a stopped electron may be written as $P_{el} = Ej_s(\vec{v},t)$, where $j_s(\vec{v},t)$ is the expected current as a function of time carried by a single electron, given that the electron is located at coordinate $\vec{v}$ at time $t = 0$, e.g., as sketched in Fig. 7b. The electron decelerates from velocity $\vec{v}$ to some bulk speed with eventually no directed motion. The amount of energy that flows into the electromagnetic field during this decleration is

$$W_s(\vec{v}) = \int_0^\infty Ej_s(\vec{v},t)\, dt \quad . \tag{2.61}$$

The quantity $W_s(\vec{v})$ is an important response function that characterizes the ramp-up process. In particular, what matters is the ratio of the incremental energy that flows into the field to the incremental energy injected into an electron using waves. We can write this efficiency as

$$\frac{P_{el}}{P_{in}} = \frac{\vec{\mathbb{S}}_w \cdot (\partial/\partial\vec{v}) W_s(\vec{v})}{\vec{\mathbb{S}}_w \cdot (\partial/\partial\vec{v}) \varepsilon(\vec{v})} \quad , \tag{2.62}$$

where the numerator is proportional to incremental energy to the field, and the denominator is proportional to the incremental energy expended. The variables P_{el} and P_{in} are defined to have dimensions of power density; P_{in} is the wave power absorbed by resonant electrons and P_{el} is the power delivered to the magnetic field.

In Fig. 2.8, we reproduce a plot of the response function $W_s(\vec{v}/v_R)$. For v/v_R small, collisions, rather than the electric field, tend to slow down the electron, and the electron kinetic energy will be converted into heat. Thus, $W_s \to 0$, for $v/v_R \ll 1$, and, consistently, $P_{el}/P_{in} \to 0$. On the other hand, for $v/v_R \gg 1$, the electron is decelerated by the electric field and is insensitive to collisions so that all of its parallel kinetic energy could be converted to magnetic field energy. Thus, for $v/v_R \gg 1$, we have $W_s \to mv_\parallel^2/2$ and if also $v_\perp \ll v_\parallel$, then $P_{el}/P_{in} \to 1$. The calculation here is applicable only for stopped electrons, which eventually slow down to $v_\parallel = 0$, but do not then run away in the negative-$v_\parallel$ direction. Such electrons are runaways and their kinetic energy would increase indefinitely at the expense of field energy.

Most relevant to ramp-up experiments is when electrons with high $v_\parallel$, but $v_\perp \ll v_\parallel$, are resonant either with lower-hybrid or with electron-cyclotron waves. The power conversion efficiencies that may be expected are reproduced in Fig. 2.9. These results will be compared to experiments in Chapter 4.

K. RF-Induced Conductivity

Analytic solutions to the adjoint equations can often be found with surprising ease. The problem of current-drive in the presence of a small dc electric field has been approached using various approximations by several researchers (Muschietti et al., 1982; An et al., 1983; Appert et al., 1983; Start, 1983). Here, we show an analytic calculation of the so-called "hot conductivity," the conductivity in the presence of a small ($E \to 0$) electric field, but in the presence of rf-induced fluxes (Fisch, 1985). Since $E \to 0$, we have $R(\vec{v}) \to 0$ for all $\vec{v}$, and hence $J \to J_s$. Thus, we may take the boundary Σ in the adjoint equation at $v \to \infty$ and apply a homogeneous boundary condition. For the initial condition we take $\psi = qv_\parallel$. Since we are not interested in transient effects, it is only necessary to calculate

$$\chi(\vec{v}) = \int_0^\infty dt\, \psi(\vec{v},t) \quad , \tag{2.63}$$

where χ solves

$$f_m \frac{eE}{m} \frac{\partial}{\partial v_\parallel} \chi + C(f_m\chi) = - f_m\, qv\mu \quad . \tag{2.64}$$

Taking the high-velocity limit form of C from Eq. (2.13), and expanding

$$x = x_0 + Ex_1 + E^2 x_2 + \cdots \quad , \tag{2.65}$$

we get to lowest order

$$\frac{\Gamma}{v^2}\left[\frac{v_T^2}{v}\frac{\partial^2}{\partial v^2} - \left(1 + \frac{v_T^2}{v^2}\right)\frac{\partial}{\partial v} + \frac{(1+Z)-v_T^2/v^2}{2v}\frac{\partial}{\partial \mu}\left(1-\mu^2\right)\frac{\partial}{\partial \mu}\right]x_0 = -q v \mu \quad , \tag{2.66}$$

from which we may solve asymptotically in v_T/v

$$x_0 = \frac{1}{\Gamma}\frac{\mu v^4}{(5+Z)}\left[1 + \frac{9}{3+Z}\left(\frac{v_T}{v}\right)^2 + \frac{9}{(3+Z)(1+Z)}\left(\frac{v_T}{v}\right)^4 + \ldots\right] \quad . \tag{2.67}$$

The first order equation then becomes

$$C(f_m x_1) = -f_m \frac{eE}{m}\left(\mu \frac{\partial}{\partial v} + \frac{1-\mu^2}{v}\frac{\partial}{\partial v}\right)x_0 \tag{2.68}$$

with solution

$$x_1 = \frac{1}{3\Gamma}\frac{e}{m}\frac{v^6}{5+Z}\left[1 + \frac{3\mu^2-1}{3+Z} + O\left(\frac{v_T}{v}\right)^2\right] \quad . \tag{2.69}$$

For a narrow spectrum of waves, one can now write

$$\frac{J}{P_d} = \frac{\hat{S}_w \cdot \partial x/\partial \vec{v}}{\hat{S}_w \cdot \partial \varepsilon/\partial \vec{v}} \quad , \tag{2.70}$$

where in the limit $E \to 0$, the leading term of x_0 gives the Fisch-Boozer (1980) result, Eq. (2.25), for steady-state current-drive efficiency. To express the rf-induced conductivity, we can expand

$$J = J_{rf} + \sigma E + O(E^2) \tag{2.71}$$

with J_{rf} representing the current proportional to x_0 (the steady-state contribution) and with

$$\sigma = \sigma_{sp} + \sigma_H(P_d) \quad , \tag{2.72}$$

where σ_{sp} is the Spitzer-Härm conductivity and σ_H is the so-called hot-conductivity that is rf-induced. Using Eq. (2.69) and an expression for P_d, we can write σ_H in the form

$$\sigma_H = P_d \frac{\vec{S}_w \cdot \partial \chi_1 / \partial \vec{v}}{\vec{S}_w \cdot \partial \varepsilon / \partial \vec{v}} \quad . \tag{2.73}$$

Thus, the rf-induced conductivity is linear in the absorbed power and strongly dependent on the spectrum location.

This approach has been pursued by Dnestrovskij et al. (1985) and by Krasheninnikov et al. (1985) who have worked out a number of interesting and practical cases. (A point of confusion: these works purport that a low-order term has been omitted in Eq. (2.69). No term is missing, but were the hot conductivity written, e.g., as a function of total power absorbed rather than rf power absorbed, then it would appear as if new terms were introduced.)

Note that finding the rf-induced conductivity, σ_H, analytically is an easier task than finding the Spitzer-Harm conductivity analytically. This is because in describing bulk plasma processes, the collision operator may not be simplified by taking in the high-velocity limit. The limit is correctly used here, however, so long as $\vec{S}_w$ is finite only for $v >> v_T$. Then the affected electrons spend much more time at high velocity, than at low velocity, before becoming randomized.

The limit $E \to 0$ is thought to be relevant particularly for start-up in a reactor. For example, in the Starfire reactor design (Abdou et al., 1982), approximately 20 minutes were required to ramp up the toroidal current. In recent experiments, however, the approximation $E \to 0$ is not valid, and a numerical solution of the adjoint equation is necessary (see Sec. IV.D).

The hot conductivity, σ_H, is valid for plasmas not in thermal equilibrium, but instead in contact with an external source or sink of heat. The contact is made through the emission or absorption of waves by fast electrons. Note that in the case of a radiating plasma, P_d and σ_H are then negative, and the hot-conductivity contribution indicates a higher resistivity.

L. Relativistic Effects

The steady-state current-drive efficiency using fast electrons is proportional to v^2 until the resonant electron velocity v becomes comparable to the speed of light c. It turns out that the maximum possible current-drive efficiency is bounded -- the maximum efficiency is attained as $v \to c$ when using lower-hybrid waves, while when using electron-cyclotron waves the maximum efficiency occurs at a somewhat slower speed. (Note: here, as elsewhere, we use electron-cyclotron waves to exemplify diffusion of electrons purely in perpendicular energy, neglecting the parallel component, which is usually unimportant. A notable exception is discussed in Sec. III.D)

The limitation in the current-drive efficiency occurs because relativistic electrons, being heavier, more easily lose energy in collisions with the lighter background electrons. Additionally, pushing relativistic electrons in the parallel direction does not immediately create current, as the current carried reaches a maximum. Each of these effects reduces the efficiency by a factor of p, where p is the electron momentum; hence, the efficiency approaches a constant of p as $p \to \infty$ for lower-hybrid current-drive. Moreover, the injection of momentum, as opposed to merely selectively increasing the perpendicular energy, is now critical. Increasing the perpendicular energy of a relativistic electron without tampering with its parallel momentum results instantaneously in that electron carrying less current, since to conserve momentum, the parallel velocity must decrease when the electron becomes heavier. Thus, for electron-cyclotron waves, this further effect implies that $J/P_d \to 0$ as $p \to \infty$.

To find the current-drive efficiency for relativistic resonant electrons, either the Langevin method or the adjoint method may be used. Fisch (1981) solved the relativistic Langevin equations and wrote the efficiency in closed form for the case of zero background temperature. Since relativistic electrons are fast compared to thermal electrons for temperatures of interest in first generation fusion reactors, this result is generally applicable. Here, however, we summarize the more accurate adjoint analysis of Karney and Fisch (1985), who included finite temperature effects and solved numerically the relativistic adjoint equation. These effects tend to increase the current-drive efficiency, as bulk electrons get dragged by resonant electrons. The efficiency increase can be about 10-25% for parameters of interest (see Fig. 2.10).

Define momentum p such that $\vec{v} = \vec{p}/m\gamma(p)$, where m is the electron rest mass and $\gamma(p) = (1+p^2/m^2c^2)^{1/2}$. The steady-state current and power dissipated may now be written as

$$J = \int \vec{S}_p \cdot \frac{\partial}{\partial \vec{p}} \chi(p)\, d^3p \tag{2.74a}$$

$$P_d = \int \vec{S}_p \cdot \frac{\partial}{\partial \vec{p}} \varepsilon(p)\, d^3p \ , \tag{2.74b}$$

where $\vec{S}_p$ is the wave-induced flux in momentum space, kinetic energy ε may be written as $(\gamma-1)mc^2$, and χ solves the relativistic adjoint equation

$$C(f_m\chi) = - q\, v_\parallel f_m \ , \tag{2.75}$$

which is a generalization of Eq. (2.64) for E = 0. Expand χ in a Legendre series, i.e.,

$$\chi = \sum_0^\infty P_n(\mu)\, \chi_n(p) \ . \tag{2.76}$$

Evidently, from Eq. (2.75), we see that the solution consists of only the first Legendre harmonic; accordingly, we set $\chi(\vec{p}) = u\chi_1(p)$. Substituting into Eq. (2.75), Karney and Fisch (1985) derive the equation for χ_1

$$\frac{1}{p^2}\frac{\partial}{\partial p} p^2 A(p) \frac{\partial \chi_1}{\partial p} - \frac{vA(p)}{T}\frac{\partial \chi_1}{\partial p} - \frac{2B(p) + \Gamma Z/v}{p^2}\chi_1 + I(\chi_1) + qv = 0 \ , \tag{2.77}$$

where

$$A(p) = \frac{4\pi\Gamma}{3n}\left[\int_0^p p'^2 f_m(p')\frac{v'^2}{v^3}\,dp' + \int_p^\infty p'^2 f_m(p')\frac{1}{v'}\,dp'\right] \tag{2.78a}$$

$$B(p) = \frac{4\pi\Gamma}{3n}\left[\int_0^p p'^2 f_m(p')\frac{3v^2-v'^2}{2v^3}\,dp' + \int_p^\infty p'^2 f_m(p')\frac{1}{v'}\,dp'\right] \tag{2.78b}$$

$$I(\chi_1) = \frac{4\pi\Gamma}{n}\left\{\frac{mf_m(p)\chi_1(p)}{\gamma}\right.$$

$$\left. + \frac{1}{5}\int_0^p p'^2 f_m(p')\chi_1(p')\frac{m}{T}\left[\frac{\gamma}{p^2}\frac{v'}{\gamma'^3}\left(\frac{T}{mc^2}(4\gamma'^2+6) - \frac{1}{3}(4\gamma'^3-9\gamma')\right)\right.\right.$$

$$+ \frac{\gamma^2}{p^2}\frac{v'}{\gamma'^3}\left[\frac{mv'^2}{T}\gamma'^3 - \frac{1}{3}(4\gamma'^2+6)\right]\Big] dp'$$

$$+ \frac{1}{5}\int_p^\infty p'^2 f_m(p')\chi_1(p')\frac{m}{T}\left[\frac{\gamma'}{p'^2}\frac{v}{\gamma^3}\left(\frac{T}{mc^2}(4\gamma^2+6) - \frac{1}{3}(4\gamma^3 - 9\gamma)\right)\right.$$

$$\left. + \frac{\gamma'^2}{p'^2}\frac{v}{\gamma^3}\left[\frac{mv^2}{T}\gamma^3 - \frac{1}{3}(4\gamma^2+6)\right]\right]dp'\Big\} \quad , \tag{2.78c}$$

where f_m is the relativistic Maxwellian (see, e.g., de Groot et al., 1980) that solves $C(f,f) = 0$ and is given by

$$f_m(p) = \frac{n}{4\pi m^2 cTK_2(\theta^{-1})}\exp(-\epsilon/T) \tag{2.79}$$

where

$$\epsilon \equiv mc^2\gamma \tag{2.80a}$$

$$\theta \equiv T/mc^2 \tag{2.80b}$$

and K_n is the nth-order modified Bessel function of the second kind. (Recently, a complete treatment of the collision operator is provided by Franz, 1986.)

Equation (2.77) has been considered nonrelativistically by a number of authors. Approximate analytical solutions are possible when χ is expressed as a sum of Sonine polynomials (Chapman and Cowling, 1970; Braginskii, 1965). Alternatively, variational approaches may be useful (Hirshman, 1980). Such solutions, however, may be employed only when the current is expected to be carried primarily by the bulk electrons. When the driving fluxes occur primarily at superthermal velocities, such as when driven by lower-hybrid waves but not by neutral beams, the asymptotic ($p \to \infty$) form of χ_1, which may not be reproduced accurately by these expansions, is critical. Numerical integrations of the nonrelativistic limit of these equations have been performed for the case of ohmic currents (Spitzer and Härm, 1953) and for applications to a number of other problems (Cordey et al., 1979).

In the limit of cold background electrons ($\theta \to 0$), Eq. (2.77) becomes particularly simple, i.e.,

$$-\frac{1}{v^2}\frac{\partial \chi_1}{\partial p} - \frac{1+Z}{vp^2}\chi_1 + \nu = 0 \quad , \tag{2.81}$$

with solution

$$\chi_1(\theta=0) = \left(\frac{\gamma+1}{\gamma-1}\right)^{(1+Z)/2} \int_0^p \left(\frac{\gamma'-1}{\gamma'+1}\right)^{(1+Z)/2} \nu' {}^3 dp' \quad , \tag{2.82}$$

which is the result derivable from the relativistic Langevin equations (Fisch, 1981). Now using $\chi_1(\theta=0)$ in Eqs. (2.74) reveals that there is indeed a limit to the current-drive efficiency both for lower-hybrid or electron-cyclotron wave current-drive. For a narrow spectrum of waves, we have

$$\frac{J}{P_d} = \frac{\hat{S}_p \cdot \partial[\chi_1(\theta=0,\mu)]/\partial \vec{p}}{\hat{S}_p \cdot \vec{v}} \quad . \tag{2.83}$$

To find the effects of finite temperature, it is necessary to solve Eq. (2.77) numerically. The numerical technique employed by Karney and Fisch (1985) was to cast Eq. (2.77) as a 1-D diffusion equation for χ_1, and then to look for the steady-state solution. The solution for χ is reproduced in contour plots given in Fig. 2.10. Here $p_t \equiv \sqrt{mT}$. The figures show how relativistic effects enter: in (a) we have the nonrelativistic treatment which is valid whenever $c >> v$ (or, equivalently, $\theta \to 0$); were that inequality to be challenged, say in a 5 keV plasma ($\theta = 0.01$) and resonant electrons with $p_\parallel/p_t \sim 5$, then the contours are stretched, as may be observed in (b), indicating less current for a given induced flux.

Most important is the question of the efficiency; this is reproduced in Fig. 2.11. (The reader should be cautioned that the energy scale at the top of the figure is only approximately linear at high energy.) The line labeled $\theta = 0$ corresponds to the zero temperature result given in Eq. (2.82). The somewhat greater efficiencies available at finite temperatures are primarily the result of resonant electrons dragging on thermal electrons. When the thermal electrons are slow, their directed momentum is quickly randomized in collisions with ions. A quick calculation of the drag effect is possible by balancing the momentum input to the drifting bulk background electrons carrying current J_B, i.e., if the resonant electrons carry current J_R, then

$$\frac{dJ_R}{dt} = -\nu^{B/i} J_B + \gamma \nu^{R/B} J_R \quad . \tag{2.84}$$

where $\nu^{B/i}$ is the collision frequency of the bulk electrons with the background ions and $\nu^{R/B}$ is the collision frequency of the resonant electrons with the bulk electrons. The steady-state drift current can then be found. The calculation is approximate because the ν's must be guessed at, but it gives roughly a 10% enhancement effect.

In Fig. 2.11, the localized excitation corresponds to a wave-induced flux at finite $p_\parallel$ but at $p_\perp = 0$. This is useful for comparing to theoretical formulas. Of more practical use is to show the efficiency as a function of the total flux induced by a lower-hybrid wave, summing over contributions to the flux at finite $p_\perp$ for the case of a narrow spectrum of waves absorbed by a Maxwellian distribution of electrons. This is depicted in Fig. 2.12. Including summation of the wave-induced fluxes (as compared to including only the contribution at $p_\perp = 0$) produces no effect for $v_\parallel >> v_T$, but results in a somewhat larger efficiency for $v_\parallel = v_T$. It is perhaps worth correcting here a misleading, but oft-cited, result in the review by Cordey (1984), who finds an efficiency $I/P = 0.15/(R_1 n_{1\parallel})$ A/W in his consideration of lower-hybrid waves driving 100 keV electrons in a 17 keV plasma. This result, based on an erroneous equation given by Hewitt et al. (1984), is too low by a factor of about 5. The correct efficiency is as shown in Fig. 2.12.

Several further remarks ought to be made about relativistic effects: First, the calculations here do not include synchrotron and bremsstrahlung emissions. For relativistic electrons, these effects can be large; in fact, it would be a worthwhile effort to derive response functions for these emissions. Presumably, in the regime where relativistic effects are the largest, these effects will render invalid the analyses offered here. Additionally, relativistic effects play a role in determining which electrons are resonant and what the diffusion path is (Fisch, 1981; Karney and Fisch, 1981). These paths are constant energy contours in the wave frame of reference. Wave propagation in a weakly relativistic plasma is considered by Fidone et al. (1982).

One helpful relativistic effect is that the absorption of the electron-cyclotron wave near the resonant surface $\omega = \Omega_e(x)$ (where x measures horizontal direction) is not symmetric with respect to that surface, so that single pass absorption is not necessary for current-drive (Cairns et al., 1983). The asymmetry is a relativistic effect; nonrelativistically,

absorption would take place equally on both sides of the resonance if the damping were very weak, so that even if after many reflections the wave were absorbed, equal currents would be generated in opposite directions.

To see this, consider that the resonance condition for a weakly relativistic electron may be written as

$$\omega - k_{\parallel} v_{\parallel} - \Omega \, (1 - v^2/2c^2) = 0 \quad , \tag{2.85}$$

where $\Omega = eB(x)/m$ is the nonrelativistic cyclotron frequency. For $v/c \to 0$, note that changing the sign of the quantity $\omega - \Omega$ produces a resonance with $v_{\parallel} \to - v_{\parallel}$, indicating that as x_c is traversed, the resonant region is mirrored about $v_{\parallel} = 0$. However, for v/c finite, a sign change in $\omega - \Omega$ no longer produces $v_{\parallel} \to - v_{\parallel}$, so that the oppositely flowing currents, that are generated on opposite sides of the resonance, need no longer be comparable. Note, however, that single-pass absorption, if not a necessary condition for the current-drive effect, does often mean a higher current generation efficiency.

III. Survey of Current-Drive Methods

A. Introduction

The most detailed experimental and theoretical attention has been paid to current-drive by fast electrons, but the eventual most useful method may well be one of the other techniques. Here we survey more briefly these other ideas, primarily with a view towards demonstrating the variety of possible current-drive effects. Included here, in addition to the neutral beam technique which has been experimentally demonstrated, are techniques that must be considered rather speculative, or at least not experimentally testable on present-day tokamaks.

Several different waves can give rise to essentially the same current-drive effect. Thus, for example, high- phase velocity whistler waves, which have propagation and absorption characteristics different from those of lower-hybrid waves, could be substituted, possibly to advantage, for the lower-hybrid waves. The current-drive effect is the same; more precisely, the current-drive efficiency depends only on the wave parallel phase velocity and

the velocity of resonant electrons. Similarly, the low-phase velocity kinetic Alfvén wave will achieve the current-drive effect (Hasegawa, 1981) characteristic of other low-phase velocity waves. Although here we are concerned more with portraying the different effects possible, rather than in compiling the number of ways each effect can be attained, different ways of attaining a given current-drive effect may be critical in realizing the utility of that effect for different reactor parameters.

The techniques presented here can generally be employed concurrently, possibly to advantage. This is especially true of passive techniques such as reflection, which could supplement, without interfering with, current driven by other means. Other methods are in effect hybrid means, such as injecting a neutral beam and then maintaining its energy with supplementary rf heating.

Some of the more speculative means of current-drive are presented here somewhat in the spirit in which they were probably suggested by the authors in the first place -- to stimulate thought on pursuing new and different avenues for, it is hoped, even more efficient, yet practical, methods of current-drive.

B. Low-Frequency Waves

The advantages and disadvantages of Alfvén waves, an example of low-frequency waves that interact with low-$v_{\parallel}$ electrons, have been remarked upon earlier. Here we consider these waves in greater detail.

In a homogeneous plasma, i.e., with aspect ratio $R/a \to \infty$, there would be no trapped electrons and the steady-state current-drive efficiency would scale as predicted by Wort (1971), i.e., $J/P_d \sim 1/v_{ph}$. This scaling leads to a relatively high efficiency, especially for hot plasmas where the collision frequencies become smaller. Note that hotter plasmas benefit current-drive techniques, such as neutral beam or Alfvén wave injection, that rely on the dynamics of bulk electrons, more than they benefit techniques, such as lower-hybrid or electron-cyclotron wave injection, which rely on the dynamics of fast, superthermal electrons, and are eventually, in hot plasmas, limited in efficiency by relativistic effects. The favorable scaling notwithstanding, the efficiency of current-drive by Alfvén waves is seriously diminished by trapped electron effects for realistic aspect ratios (Bickerton et al., 1972).

It has been conjectured (Fisch and Karney, 1981) that these trapped particle effects might not be as serious as first supposed. The conjecture runs roughly as follows: since the tokamak is axisymmetric, trapped electrons conserve canonical angular momentum. Upon absorbing toroidal mechanical momentum from a wave, they must pinch inwards towards the magnetic axis. This is analogous to the Ware pinch effect (Ware, 1970), where the trapped electrons absorb momentum from an imposed dc toroidal magnetic field rather than from rf waves. The inward pinch is not a steady-state process; eventually electron density gradients steepen near the magnetic axis. At that point, electrons will tend to diffuse outwards, driving the bootstrap current. The conjecture was that this bootstrap current might compensate for the loss of current in the first place. Unfortunately, a closer examination reveals that this rf pinch effect, while it might very well be potent in producing large gradients, does not lead to sufficient compensating current.

Were it not for the trapped electron effects, or, alternatively, near the magnetic axis in a tokamak, the Alfvén wave is an efficient current driver. Solving numerically the Fokker-Planck equation for electrons, Fisch and Karney (1981) calculate the efficiency of current-drive with low-phase-velocity waves and compare this efficiency to that using high-phase-velocity waves such as lower-hybrid waves, as reproduced in Fig. 3.1. The numerical results confirm the scaling predicted by Wort (1971). Cordey et al. (1982) show that for $v_{ph} \ll v_T$, it is possible to neglect electron-electron collisions, and they give an analytic solution agreeing with Fig. 3.1. This figure illustrates how in a homogeneous plasma it is most efficient to push either very fast or very slow electrons.

Despite its unpopularity because of the trapped-electron concern, this wave deserves experimental testing. There are enough uncertainties surrounding the physics of trapped electrons and the neoclassical bootstrap effect to shake our confidence even in the best theoretical models. Because of the high efficiency that might be attained with the readily available low frequency (10-100 MHz) power, it would be worthwhile to risk a probable negative result in testing this current-drive method.

C. Exploiting Trapped Electron and Toroidal Effects

Although the presence of trapped electrons, an artifact of the toroidal geometry, diminishes the efficiency of current-drive by Alfvén waves, these same trapped-electron effects have also been exploited, in some cases, to drive current. Ohkawa (1976) has suggested that selectively trapping or detrapping electrons can result in current. Toroidal effects have also been invoked by Parks and Marcus (1981) and Hayes and DeGroot (1981) to drive currents with electron-cyclotron waves.

Ohkawa's suggestion is illustrated in Fig. 3.2. Perpendicular heating of electrons, possibly by electron-cyclotron waves, can result in Fig. 3.2 in a circulating electron in velocity space location 1 becoming trapped in velocity space location 2. The result would be a deficit of current-carrying circulating electrons traveling to the right. An alternative method to produce a net flux of electrons to the left would be to heat in the parallel direction electrons in velocity space location 3, such that they become detrapped in velocity space location 4. This interaction, which might be accomplished by lower-hybrid waves traveling to the left, produces a surplus of left-traveling circulating electrons.

Parks and Marcus (1981) and Hayes and DeGroot (1981) play on a somewhat different, but related, toroidal effect. Circulating electrons traveling along field lines in tokamak geometry periodically decelerate and accelerate as they pass through the more intense field region near the torus hole. Imagine, then, an equivalent situation in which an electron traverses periodic magnetic mirrors as illustrated in Fig. 3.3. Parks and Marcus (1981) and Hayes and DeGroot (1981) suggest that perpendicular heating of electrons as they pass through the mirror throats (maxima of the parallel magnetic field) will, on average, increase the parallel velocity of these electrons. This occurs because as the electrons leave the mirror throats, their perpendicular energy is converted into parallel energy since each electron's magnetic moment $\mu = mv_\perp^2/2B$ is conserved over its trajectory.

The method of perpendicular heating at the mirror throats is somewhat like the method of lower-hybrid current-drive, in that waves are employed to increase the average parallel velocity of fast electrons. This likeness is more apparent when the change in velocity space coordinates at the mirror throat is related to a change in velocity space coordinates at the field

minima for the same trajectory. We shall expect, therefore, that the efficiency for this current-drive method will scale similarly to that for other methods of pushing fast electrons. Note, however, that electrons that are heated perpendicularly absorb no mechanical angular momentum. In an axisymmetric device, such as a tokamak without field ripple, there can be no exchange of momentum with the coils generating the magnetic field, and hence the canonical angular momentum of the electron is preserved. Therefore, in addition to increasing on average its $v_\parallel$ because of the heating at the magnetic throat, the electron will also increase, on average, its (radial) distance from the magnetic axis.

The equations for current-drive by rf-heating of electrons in toroidal geometry, where the effects of trapped electrons come into play, have been analyzed by Cordey et al. (1982) in the Lorentz limit, i.e., neglecting electron-electron collisons. This limit is appropriate for calculating current driven by low-parallel-phase-velocity waves, such as Alfvén waves. The kinetic theory of current-drive with electron-cyclotron waves, including resonance regions appropriate for tokamak geometry, has been pursued by Chan et al. (1982), but it is difficult to recover from their analysis the homogeneous (straight-cylinder) limit. The problem has also been considered by Belikov et al. (1982b). Current-drive by electron heating in toroidal geometry has been formulated introducing an adjoint equation by Antonsen and Chu (1982), Taguchi (1983), and Antonsen and Hui (1984). Further neoclassical effects were pursued by Yoshioka and Antonsen (1986) and Antonsen and Yoshioka (1986).

Antonsen and Chu (1982) consider the steady-state Fokker-Planck equation for electrons in toroidal geometry [see Eq. (2.3a)] and write an adjoint equation for the current response. An approximate expression for the flux-surface-averaged response function for the current is given by Antonsen and Hui (1984)

$$g \propto \begin{cases} g_h\,(1 - v_c/v_\parallel)\,, & v_\parallel > v_c \\ 0\,, & |v_\parallel| < v_c \\ g_h\,(1 + v_c/v_\parallel)\,, & v_\parallel < -v_c\,, \end{cases} \tag{3.1}$$

where g_h is the homogeneous current response function, and where v_c is the critical parallel speed (at any point along an electron trajectory) below which an electron is trapped, i.e., will not penetrate the mirror throat along its trajectory; v_c is given by

$$v_c = (1 - B(z)/B_{max})^{1/2} \sqrt{2\varepsilon/m} \quad , \tag{3.2}$$

where the kinetic energy ε is a constant of the electron trajectory and z measures the distance along the trajectory. Equation (3.1) represents a useful, although somewhat arbitrary, approximation that captures the essential features of an otherwise much more complicated function.

It is revealing to consider a schematic representation of the level curves of g, as reproduced from Antonsen and Hui in Fig. 3.4. Current production is proportional to $\vec{S}_w \cdot \partial g/\partial \vec{v}$, where $\vec{S}_w$ is the wave-induced velocity space flux; it is easy to see, therefore, how perpendicular heating near $v_\parallel = v_c$, the trapped-untrapped particle boundary, can result in current flow in a direction opposite to the sense in which current would flow in the absence of the trapped particle effects.

Current-drive by the method of perpendicular heating at the mirror throats can also be understood with reference to Fig. 3.4 if the electron velocity near the field maximum (where the heating occurs) is related to the velocity of the electron at the trajectory position indicated by Fig. 3.4. In other words, velocity space coordinate $\vec{v}$ in Fig. 3.4 is related to velocity space coordinate $\vec{v}_m$ at the mirror throat by

$$v_\perp^2 = \frac{B}{B_{max}} v_{m\perp}^2 \tag{3.3a}$$

$$v_\parallel^2 = v_{m\parallel}^2 + (1 - B/B_{max})\, v_{m\perp}^2 \quad , \tag{3.3b}$$

so that a wave-induced flux entirely in the perpendicular direction at the field maximum translates into a wave-induced flux, $\vec{S}_w$, in Fig. 3.4 with direction

$$\vec{S}_w \sim \frac{1 - B/B_{max}}{v_\parallel} \hat{i}_\parallel + \frac{B/B_{max}}{v_\perp} \hat{i}_\perp \quad . \tag{3.4}$$

Thus, a purely perpendicular flux at the field maximum has a parallel component when viewed elsewhere along the particle orbits, and the current may be found from the same response function g with the appropriately translated flux.

The efficiency can be determined as before, i.e., by Eq. (2.70) with g taking the place of χ. It should be noted, however, that in order to exploit effects associated with trapped electrons, slower electrons must be accelerated. This is because resonances affecting high-$v_\parallel$ electrons do not include many trapped or nearly trapped electrons, i.e., if $v_\perp \approx v_T$, but $v_\parallel >> v_T$, then the electron is unlikely to be trapped. If, however, slower electrons are accelerated, then their higher collision frequency indicates a lower efficiency. For this reason, among others, methods that rely solely on the toroidal effects discussed here will not be as efficient as other current-drive schemes. These effects, however, must be taken into consideration in realistic tokamak experiments especially where optimized conditions are not achieved.

On the other hand, methods that do rely upon fast electrons in order to attain the highest efficiency are not likely to be much affected, under conditions where the efficiency is highest, by effects associated with toroidal geometry.

D. Wave-Induced Diffusion Along Nearly Constant Energy Paths

Here, we remark on the possibility of exploiting at once the advantages of the two favorable wave regimes, low-phase velocity and high-phase velocity. The efficiency of steady-state current-drive via the Landau resonance in a homogeneous plasma is maximized, as depicted in Fig. 3.1, at extrema of $\omega/k_\parallel$, which correspond to these two regimes.

The advantage of high-phase velocity waves, such as lower-hybrid waves, is that they interact with superthermal electrons, which collide infrequently. The drawback is that these waves have little parallel momentum for a given energy. Waves with a high content of parallel momentum are, equivalently, waves with low parallel phase velocity, because parallel momentum is proportional to $k_\parallel$, while energy is proportional to ω. These slower waves, however, interact via the Landau resonance with low-$v_\parallel$ electrons. Apart from the inefficiencies associated with trapping effects,

depositing momentum in slow electrons suffers from the relatively high frequency of current-destroying collisions experienced by these electrons. Clearly, the best of both worlds would be to employ low parallel phase velocity waves to deposit momentum in superthermal electrons. This may be possible through a cyclotron resonance, but, as we show here, waves that accomplish this effect are probably difficult to excite in the plasma.

The interaction that we seek is depicted in Fig. 3.5. Waves with parallel phase velocity $\omega/k_\parallel$ small compared to electron thermal velocity v_T interact via a cyclotron resonance with superthermal electrons satisfying $v_\parallel = (\omega + \Omega_e)/k_\parallel$. Thus, high momentum waves accelerate relatively collisionless electrons. The advantage of using these waves can be appreciated by noting that the diffusion of resonant electrons is along contours of nearly constant energy; thus, resonant electrons convert perpendicular energy into parallel energy as they diffuse from the more densely populated low energy states to higher energy along the wave-induced diffusion path. These diffusion paths are contours of constant energy ε in the frame of reference moving with the wave parallel phase velocity, since in this frame $\omega = 0$, so that particles can exchange momentum, but, on average, not energy with the wave. Note, however, that this exchange does not take place over the full contour of constant energy; it takes place only in the resonant region of velocity space.

The contours can be found, including relativistic effects, by noting that if by interacting with a wave a particle experiences motion along $\vec{S}_w'$ in the wave frame, then we must have $\vec{S}_w \cdot (\partial/\partial p')\varepsilon' = 0$ in that frame, which implies that in the laboratory frame of reference, where the wave frequency is ω, we have

$$\vec{S}_w \cdot (\partial/\partial \vec{p})(\varepsilon - p_\parallel \omega/k_\parallel) = 0 \quad , \tag{3.5}$$

which, in turn, implies that the direction of $\vec{S}_w$ is such that

$$\vec{S}_w \sim (c^2 p_\parallel/\varepsilon - \omega/k_\parallel)\hat{p}_\perp - (c^2 p_\perp/\varepsilon)\hat{p}_\parallel \quad , \tag{3.6}$$

where $\hat{p}_\perp$ is the unit momentum vector perpendicular to $\hat{p}_\parallel$. Note that nonrelativistically, $\vec{S}_w$ traces concentric spheres in momentum or velocity space, as depicted in Fig. 3.5. In the relativistic limit, this simple

geometric relationship no longer applies and $\vec{S}_w$ traces in $p_\parallel$-$p_\perp$ space nonconcentric ellipsoids for $\omega/k_\parallel c < 1$ and nonconcentric hyperboloids for $\omega/k_\parallel c > 1$.

Using, for example, the nonrelativistic limit of Eq. (3.6) in Eq. (2.25a), we obtain for resonant electrons satisfying $v = v_\parallel >> v_T$

$$\frac{J}{P_d} = \frac{ev_\parallel^2}{m\Gamma(5 + Z)} \left[3 + v_\parallel/(\omega/k_\parallel)\right] \quad . \tag{3.7}$$

Here, for $v_\parallel = \omega/k_\parallel$ we recover the Landau resonance, and we recover in the limit of purely perpendicular heating, i.e., $\omega/k_\parallel \to \infty$, the result that these efficiencies are exactly in the ratio 4:3 as depicted in the numerical solution of Fig. 2.1. Of interest here is that in the limit $\omega/k_\parallel << v_\parallel$, there is the opportunity for substantially higher efficiencies.

To realize the substantially higher efficiency, we must assure ourselves that such waves exist in the plasma, that they can be efficiently excited, and that a substantial amount of the wave power will be absorbed by the intended resonant electrons, rather than, say, ions or electrons at the Landau resonance. Such waves do, in fact, exist in a homogeneous magnetized plasma (e.g., Stringer, 1963). The question of damping of the waves is, for the present, moot, because it does not appear that the second criteria can be satisfied, i.e., that these waves can be efficiently excited.

The excitation problem is difficult because of the following inequality. The resonant electrons satisfy

$$v_\parallel = \frac{\omega + \Omega_e}{k_\parallel} < c \quad , \tag{3.8}$$

and, since $\omega/k_\parallel << v_\parallel$ for the effect to be substantial, we have also $\omega << \Omega_e$. Thus,

$$1/k_\parallel < c/\Omega_e \quad , \tag{3.9a}$$

or the parallel wavelength $\lambda_\parallel \equiv 2\pi/k_\parallel$ satisfies

$$\lambda_\parallel < (0.1/B_{10})\text{cm} \quad , \tag{3.9b}$$

where B_{10} is the toroidal magnetic field in units of 10 tesla. For D-T reactors, where $B_{10} \sim 1$ is expected, this inequality implies that waves with 1 mm or less parallel wavelengths must be excited. It is impractical to build such small structures in the plasma, and even if built outside the plasma, which is difficult, there is likely to be an evanescent layer of about the same magnitude, i.e., 1 mm, as the wave enters the tokamaks. Unfortunately, too, parametric means of exciting this wave, say by the beating of two high frequency waves, are likely to be inefficient.

Thus, a promising approach to very much higher efficiency appears not to be implementable, although this is by no means proved. An alternative possibility in very hot plasmas might be to exploit the smaller cyclotron frequency of ultrarelativistic electrons (because of their relativistically heavier mass). Then the inequality in Eq. (3.9a) may not be quite as severe, although other deleterious effects, such as radiation, may be present.

E. Neutral Beam Current-drive

Neutral beams may be directed into the tokamak plasma largely in a tangential direction. Upon colliding with the hot plasma, they ionize and form a positively charged ion beam that circles the tokamak in the toroidal direction. Although this ion beam carries substantial toroidal current, there is a tendency for electrons to catch up and cancel the ion current. The result is that the whole plasma then rotates, but with no net current. What must be done is to exert a force on the electron fluid in the ion frame of reference.

Consider then a homogeneous plasma composed of two groups of ions, one left-streaming and one right-streaming, such that the total ion current vanishes. If, say, the right-streaming group of ions were to collide more frequently with electrons than do the left-streaming group, then electrons would experience a net force pulling them to the right, and a right-flowing electron current would develop. By assumption, the ions in this frame of reference have zero current, so on balance there is a net electric current in the plasma. Since current is a Lorentz invariant for neutral plasma, it does not matter in what frame of reference we derive its existence.

Research has focussed on ways of coaxing electrons to collide preferentially with one of the groups of ions. A method that would not be practical

is illustrated in Fig. 3.6a. This method, in analogy with the successful methods of current-drive using fast electrons, would exploit the velocity dependence of the Coulomb collision cross section. Suppose that the right-streaming group of ions were small in number but energetic. Then, even though the ion currents cancel, electrons would collide more frequently with the slower group of ions and thus tend to go to the left. Unfortunately, for this effect to be appreciable, the energetic group of ions would need a speed much greater than the electron thermal speed (which is the average relative speed between the slow ions and the electrons). Producing ions with speeds greater than the electron thermal speed in thermonuclear plasmas is impractical.

The problem was solved by Ohkawa (1970), who suggested that the disparity in the collision cross sections of the two groups of ions could be achieved if the two groups of ions are of different charge state. The Coulomb collision cross section of an ion is proportional to the square of its ion charge state Z_i, while the current it carries is only linear in Z_i. Thus, ions of disparate charge states carrying the same current collide unequally with electrons. Consider, then Fig. 3.6b, where electrons collide preferentially with ions going to the right. The net ion current is zero in this frame of reference, hence, a net electric current is produced. Ohkawa (1970) suggested producing these counter-streaming (in the zero ion current reference frame) ion beams by injecting one of the beams as neutrals into the tokamak.

Ohkawa (1970) treated the electrons as a streaming fluid with a Maxwellian velocity distribution. More precise models have been employed by Connor and Cordey (1974) and by Fomenko (1975), but only in the limit of small beam velocities, where electron-electron collisions may be ignored. These studies suggest that in tokamaks the requirement for disparate charge states may be relaxed. A full numerical treatment of the problem is provided by Cordey et al. (1979). This treatment proceeds along the lines of the solution to the electric conductivity problem (Spitzer and Härm, 1953). A variational approach, employing a polynomial expansion for the Spitzer function, was constructed by Hirshman (1980), and yielded an analytic epxression for the beam-driven current in excellent agreement with the numerical solutions. Start et al. (1980) and Taguchi (1982) extended the numerical results of Cordey et al. (1979) to include effects associated with trapped electrons.

When electrons are trapped, the near cancellation of the ion current by electrons (when only one ion charge state is present) no longer holds. Only circulating electrons can catch up to ions, so a fraction of the electrons are excluded from cancelling the ion current. The actual effect might be somewhat greater, since the circulating electrons, in colliding with the trapped electrons, are themselves restrained in catching up to the ions.

To calculate the steady-state neutral-beam-driven current, the linearized Fokker-Planck equation for electrons may be formulated as in Eq. (2.8) (Taguchi, 1982), i.e., here we have for electron distribution $f = f_m + \tilde{f}$

$$v_\parallel \hat{b} \cdot \frac{\partial}{\partial \vec{r}} \tilde{f} - C(\tilde{f}) = - \frac{\partial}{\partial \vec{v}} \cdot \vec{S}_b - \left[\frac{\dot{n}}{n} + \left(\frac{\varepsilon}{T} - \frac{3}{2}\right) \frac{\dot{T}}{T}\right] f_m \quad , \tag{3.10}$$

where $\vec{S}_b$ is the electron flux induced by collisions with the injected ion beam (or ionized neutral beam). This flux is given approximately by the collisions of the Maxwellian part of the electron distribution with the beam ions, i.e.,

$$- \frac{\partial}{\partial \vec{v}} \cdot \vec{S}_b = C(f_m, f_b) \quad . \tag{3.11}$$

For a given ion beam distribution, this flux may be computed through Eq. (2.46). In practice, the ion beam distribution must be computed too; this can be done through a separate Fokker-Planck treatment of the beam ions. Once the flux is known, the techniques discussed in Chapter 2 may be applied directly to solve this equation. It should be noted, however, that the beam-induced flux is less specific than is the rf-induced flux, so the utility of the response functions will be different. In practice, only the first Legendre component of the beam-induced flux is kept, and that is sufficient for finding the beam-induced current.

Reproduced from Start et al. (1980), the effect of trapped electrons is illustrated in Fig. 3.7. Here $\varepsilon \equiv a/R \equiv qB_\theta/B_T$ is the inverse aspect ratio, and Z_{eff} is the effective ion charge state. The number of trapped electrons is roughly $\sqrt{2\varepsilon}$. Note that for small beam velocities $v_b/v_T \to 0$ (here $v_e \equiv v_T$), and for no trapped electrons ($\varepsilon = 0$), the current obeys the Ohkawa prediction, i.e.,

$$J/J_b = 1 - Z_b/Z_i \quad , \tag{3.12}$$

where J is the net current, J_b is the beam current, and the ratio of the beam to majority ion charge states, Z_b/Z_i, gives the extent to which the electron current cancels the ion beam current. The current carried by the majority of the ions is assumed to be negligible. In the opposite limit of low temperature, $v_b/v_T \to \infty$ (here, $v_e/v_b \to 0$), there is no cancelling current; this is the impractical case depicted in Fig. 3.6a. For the more practical limit of high temperature, the analytical result of Connor and Cordey (1974) applies, i.e.,

$$J/J_b = 1 - Z_b/Z_i \left[1 - 1.46 \sqrt{\varepsilon}\, A(Z_{eff}, v_b/v_T)\right] , \qquad (3.13)$$

where A is a numerically tabulated function of two variables. In this limit, electron-electron collisions become unimportant, which considerably simplifies the analysis.

To calculate the efficiency of steady-state neutral beam current-drive, it is necessary to solve for the steady-state ion beam distribution. This can be obtained from the beam slowing-down equations, where the beam ions are assumed to collide with Maxwellian distributions of background ions and electrons (Cordey and Core, 1974; 1975; Callen et al., 1975). The electron cancelling current can then be determined through an integration over the total beam-induced fluxes. The power dissipated is the steady-state beam power that must be injected to sustain the steady-state beam distribution. The result of such a calculation is given by Start et al. (1980) and is illustrated in Fig. 3.8. The cases here illustrate the production of current in the direction of the beam current, rather than, as envisioned by Ohkawa, in the opposite direction, when the electron reverse current exceeds the beam current.

As noted by Cordey (1984), the optimum injection energy for neutral beam current-drive is about $40 A_b T_e$, where A_b is the beam atomic number. For $T_e \sim 15$ keV and using deuterium beams, an injection energy of about 1.5 MeV would be required. An approximate expression for the efficiency in the homogeneous case at this optimum energy is given by Cordey (1984) as

$$\frac{I}{P} \simeq \frac{0.6\, T_{10}}{n_{14} R_1} \left(\frac{1}{Z_b} - \frac{1}{Z_i}\right) \frac{A}{W} \quad . \qquad (3.14)$$

Thus, the largest efficiencies are achieved for either Z_b or $Z_i = 1$, with the other species having $Z \to \infty$. The high beam energy implies that a negative ion source will be required. Note that the efficiency exhibited in Eq. (3.14) does not take into account inefficiencies in producing and delivering the beam power to the plasma.

F. Minority Species Current-Drive

The method of neutral beam current-drive relies upon counterstreaming ion flows of disparate charge states to produce an electron drift. One of the main drawbacks of the method is the technological difficulty in producing and delivering efficiently high-energy neutral beams to a tokamak reactor. Technologically easier is to produce and inject rf power. The method of minority species current-drive (Fisch, 1981) seeks to employ the rf technology to produce the counterstreaming ion beams.

The basic mechanism is similar to that exploited when using electron-cyclotron waves to drive current. The idea here is to begin with a plasma containing two species of ions with disparate charge states; this may naturally occur in D-He^3 fusion reactors or in D-T fusion reactors with a minority concentration of helium ash. (Note that, if necessary, D and He^4 may be distinguished by their different thermal speeds.) Suppose that the less dense ions (minority ions) are initially distributed symmetrically in velocity space. Now if minority ions, say, moving to the right were heated in perpendicular energy (we have in mind by rf waves), then these ions would collide less with the majority ions than do the unheated minority ions moving to the left (Fig. 3.9). The result is that majority ions will be dragged to the left, and, by momentum conservation, minority ions, on average, must move to the right. Hence, counterstreaming ion populations have been produced in a manner entirely analogous to the asymmetric electron heating that produced current-drive with electron-cyclotron waves, with the minority ions here taking the place of the electrons.

In order to produce efficiently the counterstreaming ion distributions, it is necessary that the minority ions collide more often with the majority ions than with the electrons. Collisions between minority ions and electrons are not as sensitive to the speed of the minority ions as collisions between

minority and majority ions, since the electrons are, in any event, much faster than the minority ions. Hence, if collisions with electrons were to dominate the minority ion slowing down, the asymmetric perpendicular heating would not produce asymmetric slowing down.

On the other hand, the current-drive is also inefficient if collisions between the two ion populations are too frequent compared to collisions between the ions and electrons. In this case, power is expended to create and maintain the counter-streaming ion populations, but relatively little current is produced because the electrons, which are to carry the current, are not greatly affected.

The solution, therefore, is to choose waves that resonate with minority species ions with intermediate velocities, so that they collide roughly equally with electrons and with majority ions.

To derive this result, consider, in analogy to the result for electrons, that a wave-induced flux $\vec{S}_w$ of minority-species ions will produce a minority species parallel momentum p_α at a power expense P_d in the ratio

$$\frac{p_\alpha}{P_d} = \frac{\vec{S}_w \cdot (\partial/\partial\vec{v})(m_\alpha v_\parallel/\nu)}{\vec{S}_w \cdot (\partial/\partial\vec{v})\varepsilon_\alpha} \quad , \tag{3.15}$$

where $\varepsilon_\alpha \equiv m_\alpha v^2/2$ is the resonant minority ion kinetic energy, m_α is its mass, and $\nu(\vec{v})$ is a collision rate that characterizes the slowing down in parallel velocity of minority ions with velocity $\vec{v}$.

In the absence of trapped electron effects, the Ohkawa result may be used to relate the net current to the minority species momentum by

$$\frac{J}{eZ_\alpha p_\alpha/m_\alpha} = 1 - Z_\alpha/Z_i \quad . \tag{3.16}$$

Using now Eq. (3.15) to substitute for p_α, we obtain the efficiency

$$\frac{J}{P_d} = eZ_\alpha \left(1 - \frac{Z_\alpha}{Z_i}\right) \frac{\vec{S}_w \cdot (\partial/\partial\vec{v})(v_\parallel/\nu)}{\vec{S}_w \cdot \partial\varepsilon_\alpha/\partial\vec{v}} \quad . \tag{3.17}$$

The collision rate ν may be separated into $\nu = \nu_e + \nu_i$, where ν_e characterizes collisions of minority ions with electrons and ν_i characterizes collisions of

minority with majority ions. For the resonant minority ion velocity v much less than electron thermal velocity v_T, ν_e is approximately constant so that $\partial\nu_e/\partial\vec{v}$ may be neglected compared to $\partial\nu_i/\partial\vec{v}$. For $\vec{S}_W$ in the perpendicular velocity direction, only the term in Eq. (3.17) proportional to $\vec{S}_W \cdot (\partial/\partial\vec{v})(1/v)$ need be retained. It then follows that the efficiency tends to zero both for $\nu_i \to 0$ ($v \to \infty$) and for $\nu_i \to \infty$ ($v \to 0$). The maximum efficiency may be shown to occur for an intermediate resonant velocity v such that $\nu_e \approx \nu_i$, as expected. Note that were the wave to carry parallel momentum, i.e., $\vec{S}_W$ having a component in the parallel velocity direction, then the maximum efficiency would occur at the minimum of $[\nu_e(v) + \nu_i(v)]$. The global minimum occurs at the impractical limit $v \to \infty$, where ν_e, $\nu_i \to 0$. The more useful minimum, however, will occur, as before, for resonant electrons such that $\nu_e \sim \nu_i$.

The maximum efficiency for current-drive using perpendicular heating of the minority ions, occurring for resonant minority ions with velocity v such that $\nu_e \sim \nu_i$, may be calculated approximately (Fisch, 1981) as

$$\frac{J}{P_d} = 2\left(\frac{\pi}{3}\right)^{1/3}\left(\frac{M}{m_e}\right)^{1/3}\left(\frac{1}{Z_i} - \frac{1}{Z_\alpha}\right)\frac{env_T}{\nu_o n m v_T^2} \quad , \tag{3.18}$$

where $M \equiv m_\alpha m_i/(m_\alpha + m_i)$ and the maximum is typically broad as a function of v and near $v \approx 5\, v_{t\alpha}$.

Toroidal effects have been calculated by Chiu et al. (1983). For $Z_\alpha > Z_i$, the presence of trapped electrons should result in a smaller current-drive efficiency than that given in Eq. (3.18), since the trapped electrons cannot contribute to the current. For $Z_i > Z_\alpha$, electrons only subtract from the current, so the inclusion of toroidal effects should give a larger estimate for the current. The calculation by Chiu et al. actually gives an efficiency somewhat higher than that given by Fisch (1981), although with the same scaling, even when $Z_\alpha > Z_i$, presumably because of a more precise treatment of the collisions. Chiu et al. also point out that wave absorption may be asymmetric with respect to the resonance layer, so that single pass absorption, while helpful, is not necessary (cf., a similar effect in Sec. II.L). Some suggestions for wave and minority candidates to accomplish the effect are given by Longinov et al. (1986), and a detailed study of the effect is provided by Krasheninnikov (1983).

The possibility of combining both neutral beam injection with minority species heating has been suggested by Okano et al. (1983). The idea here is to inject the neutral beam as before, but to energize it with waves once it enters the tokamak. There are several advantages to pursuing this hybrid approach.

On one hand, the technology requirements on the neutral beam are relaxed, since a less energetic beam may now be adequate. Additionally, the efficiency of producing wave power in the ion-cyclotron range of frequencies (a suitable frequency range for minority species heating) is substantially greater than the efficiency with which energetic neutral beams can be produced. This advantage can be stated more tellingly when one considers the efficiency in terms of the incremental electric power necessary to produce a neutral beam that is incrementally more energetic. In other words, to produce a neutral beam of slightly more energetic ions can demand significantly more power, and that incremental power can be more efficiently provided by wave heating.

On the other hand, the requirements on the rf system are also relaxed, since the beam provides resonant ions that might otherwise be more difficult to extract from a Maxwellian distribution function. There is the possibility, for example, of using faster resonant ions, so that discriminating between the minority and majority ions might be easier. Thus, this hybrid system is an interesting suggestion, although it may still be preferable to employ just one system because it is simpler, and because, to some extent, the hybrid system may also combine the drawbacks of both systems.

Bhadra and Chu (1982) calculate how to exploit the presence of the helium ash (α-particles) in a thermonuclear plasma. Here, asymmetric minority species heating of the α-particles produces the current. It is possible, too, that the α-particle distribution in any event evolves asymmetrically, for example, because α-particles traveling in different directions have different orbits; and may be confined differently, for example, if those traveling in one direction strike the tokamak limiter (McNally, 1978; Kolesnichenko et al., 1981).

G. Thermoelectric Effects

The possibility of exploiting a thermoelectric effect in a hot plasma to maintain current has been pursued by Fisch (1984). Although this effect can

be large, and although the current-drive efficiency, in theory, can be much greater than by other techniques, this method cannot be seriously considered because of apparently insurmountable technological problems. The basic idea, however, is interesting.

A thermoelectric effect could exploit the free energy in the plasma heat itself. First, consider a "driven" thermoelectric effect as depicted in Fig. 3.10. Suppose a material barrier, possibly an injected frozen pellet of plasma fuel in the process of ablating, exists in the plasma and electrons are heated to the right of the barrier. Although the electron heating may be symmetric, electrons emanating from the heated region to the right encircle the tokamak, while electrons emanating to the left immediately slam into the barrier. As a result, there will be a surplus of electrons in the region of the barrier and a deficit of electrons in the heated region. Surplus electrons then diffuse (the short way around) along the large spatial electron density gradient that arises between the region of the barrier and the heated region. This completes the electric circuit of right-traveling electrons; a thermoelectric current has been produced.

The efficiency of creating current in this manner is easily estimated to be, at best, less than that of competing techniques. Compare, for example, to the efficiency of generating current by means of unidirectional waves. Here, only, say, the right-going current is created; no wave energy is expended to create the left-going current that slams into the barrier. Thus, the efficiency would be twice that of using the thermoelectric effect. There is a way, however, to employ the thermoelectric effect while making use of the internal plasma heat itself to drive the current, avoiding altogether the need for external heating.

Consider the injection of frozen pellets into the tokamak in a phased manner, such that succeeding pellets entering the tokamak are shadowed by preceding pellets from electrons impinging from one toroidal direction, as depicted in Fig. 3.11. An asymmetry then develops in the electron distribution function in accordance with the thermoelectric effect. The pellets essentially regulate electron traffic much in the same way that a phased array of traffic lights can favor north-heading cars over south-heading cars on a north-south oriented street.

The injection of frozen pellets of hydrogen into a tokamak reactor is something that in any event might be used to accomplish the plasma fueling. Thus, the current-drive effect comes essentially free, both in terms of power cost and capital equipment cost. Unfortunately, however, pellets in a fusion environment tend to ablate at too fast a rate for the effect to be useful. To generate an appreciable current, an impractical amount of matter would have to be injected into the tokamak.

H. Asymmetric Reflection

Dawson and Kaw (1982) suggest that the large amount of synchrotron radiation generated by a hot fusion plasma may be reflected asymmetrically back into the tokamak such that the reflected radiation sustains a current. Such a method is attractive because of its passive nature; no power need be supplied if the tokamak walls are properly constructed. The asymmetric reflection is accomplished as illustrated in Fig. 3.12.

The amount of power that must be reflected to sustain an adequate current cannot be less than the amount of power needed for current-drive by injected electron-cyclotron waves. This power might typically be $P_f/10$. The advantage here, of course, is that this power may be free. The technique, however, can be useful only when the tokamak is a very copious emitter of synchrotron radiation, typically at a power level, P_{syn}, considerably greater than $P_f/10$, in order to account for inefficiencies in the reflection of the wave power to the proper direction. On the other hand, a tokamak with $P_{syn} \approx P_f$, will not be ignitable unless the synchrotron radiation were very efficiently reflected and reabsorbed to replenish the plasma heat, let alone current. These considerations narrow the parameter window (in electron temperature) for which reflection can be useful.

The idea of radiation reflection had been considered and discounted by Ohkawa (1970) because, at that time, it was considered far too power-intensive to push fast electrons.

Dawson and Kaw calculate that the reflected synchrotron waves produce current with an electron temperature dependence $J \sim T_e^4$. For 90% reflecting walls and other parameters characteristics of tokamak reactors, the plasma current could be sustained by this means for $T_e \sim 50$ keV. This is a considerably higher temperature than is contemplated for D-T reactors, but might be useful for D-He^3 tokamak reactors.

I. Helicity Injection

Helicity density K is defined by $K = \vec{A} \cdot \vec{B}$, where vector potential $\vec{A}$ satisfies $\vec{B} = \vec{\nabla} \times \vec{A}$. It has been proposed (Taylor, 1974) that magnetically confined plasmas tend to relax to configurations that minimize the total magnetic energy while conserving the total helicity

$$K_{tot} \equiv \int \vec{A} \cdot \vec{B} \, dV \quad , \tag{3.19}$$

where the integral is taken over a volume bounded by a magnetic surface. [For a more general definition of K_{tot}, see Finn and Antonsen (1985) and Finn (1986).] The means by which the plasma attains this final state remains an open question, but some experimental evidence supports the Taylor relaxation proposal.

Relying on the Taylor relaxation proposal, Bevir and Gray (1981) proposed that steady-state plasmas may be maintained by helicity injection. Helicity is injected by oscillating toroidal and poloidal magnetic fields at the plasma periphery, and the injection balances the consumption of helicity in the presence of finite plasma resistivity.

Jensen and Chu (1984) elaborate on the Bevir and Gray proposal and derive an helicity transport equation

$$\frac{\partial K}{\partial t} + \vec{\nabla} \cdot \vec{Q} = -2\eta \, \vec{J} \cdot \vec{B} \quad , \tag{3.20}$$

where η is the plasma resistivity and

$$\vec{Q} \equiv \vec{B} \, \phi_{el} + \vec{E} \times \vec{A} \quad , \tag{3.21}$$

where ϕ_{el} is the electric potential. The right-hand side of Eq. (3.20) gives the resistive decay of helicity. (Note that this term would vanish if, say, the current were rf-driven; J here represents the difference between the total current and any noninductive current.) Jensen and Chu show that the Bevir and Gray proposal can be described by balancing the resistive decay against a time-averaged nonzero helicity flux, $\langle \vec{Q} \rangle$. The nonzero time-averaged helicity injection can be expressed as

$$\left.\frac{\partial K_{tot}}{\partial t}\right|_{inj} = 2\,V\,\Phi_T \quad , \tag{3.22}$$

where V is the loop voltage at the plasma periphery and Φ_T is the toroidal magnetic flux. Bevir and Gray suggest oscillating V and Φ_T phased such that the time-average of their product is nonzero. Bellan (1984; 1985) showed that the Bevir and Gray proposal relies on a force that can be thought of as the beating between an $\tilde{E} \times \tilde{B}$ oscillatory velocity and an oscillating magnetic field.

Although detailed calculations have not been supplied, the current/power efficiency associated with this scheme is expected to be more comparable to the efficiency of ohmic current-drive, rather than comparable to the much lower efficiency of noninductive schemes. The effect, however, relies on a key assumption: that plasma relaxation to a Taylor configuration occurs on a time scale short compared to the time scale for inward helicity diffusion. The oscillatory poloidal and toroidal field components, whose product creates the time-averaged force, can then be oscillated on an intermediate time scale, during which the plasma acts as a perfect conductor, yet allows field penetration and relaxation.

The ramifications of such oscillatory components have not yet been explored, and it is possible that deleterious effects, such as outward particle transport, could be associated with the inward helicity transport. Bellan expresses an efficiency as current generated per amplitude variation of the oscillating magnetic field, finding 2% magnetic field variation sufficient to sustain the current in a small tokamak reactor. Jensen and Chu raise questions concerning the extent to which the plasma approaches the Taylor configuration. In a true Taylor configuration, the plasma would not maintain a pressure gradient.

A similar ponderomotive force capable of current generation and relying on crossed oscillating magnetic fields occurs in the Rotamak, a containment device of somewhat different geometry (Hugrass et al., 1980). Here plasma relaxation due to finite resistance is also critical; in the limit of scarce collisions, where such relaxation does not occur, the Rotamak current-drive effect becomes more difficult (Fisch and Watanabe, 1982).

Current-drive by helicity injection is especially promising because of the possibility of low power consumption and because the oscillatory fields

can be produced relatively easily. However, the approach must be considered, at this point, highly speculative because of the lack of experimental evidence in tokamaks for even the basic ingredients of the scheme (e.g., the Taylor configuration) and because of the lack of a broader theoretical understanding of basic plasma phenomena under conditions that, in fact, differ substantially from normal tokamak operation. Also, recent theoretical studies by Liewer et al. (1986) question the amount of current that can be produced in this manner.

It should be noted that if toroidal current produced on the periphery of the tokamak can, in fact, support a toroidal current on the magnetic axis, as helicity injection would have it, then many techniques of current-drive become more attractive. For example, lower-hybrid (or other) waves can drive a current on the plasma periphery much more efficiently than on axis because the density is much lower. Also, the lower-hybrid wave has no problem penetrating the periphery. Therefore, the helicity could equally well be created by lower-hybrid or other waves, as opposed to oscillatory magnetic fields. Discussion should therefore be focused on the basic question of current penetration rather than on the specific means of achieving the boundary conditions.

IV. Theory and Experiment

A. Introduction

Experimental evidence is available for the methods of current-drive by neutral beams, electron-cyclotron waves, and lower-hybrid waves. By far the most extensive evidence has been accumulated for the lower-hybrid current-drive effect. This effect is no longer held in doubt, and the theory of current-drive efficiency has enjoyed confirmation in a large number of experiments conducted by different experimental groups.

Nonetheless, details of the effect remain the subject of debate, particularly the relation between the launched and absorbed wave spectrum. Caution must also be exercised in extrapolating results from present regimes to reactor regimes, where the higher density and temperature, and also the presence of energetic α-particles, could modify substantially the propagation and absorption of the waves considered here. The apparatus for coupling the wave to the plasma also needs to be tested in a reactor environment. For

example, it has been observed that power transmission into the plasma is sensitive to the cleanliness of the waveguide windows, and the effect of exposing these windows to a fusion plasma is unknown.

Not all of the current-drive methods suggested here have enjoyed laboratory testing. Some of these techniques, e.g., those relying on α-particles or intense plasma radiation, are testable only on fusion-grade plasma. Other techniques are perhaps too unsure or speculative at present. An interesting experiment is being devised now (Gahl et al., 1985) to test current generation by minority species heating, but no results have been reported yet. A current-drive effect using the fast Alfvén wave has been reported recently by Goree et al. (1985) and by McWilliams and Platt (1986). This wave has propagation characteristics different from those of the lower-hybrid wave, yet, in theory, enjoys the same current-drive efficiency.

B. Early Experiments

Early experimental efforts paralleled the early theoretical concerns, which centered on the possibility in the first place of generating currents with waves. Currents of one hundred amperes were generated by Thonemann et al. (1952), when 4 kW of rf power was imposed on a glass-confined cold plasma, with toroidal chamber dimensions of 9-cm major radius and 2-cm minor radius. Similar, but much scaled up, experiments were conducted by Borzunov et al. (1964) and Demirkhanov et al. (1965). Yoshikawa and Yamato (1965) observed a current on the C-stellerator in the presence of ion-cyclotron heating.

Hirano et al. (1971) imposed traveling waves on a glass-tube confined plasma, but with the plasma immersed in a toroidal magnetic field, and observed current generation maximized when a whistler wave was excited. In a similar toroidal device, Osovets and Popov (1972;1976) detected currents as large as 3 kA in the presence of a toroidal magnetic field. Here the largest currents were observed when compressional Alfvén waves were excited. Klima et al. (1978) showed dragging of electrons by waves in a small toroidal device.

A series of experiments carried out on the Synchromak device (Fukuda et al., 1976; Fukuda, 1978) examined in detail, among other things, the radial distribution of the current. The Synchromak is a small toroidal device (major radius 25 cm, minor radius 5 cm) where a cold (4-10 eV) plasma is immersed in a toroidal magnetic field and a small vertical magnetic field (see Fig.

4.1). Currents of about 200 A lasting 0.2 ms were detected when about 50 kW of rf power were absorbed from coils wrapped around a glass section of the otherwise stainless steel toroidal chamber. Rather hollow current profiles were observed even in the steady state and in spite of good penetration of the rf fields. These experiments are reasonably explained using a fluid model (Fukuda and Matsura, 1978).

Theoretical investigations during the period of these early experiments (Klima, 1972; 1973a; 1973b; 1974; 1976; Midzuno, 1973; 1975; Klima and Sizonenko, 1975; and Belikov et al., 1982a) focused on the ability of monochromatic traveling waves to drag electrons. Expressions were written for current generation based on trapping of electrons by the wave. The power dissipated was calculated based on a fluid model. Both the theoretical and experimental investigations centered on the regime $\omega/k_{\parallel} < v_T$, where it was assumed that the current-drive effect was maximized. Bickerton et al. (1972) raised serious concerns about this regime with regard to toroidally trapped particle effects, putting in doubt the optimistic calculation by Wort (1971).

These early experimental and theoretical programs established in many ways the existence of rf-driven currents and the transferability of wave to electron momentum. Electrons were assumed to flow as a fluid, and indeed in the experiments this was largely so, since $\omega/k_{\parallel} \lesssim v_T$ was the regime studied. Following these programs, the attractiveness of the regime $\omega/k_{\parallel} >> v_T$ was recognized in a theoretical model (Fisch, 1978) in which the fluid model was not employed, and later in confirmatory theoretical treatments (Klima and Longinov, 1979), although the undue emphasis placed on momentum input was not dispelled until fully two-dimensional effects (Fisch and Boozer, 1980) were appreciated.

C. Lower-Hybrid Wave

Favorable theoretical predictions concerning the efficiency of driving currents in the regime $\omega/k_{\parallel} > v_T$, and the possibility of building tokamak reactors using this regime, stimulated experimentation on the lower-hybrid wave. That the lower-hybrid wave in particular could, in fact, deposit momentum in fast electrons was first observed on a linear device (McWilliams et al., 1980; 1981; Wong, 1979), on an octopole device (LaHaye et al., 1980), and on small toroidal devices which were operated with a toroidal magnetic

field but no induced current (Wong et al., 1980; Kojima et al., 1981). These early experiments confirmed that current generation was possible not only with the waves previously reported on the Synchromak and other devices, but was also possible with the lower-hybrid wave which tended to interact with fast electrons. It remained unsure, however, whether the lower-hybrid wave could operate as intended in a tokamak, in more important parameter regimes, and with the theoretically predicted efficiency that had provided impetus for the experiments in the first place.

Experiments on tokamaks are complicated by the presence of an inductive current in addition to the rf-driven current. On toroidal devices in which there is no dc electric field, the mere detection of current in the presence of wave injection is indicative of a noninductive current-drive effect. On tokamaks, this is not so, since there is naturally a toroidal current, and just heating the electrons at constant loop voltage lowers the resistivity and increases the current. This occurs in the absence of any noninductive effect, so the unambiguous observation of a noninductive current-drive effect is more difficult in tokamaks.

The generation of noninductive current in tokamaks and other toroidal devices is generally deduced from changes in the loop voltage, for which there are two independent measurements. One method is to measure directly the voltage across the ceramic break in the vacuum vessel. This voltage may then be equated with the loop voltage at the plasma periphery. An alternative method employs a coiled conducting loop, called a Rogowski coil (see Fig. 4.1). The axis of the coils encircles the minor cross-section of the tokamak (the center of the loop coincides with the center of the minor cross-section). The poloidal magnetic field, B_θ, external to the plasma then threads these coils, so a measureable voltage is induced along the loop proportional to $\partial B_\theta/\partial t$. The line integral of B_θ gives us, by Ampere's law, the toroidal plasma current. Also, using Faraday's law, the integral of $\partial B_\theta/\partial t$ over the torus hole gives us the loop voltage at the plasma periphery. Note that both measurements of the loop voltage are made outside the plasma (the plasma is generally too hot for measurements to be taken within it - but see Secs. IV-E and IV-F), and neither measurement gives the current or loop voltage profile.

To deduce the noninductive current-drive effect, the loop voltage V is related to the toroidal current I by

$$V = -\frac{1}{I}\frac{d}{dt}\left(\frac{LI^2}{2}\right) + V_{ext} \qquad (4.1)$$

where L is the plasma inductance and V_{ext} is a voltage applied by the external transformer circuit. The current can be divided into

$$I = I_{OH} + I_{RF} \quad , \qquad (4.2)$$

where I_{rf} is the rf-induced contribution and I_{OH} is the ohmically induced current given by

$$I_{OH} = \frac{V}{R_{Sp}} \quad , \qquad (4.3)$$

where R_{Sp} is the Spitzer conductivity (Spitzer and Harm, 1953; Cohen, Spitzer and Routley, 1950). Assuming that the plasma current and the plasma inductance are approximately constant, a change ΔV in the loop voltage may be found from Eqs. (4.1) -(4.3) to obey

$$-\frac{\Delta V}{V} = \frac{I_{RF}}{I_{OH}} - \frac{\Delta R_{Sp}}{R_{Sp}} \quad , \qquad (4.4)$$

where ΔR_{Sp} is the change in the Spitzer conductivity that might arise due to the rf heating. From Eq. (4.4), it can be seen that a drop in the loop voltage ($\Delta V < 0$) can be associated with the presence of current-drive if no heating has taken place ($\Delta R_{Sp} = 0$). The first lower-hybrid current-drive experiments made use of this reasoning (Yamamoto et al., 1980; Maekawa et al., 1981; Nakamura et al., 1981; Luckhardt et al., 1982; Gormezano et al., 1983) taking pains to argue that changes in either the resistance or in the inductance could not account for the loop voltage drop. An example of this data is reproduced from Yamamoto et al., (1980) in Fig. 4.2, but note that the loop voltage is not entirely reversed and $L/R_{Sp} > \tau_{rf}$, where τ_{rf} is the duration of the rf power. Further confirmation of the current-drive effect was obtained in experiments in which the loop voltage drop was correlated with the phasing of the wave. Luckhardt et al. (1982) showed that waves traveling in the direction of the induced electron drift contribute far more to the

current than do waves phased to travel in the opposite direction, as shown in Fig. 4.3. The increase in current in the counter-traveling case is presumably due to the heating effect. Additionally, performing these experiments on Versator, a slightly smaller tokamak, Luckhardt et al. succeeded both in reversing their loop voltage and achieving $\tau_f \approx L/R_{Sp}$.

These experiments were informative, but not conclusive. It was still not clear how much current was generated due to heating and how much due to the current-drive effect. In the Versator experiment, the temperature was observed to decline during intense current-drive, but it was as though a preformed, ohmically induced tail was necessary for the current-drive effect. In the experiment by Maekawa et al. (1981), the loop voltage was actually reversed, but for a duration less than 2 ms, and in a plasma in which the electron velocity distribution was determined to be far from Maxwellian. For short times, the loop voltage measurement taken at the tokamak periphery is not a reliable indicator of the loop voltage in the plasma interior, where, presumably, the current is driven.

A series of experiments on the PLT tokamak in Princeton countered these doubts concerning the lower-hybrid current-drive effect. Bernabei et al. (1982) and Hooke et al. (1982) reported sustaining an rf current of 150 kA for 3 seconds in the absence of a loop voltage. In early experiments on PLT, the discharge was initially confined by an ohmic current before the rf power was injected. In a very encouraging experiment reported by Jobes et al. (1984), both the plasma and the current were initiated without the aid of the ohmic transformer coils. A current of over 100 kA was generated by the rf waves alone. The "start-up" experiment demonstrated conclusively the lower-hybrid current-drive effect. Additionally, it allowed tokamak reactor designers to view seriously the current-drive apparatus as having either the purpose of sustaining a transformer induced discharge, or of initiating a transformer-sustained discharge, or possibly of replacing the transformer coils altogether. The advantage of initiating the current with rf waves is that the valuable volt-seconds of the transformer coils are saved until the plasma is hotter, rather than expended on the initial colder plasma which requires a higher loop voltage to sustain the current. Thus, the waves might be useful in prolonging the pulses in otherwise ohmically sustained reactors; additionally, the waves would help to heat the plasma to ignition.

Nonetheless, despite these possibilities, the primary hope remains to use the waves to achieve truly steady-state currents.

While the PLT data exhibited agreement between theory and experiment, these experiments were performed at relatively low density ($n < 10^{13}$ cm^{-3}). Higher density experiments, more relevant to the reactor regime, were performed on the Alcator C tokamak at MIT, and, in particular, the theoretical efficiency scaling $J/P_d \sim 1/n$ was confirmed by Porkolab et al. (1984b) in a more interesting (high density) parameter regime as reproduced in Fig. 4.4. In these experiments a normalized efficiency $J/P_d \approx 50$ was reported, and found to be consistent with theoretical estimates using the modeling code (which included the propagation of the waves) of Bonoli et al. (1983).

The high-density operation of the current-drive experiments on the Alcator C tokamak was possible because of the relatively high frequency (4.6 GHz), the high magnetic field (11 T), and the relatively high power (1.1 MW) employed. In general, it has been observed that efficient current-drive is obtained only when $\omega/\omega_{LH} > 2$, where ω_{LH} is the lower-hybrid frequency ($\omega_{LH} \approx \omega_{pi}/(1 + \omega_{pe}^2/\Omega_e^2)$, where ω_{pi} is the ion plasma frequency). A systematic experimental study of this observation (Mayberry et al., 1985) suggests that there is no absolute density limit for the current-drive effect, but that when $\omega/\omega_{LH} \gtrsim 2$, the lower-hybrid power tends to be deposited in ions rather than in electrons. Recently, Knowlton et al. (1986) characterized the tail energy content and confinement properties of lower-hybrid-current-sustained discharges on the Alcator C tokamak.

Confirmatory evidence of the lower-hybrid current-drive effect has been reported by a number of other experimental groups. In a series of experiments in the Petula tokamak (Gormezano et al., 1985), there were observed large rf-driven currents, consistent with theoretical predictions and over a wide parameter range of density, magnetic field, and waveguide phasing. The effect was reported also on the Ioffe FT-2 tokamak by Budnikov et al. (1984) and on the JAERI JFT-2M tokamak by Uesugi et al. (1985). Lower-hybrid waves were used to initiate and sustain ("start-up") the current on the Nagoya T-IIU tokamak (Toi et al., 1984). Significant in this experiment was the long pulse width of the rf power compared to the L/R_{Sp} time of the tokamak. Additionally, the turn-on time for the current was found to be in rough agreement with Eq. (2.33). Start-up was achieved also by using an electron-

cyclotron wave (ECW) produced target plasma (Kubo et al., 1983; 1984) in the Kyoto WT-2 tokamak. Shimozuma et al. (1985) have numerically simulated the Kyoto experiments using quasilinear theory. Successful lower-hybrid current-drive experiments were carried out on the Kurchatov T-7 tokamak (Alikaev, 1983; 1985), where, recently, lower-hybrid start-up was achieved in an ECW initiated plasma. Measurements of the hard x-ray emissions in the PLT experiments [von Goeler et al. (1985); Stevens et al. (1985)] showed that energetic tail electrons were distributed in velocity space consistent with quasilinear theory (see Fig. 2.4b).

D. Converting Wave to Magnetic Field Energy

The most compelling evidence for the theory of steady-state current-drive came, ironically, from experiments in which the current was either increased (ramp-up) or not quite maintained (ramp-down) by the injected lower-hybrid waves. The evidence was compelling because the steady-state problem was embedded in the larger problem of current-drive in the presence of a dc electric field. Thus, data obtained under very different plasma conditions could be related and combined to support a single theory.

During steady-state current-drive, rf power is injected into the tokamak, maintaining the current, but this power is eventually lost as heat. During current ramp-up, the current increases and, consequently so does the storage of poloidal magnetic field energy, W, where $W = LI^2/2$. The important efficiency parameter during ramp-up is the ratio of the electric power flowing into the magnetic field, P_{el}, to the power absorbed by the resonant electrons, P_{in} (see Eq. 2.62). Under steady-state conditions, $P_{el} = 0$, and this efficiency is zero. Nonetheless, this efficiency is intimately related to the efficiency commonly used for steady-state operation, i.e., J/P_d, since we have

$$\frac{J}{P_d} = \lim_{E \to 0} \left(\frac{1}{E} \frac{P_{el}}{P_{in}} \right) \quad . \tag{4.5}$$

This suggests that P_{el}/P_{in} is the more general efficiency parameter, and that the problem of accumulating experimental evidence for the theoretical prediction of J/P_d might be alleviated by broadening the parameter space on which evidence is defined.

The ramp-up results on the PLT tokamak (Stevens et al., 1982; Motley et al., 1984; Jobes et al., 1985) were remarkable in that a large fraction of incident rf energy appeared to have been converted to magnetic field energy. Figure 4.5, reproduced from Jobes et al. (1985), shows the ramp-up phenomenon. A raw measure of the efficiency, given by $\dot{W}/P_{rf}$, is shown in Fig. 4.6, where $\dot{W} \equiv d\,(LI^2/2)/dt$ and P_{rf} is the incident of power. This raw measure of the efficiency, which differs from the efficiency defined here (P_{el}/P_{in}), can be seen to approach 20%. That a fifth of the incident energy is converted to field energy is viewed as notable, especially in light of various inefficiencies that are unavoidable in these experiments. These inefficiencies arise, for example, because a fraction of the rf energy may be launched in the wrong direction, may be scattered off various plasma inhomogenieties, or, for other reasons, may not be absorbed by the intended electrons.

This significant experimental finding served as an impetus for a theory of current-drive in the presence of a dc electric field (Fisch, 1985; Fisch and Karney, 1985). Very close agreement between the theory and experiment was shown by Karney et al. (1985). The method of comparing theory and experiment bears examining in some detail, in part because of the unusually close agreement over a wide parameter range, and in part because of the very narrow specificity (in order to isolate the critical mechanism) in what was actually compared.

First, we review briefly the major microscopic physical processes we seek to describe. Electrons absorbing wave energy and momentum may slow down either by colliding with the background plasma, or by decelerating under the effect of the dc electric field as depicted schematically in Fig. 4.7. In the former instance (Region A in the figure), the wave energy is eventually dissipated as heat and $P_{el}/P_{in} \to 0$. In the latter instance (Region B), the background plasma does not participate; hence, by energy conservation all energy must go into the field, i.e., $P_{el}/P_{in} \to 1$. These regimes correspond, respectively, to $v/v_R \ll 1$ and to $v/v_R \gg 1$, where the runaway velocity v_R, given by Eq. (2.56), serves to divide these two regimes. The Landau resonance, $v_\parallel = v_{ph}$ ($v_{ph} = \omega/k_\parallel$), determines which regime applies.

It is advantageous, therefore, to use high phase-velocity waves (v_{ph} large), or, alternatively, to try to ramp-up quickly (v_R small). Quick ramp-up

might be achieved by operating at low density or at high rf power (we avoid discussing, for the moment, the cost of high power operation). Unfortunately, if v_{ph}/v_R is too large, the resonant electrons tend to run away, since $R(\bar{v}/v_R)$, given by Eq. (2.54), rapidly increases with v/v_R for $v>v_R$. In the PLT experiment, even if only a small fraction (1%) of the resonant electrons were to run away yet remain confined there would be a significant diminishing of the efficiency (Valeo and Eder, 1985). An electron decelerated by the dc electric field first gives up its kinetic energy to the field, but, as it changes direction, i.e., as $v_\parallel$ passes through zero, it is then accelerated as backward runaway to higher kinetic energy at the expense of the electromagnetic field energy. Therefore, the regime $v_{ph}/v_R \gg 1$ must be avoided if there is to be both efficient energy conversion and good particle confinement.

It turns out that between the regimes of collisional inefficiencies (v/v_R small) and rf-induced runaways (v/v_R large), there exists an intermediate regime where efficient energy conversion is possible without inducing too many runaways. This conclusion may be reached by observing Figs. 2.7 and 2.8. The PLT experiment evidently operated in this favorable regime.

To relate the experimental observables to the theoretical analysis, we express the data in terms of the critical dimensionless parameters, P_{el}/P_{in} and v_{ph}/v_R, that characterize the theoretical results. To carry out this program, first note that the circuit equations give

$$P_{el} = \dot{W} + \frac{V^2}{R_{sp}} - P_{ext} \quad , \tag{4.6}$$

which can be understood easily by inspecting the schematic power flow diagrammed in Fig. 4.8. Some fraction η of the rf power P_{rf} that is injected at the plasma periphery is absorbed by resonant electrons in the plasma interior. The absorbed power, P_{in}, then flows, as argued above, either into heating the bulk electrons (and, on a longer time scale, into heating the ions, too), or into increasing the storage of poloidal magnetic field energy, W. This stored inductive energy, in turn, flows by ohmic heating (V^2/R_{Sp}) into the bulk particles. Alternatively, the inductive energy can be exchanged through mutual inductance with an external magnetic field necessary for plasma equilibrium, or, if connected, the transformer circuit that provides the usual

toroidal current in tokamaks. Power flowing from an external circuit into the tokamak is represented in Fig. 4.8 by P_{ext}, and Eq. (4.6) follows accordingly.

The right-hand side of Eq. (4.6) may be measured experimentally or reasonably surmised. The dimensionless parameter P_{el}/P_{in} may then be formulated in terms of experimental observables by using, together with Eq. (4.6), the expression for P_{in}

$$P_{in} = \eta P_{rf} \quad . \tag{4.7}$$

The input power, P_{rf}, is generally a known quantity, and the fraction absorbed, η, may be calculated in principle by means of a numerical code that solves the propagation and damping equations for the waves. The other critical dimensionless parameter, v_{ph}/v_R, may also be expressed in terms of experimental observables; the runaway velocity, v_R, is dependent on the loop voltage and the density, which are measurable.

The calculations of v_{ph} make use of the parallel index of refraction, $n_\parallel$, at the plasma periphery, which is determined through a Fourier analysis of the launched spectrum. As the waves propagate into the plasma interior, the index of refraction at the point of power absorption is generally upshifted by some factor β, so that

$$v_{ph} = c/n_\parallel \beta \quad , \tag{4.8}$$

where c is the velocity of light, $n_\parallel$ is given by the waveguide phasing, and β may be determined by solving the propagation and damping equations for the waves.

The experimental data from PLT, which included a large (over 250) number of shots with various values of density, waveguide phasing, and rf power, were plotted by Karney et al. (1985) in terms of P_{el}/P_{rf} and v_{ph}/v_R as reproduced in Fig. 4.9. Based on x-ray emissions, the ion charge state was chosen to be 5. The relatively small scatter in the experimental data, when plotted in this way, is strongly indicative that the critical dimensionless parameters were correctly identified, and the resemblance of the data to curves shown in Fig. 2.9 shows that a reasonable theoretical interpretation is at hand. Karney et al. (1985) noted that the absorption fraction η and the $n_\parallel$-upshift

factor β could reasonably and most simply be assumed to be constants, in which case they merely serve to scale the axes in Fig. 4.9 without changing the shape of the curves. The theoretical fit in Fig. 4.9 was then chosen by optimizing over choices of η and β. This optimization procedure did not detract from the very close agreement (only two adjustable parameters in fitting over 250 points), while it made it possible to compare the theory and experiment without solving the wave propagation equations. In solving these equations, further debatable assumptions would have had to be introduced in the model of the plasma, and further debatable choices would have ha to be made in the theoretical treatment. The theoretical treatment ignored also the presence of runaway electrons, which, in view of the powerful agreement, would appear to be justified.

The data in Fig. 4.9 correspond to several different current-drive regimes, and serve to corroborate at once the current-drive theories derived for these regimes. The point $v_{ph}/v_R = 0$ corresponds to steady-state current-drive, where the ramp-up efficiency vanishes. The second derivative of the theoretical curve, taken at the origin, however, is the steady-state efficiency (J/P_d). The regime $|v_{ph}/v_R| << 1$ corresponds to a small electric field, where the rf-induced so-called "hot conductivity" theory holds. The regime $v_{ph}/v_R > 0$ corresponds to current ramp-up, whereas the regime $v_{ph}/v_R < 0$ corresponds to the case where rf power is either insufficient or is misdirected so that the current decreases. Interestingly, in this latter regime, $P_{el} < 0$, which means that power flows from the field energy into kinetic energy of resonant electrons. The close fit of the data over all these regimes clearly indicates solid confirmation of the theories.

Moreover, the two free parameters η and β, are in fact related through the wave damping mechanism. Heavy damping should accompany large upshift (because bulk electrons become resonant). The fact that the values for these parameters that optimize the numerical fit are also consistent with the quasilinear damping mechanism can be viewed as further confirmation of the theory.

Other experiments on current ramp-up have also been shown to agree with the theories of current-drive efficiency. Leuterer et al. (1985) ramped-up the current in the ASDEX tokamak at a rate of 50 kA/sec by injecting 675 kW of lower-hybrid power. Ramp-up experiments were also performed on the MIT

Alcator C device, and the data were plotted (as in Fig. 4.9) in terms of the dimensionless parameters P_{el}/P_{in} and v_{ph}/v_R (Porkolab, Varenna, 1985). In these experiments, performed at higher density, the parameter v_{ph}/v_R was generally smaller than in the PLT experiments, and the theory of hot conductivity alone was sufficient to explain the data.

Because the efficiency of converting wave energy to poloidal field energy depends only on the ratio v_{ph}/v_R, we may contemplate easily how to extrapolate the favorable results achieved on PLT to ramp-up current on larger devices. In this regard, a useful formula is

$$\frac{dI}{dt} \simeq \frac{5\ E_1}{\ln R/a} \quad \frac{MA}{sec} \ , \tag{4.9}$$

where E_1 is the electric field in units of volt/meter. To maintain the PLT parameter regime we keep both E/n and v_T approximately unchanged from the PLT experiment, so that both the efficiency and the wave damping can be reasonably extrapolated. An example given by Fisch and Karney (1985) gives E = 0.6 V/m, $n = 5 \times 10^{12} cm^{-3}$, T = 1 keV, and Z = 1 in order to ramp current to 10 MA in 50 seconds in a large tokamak (L = 8μH). Assuming then a 33% efficiency, 40 MW of rf power is required.

In designing such ramp-up possibilities, Eq. (4.9) is used to relate the ramp-up rate to E, the electric field, while to maintain the PLT regime, E is further related to n. The power required to maintain the ramp-up may be written as

$$P_{rf} = \frac{LI^2/2}{eff \times T_{ramp}} \ , \tag{4.10}$$

where eff is the conversion efficiency, P_{el}/P_{in}, and T_{ramp} is the current ramp-up time. Thus, less power need be used if the ramp-up is slow (T_{ramp} small), but then to maintain similar efficiency, the density must be kept low. At high density, but the same ramp-up rate, somewhat faster waves may be employed, but then the plasma must be hotter in order to absorb these waves. The danger in hotter plasma is that there may be significant energy loss due to Joule heating. This implies that the plasma must be kept resistive, and a short bulk energy confinement time is necessary (about 30 ms in the above example). In the above example, care was taken not to produce backward

runaways. If, however, some method of removing these runaways were possible, then somewhat higher efficiencies could be obtained by employing higher v_{ph}/v_R. Alternatively, should the backward runaways lose energy to collisionless instabilities, their effect would be mitigated. This latter possibility was studied recently by Chan et al. (1986).

E. Launched and Absorbed Waves

One of the curiosities of lower-hybrid current-drive experiments has been that the spectrum launched at the plasma edge often appears not to be slow enough to interact with a substantial amount of resonant electrons. From hard x-ray measurements (e.g., Bernabei et al., 1982), it is known that many very energetic electrons are created, with energies as large as 200 keV in a 1 keV plasma. This is consistent with the presence of very fast parallel phase velocity waves in the spectrum. The presence of many of these electrons, however, also implies a wave spectrum that extends into the bulk of the distribution function that can interact with less energetic electrons, on the order of only several keV. The apparent absence of low parallel phase velocity waves in the exciting spectrum, i.e., waves that could extend the resonant region in velocity space into the plasma bulk, has been termed the problem of the "spectral gap." Several researchers have contributed ideas on how waves, that apparently have not been launched at the plasma periphery, appear nonetheless in the plasma interior to "plug this gap."

One possibility is that there is an upshift in the $k_{\parallel}$-spectrum merely as a result of a focusing effect, possibly in conjunction with multiple reflections of the lower-hybrid wave before it is absorbed (Bonoli et al., 1984; Englade et al., 1983). What is conserved as waves propagate from the tokamak periphery to the tokamak interior is by axisymmetry only the toroidal mode number. Solutions of the ray tracing equations (e.g., Ott et al., 1979; Ignat, 1981), reveal that there is a significant variation in $k_{\parallel}$ as the wave propagates towards the interior. This is due to two effects: at smaller major radii the toroidal wavelength decreases due to focusing, and at small minor radii, the parallel wavelength, to the extent that the parallel direction coincides with the poloidal direction, decreases due to a radial focusing effect. The result is an explanation of the "spectral gap" problem based entirely on linear propagation theory; the possible difficulty with this

explanation occurs only to the extent that the ray-tracing trajectories are often very sensitive to the initial conditions of both wave and plasma, and the number of reflections can become large. Results of a numerical code using the ray-tracing equations together with models evolving the electron distribution function and the plasma current (Valeo and Eder, 1985) show that minority hydrogen ions could explain a density limit to current-drive experiments conducted in deuterium plasmas (Stevens et al., 1982). The numerical code also gives a reasonable picture of ramp-up experiments.

One result of the ray-tracing calculations is that it makes a difference where on the torus periphery waveguides are placed. The importance of waveguide placement was brought out in experiments by Lloyd et al. (1983), who showed how launching the waves from the side rather than the top of the tokamak could lead to better coupling to the electrons. Bernabei et al. (1986) performed confirmatory experiments on the Princeton PLT tokamak, and showed that to some extent launching faster waves at the top can reduce the discrepancy in the coupling.

Alternative explanations for the spectral gap involved nonlinear effects (Canobbio and Croci, 1984), which could broaden the resonances, i.e., the extent to which $\omega - k_{\parallel}v_{\parallel} = 0$ need be satisfied exactly. It is also possible that, as the wave passes through a turbulence layer on the periphery of the tokamak, it could be scattered in angle off local inhomogeneities in the parallel direction (Ott, 1979; Andrews and Perkins, 1983; Andrews et al., 1985). Some properties of the equation that describes this effect are discussed by Fisch and Krusdal (1980). If the initial distribution of waves were to cause a large anisotropy in the distribution function, the plasma could be unstable to other waves that would seek to diminish the extent of the anisotropy. Such instabilities often occur during low density ohmic discharges with large runaway or slide-away current (Parail and Pogutse, 1976). (A fine examination of the slide-away regime in an ohmic discharge, but relevant to the parameter regime most useful for current-drive was performed on Asdex (Fussmann et al., 1981.) It has been suggested that such an instability could excite low parallel phase velocities that plug the gap (Liu et al., 1982; Parail and Pereverzev, 1983; Liu et al., 1984; Chan et al., 1984). Its presence is thought to explain, for example, lower-hybrid wave experiments on the FT tokamak (Santini et al., 1984). Other nonlinear effects

in current-drive have been brought out by Chan and Liu (1985). A treatment of the effect of low-phase-velocity components of the wave spectrum, however generated, is provided by Succi et al. (1984).

The Parail-Pogutse instability appears to have been observed in several current-drive experiments, where it has also been quenched by the simultaneous application of electron-cyclotron waves to the plasma. (Luckhardt et al., 1982; Maekawa et al., 1983; Nakamura et al., 1984.) These waves presumably isotropize the distribution function enough to stabilize the low parallel phase velocity modes. In a steady-state reactor, however, this instability will not be present because the distortion of the distribution function is relatively small; it involves relatively few electrons and these electrons are only several times as fast as thermal electrons. In higher density, higher temperature, or more completely steady-state experiments, this instability is not observed to occur. For example, on high-density experiments on Alcator C, instabilities appear only after the rf power is terminated (Porkolab, 1984). In such experiments the distortions to f are similarly not dramatic.

Recent experiments by Ando et al. (1986) on the WT-2 tokamak also employed both lower-hybrid and electron-cyclotron waves, and exhibited a dependence of the current-drive efficiency and the current ramp-up rate on the location (bulk or tail) of the ECH-heated electrons. The reason here is unclear; confinement properties of the heated electrons may be important. Such confinement properties, incidentally, have been investigated recently under similar but not identical conditions by Luckhardt et al. (1986) on the Versator tokamak.

Two observations may be in order here. First, the latest theoretical work exhibits a shift in emphasis from establishing the existence of the current-drive and other physical effects to understanding often complicated experiments. More complete and complicated wave and particle transport models are then often needed [see, e.g., Dnestrovskij et al. (1983); Parail et al. (1985).] Second, as difficult as it may seem to relate in tokamaks the absorbed to the launched spectrum of waves, the problem in tokamaks is still far more tractable than in other devices where the current-drive effect may be useful. A recent theoretical study of current-drive using electron-cyclotron waves in spheromaks was performed by Yoshioka et al. (1986).

F. Observation of Neutral Beam Currents

Currents driven by neutral beams were observed by Start et al. (1978). These observations were made on the Culham Levitron, a small, cold, toroidal plasma confinement device in which the poloidal magnetic field is generated by an internal superconducting toroidal current ring. The major radius is about 30 cm and the minor radius is about 6.5 cm. Experiments are carried out with temperatures in the range of only several eV. This allows probes to be inserted directly into the plasma to measure the local current and temperature. The Levitron is not a design for fusion reactors, which are too hot to permit the internal ring. As a device for basic physics experiments, however, the Levitron is an eminently suitable device. The ability to measure local currents was especially helpful in discerning currents driven by electron-cyclotron waves near the cyclotron resonance (Start et al., 1980).

Neutral hydrogen beams, with energy of abut 8.5 keV were injected into a hydrogen plasma with typical parameters $2 \times 10^{11} cm^{-3} < n < 1.5 \times 10^{12} cm^{-3}$ and $1 \text{ eV} < T_e < 4.7 \text{ eV}$. The beams were pulsed on a time scale (kHz) long compare to current penetration plasma induction times, which are only about 30 μsec for such cold plasmas. Since $Z_b = Z_i$, the primary current-drive effect should vanish if $v_b << v_{Te}$, while in the limit $v_b >> v_{Te}$, net current would flow in the beam direction. In the experiment, however, the beam current was cancelled by an electron backcurrent for T_e as low as 4.7 eV, which still is in the regime $v_b/v_{Te} \approx 40$. This is a result that could not be explained either by trapped electrons or a direct ($Z > 1$) plasma, since these effects tend only to decrease the electron backcurrent. The quizzical result might be explained either by a collisionless mechanism that slows down the beam ions, or by a large distortion of the electron distribution function.

The first measurement of a beam-driven current in a tokamak was made by Clark et al. (1980) in experiments on the Culham DITE tokamak. The DITE tokamak has major radius R = 1.17 m and minor radius a = 0.26 m and operates with a toroidal current of somewhat less than 250 kA. The experiments consisted of injecting atomic hydrogen beams with energies up to 24 keV into deuterium or helium target plasmas. The presence of the beam-driven current was then inferred from a drop in the loop voltage.

These experiments confirm the presence of the beam-driven current, although only the parameter regime $Z_b < Z_i$ was investigated. The loop voltage

drop could not be accounted for merely by plasma heating, although no overdrive data ($\Delta V > V$) were taken. The experiments appear to be explainable by theory, and trapped electrons appear to play a negligible role.

In these experiments, about half of the toroidal current (half of 250 kA) appears to be beam driven. It appears, too, that the electron countercurrent is as much as a half the injected beam current, which would be consistent, using Eq. (3.12), with a $Z_{eff} = 2$ background plasma.

G. Currents Driven by Electron-Cyclotron Waves

Start et al. (1982) observed the electron-cyclotron wave current-drive effect on the Culham Levitron device, the same device on which they had observed neutral-beam-driven current (see previous section). Up to 120 W of rf power were injected into the Levitron from the low field side of the device (large major radius). Plasma conditions were in the range $n \approx 3 \times 10^{11} cm^{-3}$ and $T \approx 7.5$ eV.

The primary result was the observation of the effect. This experiment was well-suited to observe the effect because the plasma was cold enough that internal probes could be used to obtain a current profile. Currents were observed to flow in opposite directions near the cyclotron resonance layer $\omega = \Omega_e(x)$, where x here measures distance from the torus axis of symmetry (i.e., along the major radius). As a function of x, Ω_e is monotonically decreasing, so that as waves with, say $k_\parallel > 0$ enter the torus, they are first absorbed by electrons satisfying $v_\parallel = [\omega - \Omega_e(x)]/k_\parallel > 0$, but once the wave crosses (at some critical x_c) the so-called resonance layer, then only electrons satisfying $v_\parallel < 0$ absorb energy from the wave. In the event that the wave is attenuated only mildly in one pass through the plasma, the absorption should be very nearly symmetric (only the nonrelativistic equations apply here) with respect to x_c, so that, according to the theory [Eq. (2.25)], nearly equal, but oppositely flowing, currents should be generated on either side of x_c. Thus, by obtaining the current profile, this artifact of the theory could be observed.

Start et al. observed the current to depend linearly on injected power, and inversely with density, again as would be predicted by theory. In addition, the current per power dissipated was observed to depend linearly on electron temperature. This, too, would be in agreement with theory provided

that the damping of the wave take place at a characteristic resonant velocity that scales linearly with v_T. This is eminently likely since, at low levels of power, v/v_T is the only dimensionless parameter that governs the damping process. The experimental findings are summarized by Figs. (4.10) and (4.11).

The net plasma current generated obeyed an efficiency of about 30 mA/W, which is reasonably consistent with theoretical expectations too. It should be remarked, however, that the plasma parameters attained here are very far from what is required in the useful implementation of the electron-cyclotron wave current-drive effect. It is heartening, nonetheless, to see major aspects of the theory in agreement with the experimental observations, in apparent isolation from other competing or complicating processes.

V. Quasisteady Methods

A. Introduction

The original, and still primary, goal of current-drive research is the completely steady-state tokamak reactor. There may be advantages, however, in generating instead only nearly steady-state currents. These methods are known as pulsed, cyclic methods, or as transformer recharging.

The quasisteady methods have in common a two-phase cycle of operation, wherein the rf or other external power is injected for part of the cycle, the "on" phase, and then shut off during the "off" phase. The current increases during the (rf) on phase and then relaxes during the (rf) off phase. As depicted in Fig. 5.1, concomitant with the cyclic injection of power, other plasma parameters may be caused to vary. These methods seek to exploit the disparity in the resistivity laws. For ohmic current drive, the dissipated power obeys $P_d \sim J^2/\sigma$, where $\sigma \sim T^{3/2}/Z$. For most nonohmic current-drive techniques, $P_d \sim nJ$.

Transformer recharging can occur during the (rf) on stage. During the off stage, the tokamak current may be driven inductively. When the transformer volt-seconds expire, the dc electric field reverses direction to recharge the primary coil before the field can again point in the same direction. In normal pulsed tokamak operation, during the recharging the plasma is evacuated. Alternatively, if the plasma is not evacuated a noninductive current-drive means may be used to maintain the current during

the recharging stage. The noninductive current must be greater than the equivalent steady-state current, to the extent that it must also cancel the ohmic current produced by the reverse electric field.

The most straightforward variation of a parameter is to lower the density during the (rf) on stage, since the efficiency of noninductive current-drive tends to increase with lower density. The density may then be raised during the off stage, since the relaxation time of the current is independent of density. This scheme was first proposed in connection with neutral-beam current-drive by Bolton et al. (1978) and then elaborated on in connection with other schemes of current-drive by Fisch (1981b).

In this chapter, we present the theory of these quasisteady methods and explore the effects of further permutations of parameters. The advantage of these techniques is generally lower average power requirements. Not all of the advantages of steady-state operation are retained, and a higher peak power may be required.

The technological feasibility of these techniques is not explored here in detail. However, one may assume that the composition of the plasma may be varied on the time scale in which particles are confined, which is in the range of several seconds. This is ample time for most applications here, which require oscillating parameters only with periods shorter than the plasma L/R time, which is in the range of several hundred seconds. The experiments discussed in Sec. IV.D, exemplifying rf ramp-up, provide support for the reasonableness of the suggestions proposed here.

B. Circuit Equations

Following Fisch (1982) consider that the total toroidal current density J satisfies during the current generation stage

$$\frac{dJ}{dt} + \frac{J}{\tau_g} = \frac{J_{rf}}{\tau_g} \quad , \tag{5.1}$$

where $\tau_g \equiv L/R_{Sp}$ is the so-called "L over R" time during the current generation stage, where L is the torus inductance and R_{Sp} is the torus resistivity during this stage. For constant rf-induced current J_{rf}, the steady-state current will be reached in the characteristic time τ_g. During the current relaxation stage, there is no driving term to Eq. (5.1) and the current obeys

$$\frac{dJ}{dt} + \frac{J}{\tau_r} = 0 \quad , \tag{5.2}$$

where $\tau_r \equiv L/R_{Sp}$ with parameters defined during the relaxation stage so that τ_r is not necessarily equal to τ_g. We envision that the relaxation cycle of duration T_r alternates with a generation cycle of duration T_g. The electric field during the generation phase obeys Ohm's law

$$E = \eta(J - J_{rf}) \quad , \tag{5.3}$$

where η is the Spitzer parallel resistivity for the parameters present during the generation phase.

The circuit equations (5.1) - (5.3) are supplemented by the constitutive relation

$$\frac{P_{el}}{P_{in}} \equiv \frac{EJ_{rf}}{P_{in}} = G(E) \quad , \tag{5.4}$$

where G(E) is the response function for energy conversion efficiency. When using fast electrons, it is given by Eq. (2.62). [Fisch (1982) uses a constitutive relation less precise than Eq. (5.4), and strictly valid only for $E \to 0$, but then goes on to derive Eq. (5.5b). The approach we adopt here derives the more precise Eq. (5.5a), and shows more clearly the approximation involved in writing Eq. (5.5b).] Neglected in these circuit equations are mutual inductances with, for example, coils that provide the tokamak vertical field, and many other important details of tokamak operation. The approach here, however, is expected to yield the main effects. Further discussion of model circuits in current-drive problems is found in Mitarai and Hirose (1984).

The average efficiency is defined as the time-averaged current over the time-averaged power dissipated, where the time average is taken over a complete (generation plus relaxation) cycle. Note that power is absorbed only during the generation stage. Using Eqs. (5.1) - (5.4), and considering the case when $T_g \ll \tau_g$, $T_r \ll \tau_r$, i.e., oscillating the parameters on a time scale short compared to the current relaxation time so that J_{rf}, J, and E can all be considered constant over the generation stage, the average efficiency can be written as

$$\left\langle \frac{J}{P_d} \right\rangle = \left(\frac{G(E)}{E}\right)\left[1 + \left(\frac{\tau_r - \tau_g}{\tau_g}\right)\left(\frac{J_{rf} - J_o}{J_{rf}}\right)\right] \quad , \tag{5.5a}$$

where J_o is the current minimum (see Fig. 5.1) and J_{rf} is the current that would flow were the current to saturate during the generation phase (i.e., were $T_g > \tau_g$). In deriving Eq. (5.5a), we assumed that negligible kinetic energy is stored in the resonant electrons (but see Sec. 5.5). Note that for $E \to 0$, Eq. (5.4) reduces to the equation for the steady-state efficiency, i.e., $J/P_d = \lim E \to 0\ [G(E)/E]$. In this limit we can write Eq. (5.5a) as

$$\left\langle \frac{J}{P_d} \right\rangle = \left(\frac{J}{P_d}\right)_g \left[1 + \left(\frac{\tau_r - \tau_g}{\tau_g}\right)\left(\frac{J_{rf} - J_o}{J_{rf}}\right)\right] \quad , \tag{5.5b}$$

where $(J/P_d)_g$ is the steady-state efficiency, given plasma parameters characteristic of the generation stage. Equation (5.5b) is valid then for $v/v_R \ll 1$, where v is the resonant electron speed.

Note that if $\tau_r = \tau_g$, then the average current-drive efficiency is just the current-drive efficiency available during the generation stage, yet the plasma parameters during the relaxation stage could be very different. For example, the density during the relaxation stage (on which τ_r does not depend) could be much larger than during the generation stage. This is the scheme of density oscillation and it has utility in conjunction with any noninductive current-drive mechanism that operates more efficiently in low density than in high density plasmas. Most current-drive schemes fall into this category, including current-drive with neutral beams and with lower-hybrid waves.

C. Resistivity Oscillation

Of particular interest is the case $\tau_r \gg \tau_g$. Here, with significant overdrive, i.e., $J_{rf} \gg J_o$, and using Eq. (5.5b), the average efficiency takes the form

$$\left\langle \frac{J}{P_d} \right\rangle \approx \left(\frac{J}{P_d}\right)_g \frac{\tau_r}{\tau_g} \quad , \tag{5.6}$$

from which it is clear that over and above the advantages of parameter oscillations of quantities such as the density which do not affect the relaxation times τ_r and τ_g, there is a factor of τ_r/τ_g to be gained in the

efficiency. Since τ_r and τ_g are inversely proportional to resistivity, the statement is that current-drive can be more efficient either by making the plasma less resistive in the relaxation stage or more resistive in the generation stage. The first possibility comes as no surprise, but presumably τ_r is determined primarily by the parameters that optimize for fusion production. During the generation stage, however, there is the opportunity to design for current-drive efficiency. It is somewhat surprising that it could be advantageous to minimize τ_g, which is proportional to $T^{3/2}/Z$. This might involve running the tokamak in the counter-progressive downgraded regime of dirty (high-Z impurities) and cold, possibly in addition to underdense, plasma.

Not all current-drive mechanisms can exploit the full τ_r/τ_g factor, because the steady-state efficiency $(J/P_d)_g$ might also suffer when τ_g is minimized. For example, in pushing slow electrons, $J/P_d \sim 1/Z \sim \tau_g$, so the two effects cancel and there is no advantage to increasing the ion charge state Z during the generation stage. On the other hand, several leading current-drive methods could exploit this low-τ_g regime. Two examples are offered in Fisch (1982).

Consider the class of current-drive techniques that rely on pushing fast electrons, such as by lower-hybrid or electron-cyclotron waves. For these techniques, $J/P_d \sim (5 + Z)^{-1}$. Then by employing $Z = Z_g$ during the generation stage, we have by Eq. (5.6)

$$\left\langle \frac{J}{P_d} \right\rangle = \left(\frac{J}{P_d}\right)_{Z=1} \left(\frac{\tau_r}{\tau_g(Z=1)}\right) \frac{6Z_g}{5+Z_g} \quad , \tag{5.7}$$

so that for $Z_g \to \infty$, there is an improvement by a factor of 6 over the average efficiency obtained for $Z = 1$ during the generation stage.

The second class of current-drive techniques are those that employ disparate ion charge states, such as through neutral beams or minority species heating. For these techniques, $J/P_d \sim |Z_i^{-1} - Z_b^{-1}|$, where Z_i is the majority ion charge state and Z_b is the beam or minority ion charge state. For $Z_b \gg Z_i$, we have $J/P_d \sim 1/Z_i$ which cancels out any advantage associated with increasing Z_i. On the other hand, for $Z_i \gg Z_b$, we have $J/P_d \sim 1/Z_b$, which is independent of Z_i, so the full factor τ_r/τ_g is available by increasing Z_i during the generation stage.

The reason that polluting the plasma (increasing Z) helps out is because the immediate presence of the noninductive current induces an ohmic countercurrent. This countercurrent, which subtracts from the total current, is impeded by a more resistive plasma.

In practice, the effects described here may be employed simultaneously. Thus, density, temperature, and ion charge state may be caused to vary at once in an effort to improve the average current-drive efficiency. Other means of increasing the resistivity during the generation stage, such as by rippling the toroidal magnetic field to increase the number of trapped electrons, could also be considered. The drawback in all these variations is that while less average power might be required, the peak power required is a factor J_{rf}/J_o greater than in the corresponding steady-state method.

As a practical example to illustrate the multiplicative effect in simultaneously varying parameters, consider oscillating parameters in a tokamak of 8 m major radius and 3 m minor radius. The parameters characteristic of the current generation stage are to be $n = 10^{13} cm^{-3}$, $T = 1$ keV, and $Z = 4.5$. The parameters characteristic of the current relaxation, fusion power generation stage are to be $n = 10^{14} cm^{-3}$, $T = 15$ keV, and $Z = 1$. The fusion output of this D-T reactor is about 2 GW and perhaps 150 MW of continuous lower-hybrid wave power would be required to sustain 8MA of current. Alternatively, oscillating the parameters for about 20 seconds in synchronism with about 50 MW of rf power could sustain the current for a relaxation stage lasting about 1500 seconds. Confinement would then be achieved with peak power of 30% and circulating power of 0.5% of the steady-state case.

Achieving these parameters might require the injection of perhaps a 50% neon impurity concentration during current generation to obtain high Z. Means of removing the neon within several seconds would then also be required. The electron temperature would also need to be regulated to prevent overheating. Note, however, that these ramp-up parameters correspond closely to those employed in the very successful PLT experiment (Jobes et al., 1985).

Lost in this scheme are several advantages of fully steady-state operation, including the constant heat load to the reactor blanket, the constant magnetic fields in the possible presence of superconducting coils, and, possibly most important of all, the minimal tampering with plasma regimes

present in the true steady-state mode. On the other hand, the ohmic coils may not be needed and the plasma need not be restarted entirely afresh with each pulse.

D. Inverting the α-Particle Distribution

Very quick cycling of tokamak parameters, such as the fusion reaction rate, may be equivalent to steady-state operation if the cycling occurs faster than the important time constants for temperature changes in the first wall and the blanket of the reactor. It may be the case that other advantages of steady operation, such as a lessened tendency for disruptions to occur, removal of the ohmic coils, and smaller variations in the magnetic field near the superconductor coils may also be present. These thoughts are entirely speculative, although it seems reasonable that at some very quick cycling rate (perhaps with period of a second or less), the plasma appears to be in an averaged steady state.

Accepting for the moment this possibility, we describe now a speculative suggestion for making available free energy in the fusion products to drive the plasma current.

In a D-T tokamak reactor, energetic α-particles (He^4) are produced through the reaction

$$D + T \rightarrow He^4(3.5\ MeV) + n(14.1\ MeV) \quad . \tag{5.8}$$

This reaction serves a source of α-particles isotropic in α-particle velocity space as depicted in Fig. (5.2a). For typical D-T fusion reactor temperatures, the α-particles are subsequently slowed down primarily by electrons, since typically $v_{Ti} \ll v_o \ll v_{Te}$. The slowing down is independent in this regime of the α-particle velocity since the electrons are so much faster. The slowing down equations may be written as

$$\frac{\partial f}{\partial t} + \frac{\partial \vec{v}}{\partial t}\frac{\partial f}{\partial \vec{v}} = S_\alpha\, \delta(v - v_o) \quad , \tag{5.9}$$

where in this regime

$$\frac{\partial \vec{v}}{\partial t} = -\nu^{\alpha/e}\,\vec{v} \quad . \tag{5.10}$$

The solution to Eq. (5.9) is evidently

$$f = \begin{cases} v_o S_\alpha / v^{\alpha/e} v^2 & , \quad v_{Ti} << v < v_o \\ 0 & , \quad v > v_o \end{cases} \tag{5.11}$$

where the α-particle flux S_α is given by

$$S_\alpha = (P_\alpha/\varepsilon_\alpha)/4\pi v^2 \quad , \tag{5.12}$$

where $P_\alpha = P_f/5$ is the amount of fusion power carried by the α-particles. For $v \approx v_{Ti}$, the α-particle distribution, thermalizing quickly with the ion distribution, will become Maxwellian. Of the most interest here, however, is the $1/v^2$ dependence of f in the regime $v > v_{Ti}$, as depicted in Fig. 5.2b. Because the α-particle distribution is monotonically decreasing, it may effectively damp waves such as the lower-hybrid wave, which may satisfy the unmagnetized resonance condition $\omega/k \approx \omega/k_\perp \approx v_o$. [This question has been raised by Perkins (1982).] For efficient current-drive by lower-hybrid waves, it is important to choose the wave characteristics (ω and $k_\parallel$) such that damping by electrons far exceeds the damping by α-particles.

While there is a worry in steady-state current-drive that α-particles may absorb lower-hybrid waves, consider, instead, a speculative possibility of cycling the fusion production of α-particles. This cycling might be accomplished either by altering the ion mix of fusion reagents in the plasma, by rf heating of energetic ions, or possibly by neutral beam injection. Suppose that α-particle production is begun, but then stopped in a time t less than τ_s, the characteristic slowing down time for energetic α-particles. The distribution function for α-particles then assumes the inverted profile depicted in Fig. 5.2c.

It is tempting now to consider exploiting the free energy in the inverted distribution. There has been the suggestion (Fisch, 1985) that lower hybrid waves could be amplified by the inverted distribution, much in the same way that they are damped by the steady-state distribution. Injecting and amplifying waves in one direction becomes a means then of channeling

α-particle energy to fast electrons traveling in that direction. Unfortunately, this suggestion is mistaken; such waves are not amplified, because even a monoenergetic distribution of α-particles is monotonically non-increasing when projected onto the direction of the wave phase velocity. A more fruitful approach might be to try waves in the ion-cyclotron range of frequencies, where the finite gyroradius of α-particles may allow for wave amplification. Alternatively, a combination of waves or waves and neutral beams might be able to tap this energy. Of course, once the α-particles slow down ($\tau_s \sim 1$ sec), it would be necessary to suspend temporarily both the injection of lower-hybrid waves and the production of new α-particles, so that conditions for obtaining a new inversion can be repeated. In practice, therefore, the cycling period must be less than the slowing down time of the α-particle for maximum exploitation of the effect.

How useful can this effect be, assuming that both the inversion and its exploitation can be accomplished? The available power in α-particles is $P_f/5$. Suppose half of the α-particle energy is extractable and only half of the α-particles may participate. This gives 5% of P_f as a rough bound to the available current-drive power. This is very near the window of utility: if a current-drive mechanism normally requires say 30% of P_f to drive the toroidal current, then the α-particle enhancement is not large enough to make the scheme attractive; on the other hand, if the mechanism requires only 3% of P_f to produce the current, then the α-particle effect is not needed and needlessly complicated. In the regime, however, where the mechanism needs 10% of the fusion power to produce the current, then the α-particle effect can be telling, reducing the required injected power by perhaps 50%.

The ideas here are clearly speculative and vague. Nonetheless, it is perhaps worth bearing in mind that unusual distributions of α-particles in a fusion producing plasma are possible and might be exploitable, even if not as directly as first thought.

E. RF-Assisted Current-Drive

There is a preferred order for combining rf and ohmic current generation means. Such a combination is often known as rf-assisted current-drive, since the rf current supplements the ohmic current to achieve a larger plasma current than could be achieved by ohmic means alone. The advantage of the

combination could be to reduce the volt-second requirements, and hence the size, of the primary coil.

The preferred order is first to inject the rf waves in a low density, low plasma current plasma, and then to employ the ohmic current in a high density, high current and possibly higher temperature plasma. This order is advantageous because at constant capital cost rf-driven current is energy limited, while ohmic-driven current is flux limited. The inductively stored magnetic energy is given by $LI^2/2$, so that, for example, increasing the current from zero to say I/2 requires 1/3 the energy necessary in increasing the current from I/2 to I. Injecting the rf-energy to provide the first I/2 rather than the second I/2 would therefore require 1/3 of the rf energy. Providing this current at lower density might, in addition, relax the rf power requirements, since the same energy conversion efficiency P_{el}/P_{in} could be achieved at lower ramp-up rates (i.e., since $v_R^2 \sim n/E$).

In some instances, the preferred order may not be achievable, possibly because of the cooling requirements on the transformer primary coil, that are more severe if its use is delayed. In such an event, there is a speculative possibility to store energy injected into the tokamak during the ohmic current stage and then to make use of it during a later rf current stage.

This possibility relies on the good confinement of runaway electrons. Supplying the first half of the current by ohmic means provides, in addition to the magnetic stored energy of $LI^2/2$, additional particle kinetic energy. Some of that particle kinetic energy is in the form of heat, but, if the initial discharge is at low density, a large amount of kinetic energy can be injected into runaway relativistic electrons (typically at 10-20 MeV). The fewer and more energetic the runaways, the more stored energy. These electrons, if very energetic, store large amounts of energy, but not current. When the rf waves are then injected to ramp-up further the current, a reverse electric field is induced that opposes both the rf-generated current and the confined relativistic electrons. When these relativistic electrons are decelerated by this counter electric field, their kinetic energy is converted to inductive energy. The rf energy then required can be as low as when the preferred order is used. The method described here is considered speculative, however, because the runaway electrons may not be well-confined and storing several MJ of kinetic energy increases the vulnerability of the tokamak to disruptions.

VI. Reactor Considerations

A. Introduction

Methods of driving current are all suggested with application to an eventual tokamak fusion reactor in mind. In order to assess the utility of these methods, several questions must be answered both with regard to the method and with regard to the reactor on which the method is to be practiced. The method must operate reliably in a fusion environment and the power requirements must be small compared to the fusion power output. Additionally, the capital cost of the apparatus must be small. At the same time, the reactor must benefit from steady-state operation and, of course, the larger the benefit, the more relaxed the requirements on the current-drive method.

A rough and not quite well-defined measure of reactors is the Q value that is attained, where Q is defined as the ratio of power out to power in; $Q > 1$ is necessary for viability and $Q \gg 1$ is necessary for economic competitiveness. The use of currents produced by nonohmic means is likely to limit the attainable Q. Rather than examine the effect on Q in each reactor design, we focus on the quantity P_d/P_f. For P_d/P_f small, the effect on Q will be minimal, although Q must certainly be less than P_f/P_d.

It is difficult to quantify the advantages of nonohmic current-drive. Several features were listed in Sec. I-H, but even a rough cost-benefit analysis is elusive. The most comprehensive attempt to quantify the advantage of steady-state current-drive in reactors was the Starfire reactor study (Abdou et al., 1982). This study was commissioned with the objective of identifying an economically attractive practical reactor (something like a best-case scenario). In this study, the lower-hybrid wave was selected as the driver of steady-state current. The reactor was designed to produce a hollow current profile, because the plasma was too hot (~17 keV) to allow the waves to propagate to the plasma center. Such a profile is likely to be unstable to tearing modes. Were it possible, however, to maintain a plasma with such a current profile, then the efficiency of doing so could be high, because peripheral currents flow in a less dense plasma than do central currents. The result of the Starfire study, therefore, was a desirable, but highly controversial, design. By focusing on a particular realization of what was to

be an economically attractive fusion reactor, the Starfire study did construct, however, a strong case for the desirability of steady-state operation. This point of view is expanded upon by Sheffield (1986).

To attain more centrally peaked current profiles, Yuen et al. (1980) suggest lower density, higher magnetic field operation, so as to allow the lower-hybrid wave to be accessible to the plasma center. Ehst et al. (1982) present an improved account of the Starfire approach, including a discussion of the physics issues regarding stability and integrating the rf system into the overall power plant design.

The utility of nonohmic means of current-drive in reactors may be broader than merely providing for steady-state operation. Reiman (1983) has suggested that lower-hybrid-driven currents might be stable to tearing modes, and there is now some experimental evidence (Cavallo et al., 1985; Parlange et al., 1985; McCormick et al., 1985; Söldner et al., 1986) for the suppression of sawtooth oscillations in current-drive experiments. Chu et al. (1986) report suppression of internal disruptions in inductively driven tokamak discharges through the use of lower-hybrid current-drive. These experiments point to higher central electron temperatures and better energy containment. Rutherford (1985) and Ignat et al. (1985) have suggested that the periodic production of lower-hybrid current at the frequency of magnetic island rotation may control the island growth. Cho et al. (1986) show that lower-hybrid current-drive can provide enough current to stabilize relaxation oscillations in an electron-cyclotron-resonance-produced discharge. There have also been suggestions to use the current-drive effect to pump impurities out of the tokamak (Sperling, 1978; Klima, 1980; Antonsen and Yoshioka, 1986).

Here, we present the main issues concerning current-drive in reactors, with regard to electron-based and ion-based current-drive methods. Electron-based methods rely on the penetration of the tokamak by waves. Trapped-particle effects make impossible, we think, current-drive by low parallel phase velocity waves. The efficiency of schemes which rely on fast electrons is then limited in hot plasmas by relativistic effects. Ion-based schemes, on the other hand, rely on pushing thermal electrons and, subject to the production in the plasma of counterstreaming ion populations, the efficiency of these schemes is higher in hotter plasmas. The main problems are technological.

Both electron-based methods and ion-based methods could be assisted by other passive means of current production, e.g., by the bootstrap effect or by asymmetric reflection of waves back into the plasma. Additionally, it may be useful to employ these methods in a quasisteady manner, as discussed in Chapter V. Here, however, we confine the discussion to the major methods. Considerations of quasisteady methods in reactors have been made by Ehst et al. (1984) and by Singer and Mikkelsen (1982). Here, we focus on the goal of entirely steady operation.

A main conclusion here is that, in terms of efficiency alone, both electron-based and ion-based methods are satisfactory, although in each case there are other concerns. These concerns include the propagation and damping of waves and the development of efficient neutral beam sources. In an attempt more to outline the issues than to present reactor blueprints, these concerns are left unanswered here, although relevant literature is cited. This approach is adopted because even a more thorough consideration now would not yield conclusive answers. The message here is that these methods of current-drive are promising and cannot be ruled out, but they are far from sure.

B. Electron-Based Methods

The most extensive experimental investigation and theoretical scrutiny has been given to the method of generating current by lower-hybrid waves. Accordingly, probably more concerns have been raised in connection with this method than any other method, with the result that, in addition to the concerns, the method per se enjoys the most confidence. The most difficult remaining concern here is whether results obtained on present-day experiments can be extrapolated to the reactor regime, where relativistic effects are thought to limit the current-drive efficiency and where penetration of the wave to the plasma center may be more difficult to achieve.

In other respects, the method of accelerating fast electrons, either by lower hybrid waves or by other fast waves, appears eminently viable. The rf power may be generated efficiently (70% electric to rf power is typical) and may be brought conveniently to the tokamak by means of waveguides. The fraction of the tokamak wall area that need be taken up by the waveguides is small, perhaps 1% if modest demands on waveguide capabilities are assumed (~ 20 MW/m^2), and possibly an order magnitude lower for state-of-the-art

waveguides. This calculation is arrived at by noting that the neutron wall loading, H, is at most 2-4 MW/m^2. The waveguide power required to sustain the current can then be written as

$$P_{wg} = (1/\eta_D)(H/0.8)(A/A_{wg})(P_d/P_f) \quad , \tag{6.1}$$

where η_D is the fraction of rf power absorbed and A_{wg}/A is the fraction of available wall area devoted to the waveguide opening. Since the current-drive efficiency must in any event be designed for circulating power P_d/P_f less than 10%, and $\eta_D \to 1$ is quite reasonable, the modest demand on the waveguides themselves results.

In order for the lower-hybrid wave to be accessible to the tokamak center, its parallel phase velocity must not be too large. This condition may be expressed approximately as

$$n_\parallel \equiv ck_\parallel/\omega > 1 + 0.6\beta_{4\%}/T_{10} \quad , \tag{6.2}$$

where $n_\parallel$ is the parallel index of refraction, $\beta_{4\%}$ is the ratio of plasma to magnetic pressure in units of 4% (a typical value), and T_{10} is the electron temperature normalized to 10 keV. While the necessity for accessibility of the wave represents a lower bound on the index of refraction or, equivalently, an upper bound to the parallel phase velocity for the lower-hybrid wave, the requirement that the plasma not absorb all the wave energy before the wave penetrates the plasma center implies that too low a parallel phase velocity is also not possible. Low parallel phase velocities imply an interaction of the wave with the bulk of the electron velocity distribution, which more easily absorbs the wave power than does the tail of the distribution (where there are fewer electrons). The damping of the wave can, in principle, always be made manageably small if the spectrum of waves could be focussed in only a narrow range of parallel phase velocities. Fewer resonant electrons imply a smaller damping rate, since the velocity distribution of electrons, once a quasilinear plateau is formed, is unaffected by higher wave power. It is unclear, however, whether such focusing can be achieved; it would require more waveguides and it would be more susceptible to processes that tend to spread the spectrum. An example of such a process is the deflection of the entering lower hybrid waves by drift wave turbulence at the plasma periphery.

Although reactors require more current and, hence, more rf power than today's experimental tokamaks, effects nonlinear in the rf power will actually be less likely to occur in reactors. This implies the absence of some possibly worrisome effects. There are several reasons why such effects are less likely to occur. Because reactors are larger, the current density J, which scales as B_p/a, can be smaller given constant peripheral poloidal magnetic field B_p but larger minor radius a. Lower current density then implies lower rf power density. The current density may be written as $J = -env_D$, where v_D is the electron drift velocity. Because the density and temperature in reactors is relatively high, together with the fact that the current density is relatively low, the parameter v_D/v_T will be small. This parameter is a measure of the distortion of the electron velocity distribution function from a Maxwellian distribution (which tends to be stable). The same reasoning leads to small distortions of the distribution function when all of the current is assumed to be carried by high energy electrons. Because the reactor plasma is hot and dense, resonant electrons are numerous and fast so that only relatively few and mildly energetic electrons (in comparison to thermal electrons) need carry the current.

For example, a variety of nonlinear parametric decay effects are sensitive to the parameter $(E_\perp/B)/(T_e/m_i)^{1/2}$ (Porkolab, 1977). When lower-hybrid waves are employed to sustain the current in a reactor plasma, this parameter can be shown (Fisch, 1978) to be approximately $\beta n_\parallel^3(v_o/\omega_{pi})(a/R)$, which is quite small and indicative that parametric effects are likely absent. Other nonlinear effects that may concern us include resonance broadening (Dupree, 1966), which has also been shown to have little effect for parameters of interest here (Kritz et al., 1981). Some present-day experiments are thought to exhibit large enough asymmetry in the electron distribution function so as to excite the Parail-Pogutse instability (e.g., Liu et al., 1985). This effect does not always occur in present-day experiments, and there is some debate concerning its importance when it might occur. However, in any event, in a steady-state reactor, the electron anisotropy would be far too small to support this instability.

The efficiency of current-drive by a narrow spectrum of lower-hybrid waves, taking into account both relativistic resonant electrons and reactor regime background temperatures, was exhibited in Fig. 2.12. The relevant

electron temperature regime for first generation D-T reactors is $1 \lesssim T_{10} \lesssim 2$, and in order to resonate with sufficiently many electrons to produce the required current, the waves must have wave phase velocities in the vicinity $\omega/k_\parallel \approx 4.5\ v_T$. For $T_{10} = 1$, this corresponds to a wave refractive index $n_\parallel = c/(\omega/k_\parallel) \approx 1.8$ and to resonant electrons of about 100 keV. From Fig. 2.12, we have approximately

$$\frac{I}{P} \approx \frac{0.6}{n_{14}R_1}\left[1 + \frac{T_{10}-1}{3}\right]\frac{\text{Amps}}{\text{Watt}}, \quad (n_\parallel \approx 1.8,\ 1 \lesssim T_{10} \lesssim 2.5) \quad . \qquad (6.3a)$$

Note that waves with $n_\parallel \lesssim 1.8$ satisfy the accessibility condition, Eq. (6.2), for typical β in the indicated temperature range.

In many experiments, it is believed that electrons with energy on the order of 200 keV have been excited. Waves that resonate with these electrons would have a parallel index of refraction $n_\parallel \approx 1.4$. Such waves have parallel velocity $\omega/k_\parallel \approx 4.5\ v_T$ for electron temperature $T_{10} \approx 2$, so that for $T_{10} \gtrsim 2$, there are sufficient resonant electrons to produce the needed current. For such a parameter regime, we have from Fig. 2.12

$$\frac{I}{P} \approx \frac{1.1+0.2(T_{10}-2.5)}{n_{14}R_1}\frac{\text{Amps}}{\text{Watt}}, \quad n_\parallel \approx 1.4, \quad 2 \lesssim T_{10} \lesssim 5). \qquad (6.3b)$$

Note that waves with $n_\parallel \approx 1.4$ satisfy the accessibility condition, Eq. (6.2), for typical β in the indicated temperature range, although this temperature range is unlikely for first generation D-T fusion reactors.

It is important to bear in mind that the application of Eqs. (6.3) is limited also by the ability of lower hybrid waves to penetrate the plasma center. Here, we must be guided by ray tracing and other wave propagation studies and by experiments employing different launch structures. Although we discount as unlikely the possibility of unwanted effects nonlinear in the lower-hybrid energy, linear effects such as given by the ray-tracing studies or scattering by plasma turbulence may prove worrisome, but conclusions now are premature.

Other waves, with different propagation characteristics, may be brought to bear on fast electrons. The efficiency possible using electron-cyclotron waves is only somewhat lower than that available with lower-hybrid waves as indicated in Fig. 2.11. Reactor possibilities utilizing this wave have been

explored by Firestone et al. (1985). Electron-cyclotron waves, which are free space waves, may more easily penetrate the plasma center. The technology of generating these higher frequency waves continuously and efficiently is considerably more difficult. In addition, these waves tend to deflect away from high density plasma. A third wave that interacts with high velocity electrons is the fast wave. This wave, like the lower-hybrid wave, diffuses electrons in the parallel direction, and so enjoys the same efficiency of current production. In addition, high power, high efficiency sources are available. The propagation characteristics differ from both the cyclotron wave and the lower-hybrid wave, and so this wave may penetrate where the others fail. Theoretical calculations of current-drive employing this wave were performed recently by Andrews and Bhadra (1986). Also Ehst et al. (1986) calculate the propagation of this wave consistent with the magnetic equilibrium arising from the wave-generated current. Again, however, firm conclusions are not yet possible and there is no experimental evidence in tokamaks for the current-drive effect using this wave.

C. Ion-Based Methods

Ion-based methods of steady-state current-drive include current-drive by neutral beams or by other schemes that exploit counterstreaming ions. These other schemes produce or maintain the counterstreaming ion populations, for example, by minority species heating or by direct rf-heating of the injected ions.

The overall efficiency, E_{ff}, of producing current by neutral beams might be expressed as

$$E_{ff} = (I/P) \times \eta_{ads} \times \eta_{beam} \quad , \tag{6.4}$$

where I/P represents the current-drive efficiency given by Eq. (3.14), η_{ads} is the fraction of the beam absorbed near the plasma center, and η_{beam} is the efficiency of producing the beam. This last term is important because the maximum efficiency tends to occur at energies (several MeV) for which the technology of high efficiency sources (η_{beam} high) is presently only in a developmental stage.

A comprehensive study of the optimization of steady-state beam-driven tokamak reactors was performed by Mikkelsen and Singer (1983). Here, we limit ourselves to discussing the important scalings and trade-offs.

The fraction of beam energy that is usefully absorbed, η_{abs}, is a sensitive function of the plasma density, the plasma size, and the beam energy. Mikkelsen and Singer find that for INTOR (an International Tokamak Reactor study) parameters ($n \sim 10^{14}cm^{-3}$, $R \approx 5.3$ m) the optimum beam absorption occurs for beam energies of 1 to 2 MeV/amu. For denser or larger plasmas, the beam energy would have to be larger in order to penetrate the plasma center. For less dense or smaller plasmas (not a typical reactor regime), the beam must be less energetic, or else it would merely pass through a relatively transparent plasma.

To appreciate the scaling for neutral-beam current-drive, or, more generally, all current-drive schemes that exploit counterstreaming ion populations, let us reiterate a rough derivation of the current-drive efficiency, I/P. The leading order effect is

$$J/J_b = 1 - Z_b/Z_i \quad , \tag{6.5}$$

as given in Eq. (3.13). A crude measure of the power dissipated is given by

$$P_d = \nu n_b m_b v_b^2/2 = m_b v_b J_b(\nu_s^{b/i} + \nu_s^{b/e})/2eZ_b \quad , \tag{6.6}$$

where $\nu_s^{b/i}$ and $\nu_s^{b/e}$ depict slowing down rates of beam ions on, respectively, bulk ions and bulk electrons. Thus

$$\frac{J}{P_d} = \frac{2e\, Z_b^2(1/Z_b - 1/Z_i)}{m_b(\nu_s^{b/i}+\nu_s^{b/e})v_b} \quad . \tag{6.7}$$

Now $\nu_s^{b/i} \sim 1/v_b^3$, while $\nu_s^{b/e} \sim 1/T_e^{3/2}$ (and is independent of v_b). Therefore, the efficiency J/P_d is maximized when $\nu_s^{b/i} \sim \nu_s^{b/e}$, which implies that the maximum efficiency occurs at some $v_b = v_*$, where $v_* \sim T_e^{1/2}$. Typically, $v_* \sim 10\, v_{Ti}$, corresponding to several MeV in a reactor plasma ($T_i > 15$ keV). For $v_b < v_*$, $J/P_d \sim v_b^2$, and for $v_b > v_*$, $J/P_d \sim 1/v_b$. Using $v_* \sim T_e^{1/2}$ and $\nu_s^{b/i} \approx \nu_s^{b/e} \sim n_e z_b^2/T_e^{3/2}$, it can be seen that (except for a fairly insensitive

dependency on m_b and m_i), the optimum efficiency scales as given in Eq. (3.14), namely $I/P \sim T_e/nR$.

The regime $v_b < v_*$ presents an important trade-off: decreased current-drive efficiency [$\sim(v_b/v_*)^2$] vs. increased beam production efficiency η_{beam}, since less energetic beams can be produced more efficiently. The regime $v_b > v_*$ is of marginal interest, since both the current-drive efficiency decreases ($\sim v_*/v_b$), and these more energetic beams are even more difficult to produce (smaller η_{beam}). Unless the plasma were so dense or so large that a less energetic beam could not penetrate, this regime is not of particular interest for driving current.

Note that the efficiency (I/P) of current-drive by neutral beams can be quite large near $v_b = v_*$ [Eq. (3.14)]. Moreover, since thermal electrons contribute to the effect, the favorable scaling with electron temperature persists even at higher temperatures, for example, when superthermal electrons become relativistic. The primary concerns with this method are the production and absorption of the beam ions. These concerns encompass both the efficiencies of production and absorption, as well as the maintenance of hardware in a fusion environment. Neutral beam sources must be placed close to the reactor, and since, as opposed to rf waveguides, bends and windows are not permitted in the structures that deliver the beam to the plasma, the source itself may be subject both to direct bombardment by fusion neutrons and to contamination by tritium. Additionally, for tangential injection, the neutral beam source must itself be oriented tangential to the tokamak, which can add to the shielding difficulties.

Should it be possible to produce or maintain these beams by rf waves, some of these concerns could be alleviated. The beam could be optimized for penetration only, for example, while rf waves might then accelerate the injected beam. Note that in the scheme of minority species heating, where the beam is produced entirely by rf waves, the efficiencies η_{abs} and η_{beam} may be, effectively, quite high, while the technological problems associated with neutral beam injectors are absent. Note too, however, that the current-drive efficiency, I/P, of minority species heating is less than that attainable directly with neutral beams, and the scheme relies upon physics of the injected wave. Methods of producing counterstreaming ions, or maintaining counterstreaming ions, with waves do share with the neutral-beam method the

same attractive scaling with electron temperature. A fair summary is that there may be considerable advantages associated with using waves in this manner, but using these waves is still untested and speculative.

Let us compare generating current by neutral beams with generating current by lower-hybrid waves. In a first generation D-T reator, operating at about 20 keV, both methods may yield an efficiency as high as 0.5 amp/watt. The possibility exists that the lower-hybrid current-drive efficiency could be a factor of 2 higher should lower $n_{\parallel}$ waves penetrate the tokamak. The efficiency of producing neutral beams as energetic as several MeV, however, is likely to be considerably smaller than the efficiency of producing lower-hybrid waves. A second distinguishing concern is the plasma purity. The neutral beam current-drive effect relies here on an impure plasma, say effective ion charge state $Z_{eff} = 2$, if deuterium beams are to be employed. Such impurities contribute to the plasma pressure and are confined at the expense of the fusile hydrogen. It may be, however, that such impurities are in any event unavoidable. The effect of such impurities on the lower-hybrid current-drive efficiency is slight; e.g., nonrelativistically the efficiency scales as $1/(5+Z_{eff})$. The remaining comparisons concern the possible individual problems associated with each method: on one hand, whether the neutral beam apparatus can withstand the reactor environment and whether the energetic ion sources can be developed; and, on the other hand, whether lower-hybrid waves can successfully propagate to the plasma center. At present, the experimentation on the lower-hybrid method is far more advanced, and, in the best of theoretical worlds, wave current-drive is preferable. However, insurmountable problems associated with either method cannot be ruled out.

D. Steady-State Reactors

Ehst et al. (1985a) compare steady-state and pulsed operation, including quasisteady-state methods, with particular concentration on costs associated with thermal fatigue in the first wall, the limiter or divertor, the breeder material, and the blanket structure. In addition, the capital cost associated with thermal storage between pulses is examined. A companion paper (Ehst et al., 1985b) considers the mechanical fatigue of structures associated with the magnetic fields and compares reactors with different burn cycles. Ehst et al. conclude that burn pulses longer than one hour should be sought because of

costs associated with thermal and mechanical fatigue. Additionally, unless plasma disruptions can be guaranteed by other means to be rare (less than once in 10^4 pulses), to release little energy (less than 200 J/cm^2), or to be directed away from the first wall, they are likely to be a dominant issue. Steady-state operation is thought to be helpful in reducing significantly the likelihood of occurrence of these disruptions. Ehst et al. set a goal of $0.49/R_1$ A/W for the efficiency of current generated by noninductive means. The meeting of this goal, expressed by Ehst et al. as 0.07 A/W in a 7 m major radius reactor, then implies that the steady-state tokamak with current provided by the nonohmic means is to be preferred over the conventional pulsed tokamak.

The raw criteria of 0.07 A/W is, in principle, attainable either by electron-based or by ion-based methods. The theoretical maximum no doubt, however, will not be attained because of various inefficiencies such as those arising from unwanted reflections of the waves or the lack of a perfect endfire antenna or waveguide array.

On the other hand, there are some possibly helpful effects not accounted for in the present calculations. The most hoped for effect is the so-called neoclassical bootstrap current (Bickerton et al., 1971). The theory of the bootstrap current is that sources of charged particles or heat at the magnetic axis produce toroidal current as the particles or heat flow towards the plasma periphery. The effect has not been verified experimentally. Were it present, however, the bootstrap current in a fusion plasma might provide more than half the required current, halving or more the noninductive power requirements.

Additionally, these calculations have not taken into account passive current-drive effects, such as arising from the asymmetric reflection of plasma radiation or the asymmetric loss of α-particles. Any current arising from these effects, while not likely to provide the total required current, reduces the amount of additional current required of the nonohmic current-drive means.

All noninductive current-drive schemes appear to work best in low density, large, high temperature reactors. The scaling is derived as follows: By Ampere's equation, to produce a poloidal magnetic field B_p, a uniform current density,

$$J = 2B_p/\mu_o a \quad , \tag{6.8}$$

is required. Tokamaks are thought to operate best in the regime

$$\beta_p \equiv \frac{n(T_e+T_i)+E_\alpha}{B_p^2/2\mu_o} < \frac{R}{a} \quad , \tag{6.9}$$

where E_α is the α-particle pressure. The fusion power density in a D-T reactor is given approximately by

$$P_f = 8.8 \times 10^5 \, n_{14}^2 \, (3T_{10}-2) \ W/m^3 \ , \ 1 < T_{10} < 3 \quad . \tag{6.10}$$

Taking $\beta_p = R/a$, and using Eq. (6.8) and Eq. (6.9) neglecting E_α, it is possible to write Eq. (1.5). A convenient formula relating the normalized efficiency J/P_d (J normalized to $-env_T$ and P_d normalized to $\nu_o n m_e v_T^2$) to the current/power I/P used in Sec. VI.B and VI.C is

$$\frac{I}{P} = 2 \times 10^{-2} \left(\frac{T_{10}}{R_1 n_{14}}\right) \left(\frac{J}{P_d}\right) \frac{\text{Amps}}{\text{Watt}} \quad . \tag{6.11}$$

Accordingly, Eq. (1.5) for the fraction of circulating power can be written in an alternative notation as

$$\frac{P_{rf}}{P_f} = \frac{0.3 \, T_{10}}{(I/P)R_1 n_{14}} \frac{1}{(n_{14}T_{10}a_1R_1)^{1/2}(3T_{10}-2)} \quad , \ 1 \leq T_{10} \leq 3 \tag{6.12}$$

and I/P is given in amps/watt, *e.g.*, from Eqs. (6.3) or Eq. (3.14).

Optimization of tokamak parameters is a separate art in itself. From Eq. (6.12), it is apparent that large, high temperature tokamaks minimize the *circulating power required for steady-state operation*. Low density is desired because it allows the temperature and size to be large, keeping the wall loading and magnetic field constant. For example, we can write the approximate relation

$$a_1 n_{14}^2 \, (3T_{10}-2) = 10 \ H/(3.5 \ MW/m^2) \quad , \tag{6.13}$$

where H is the wall loading (power of fast fusion-produced neutrals per wall area). Large wall loading is efficient for energy conversion; too large

implies deterioration of the wall ($H < 3.5$ MW/m^2 is a typical design parameter). While large reactors may be relatively cheaper, in terms of circulating power, to operate continuously using noninductive currents it is also true that these tokamaks could anyway operate in somewhat longer pulses using inductive means. Such consideration may be moot, however, in view of the preference at present for smaller tokamaks (e.g., Design 1 in Table 1).

Application of noninductive current-drive techniques to later generation tokamak reactors, relying on reactions other than the D-T reaction, is unlikely. This is because the fusion cross sections for these reactions are much smaller, so in order to extract the same fusion power density, these reactors tend to be designed much denser.

E. Conclusions

The purpose of this review has been to summarize recent exciting developments in the theory of current generation. One must hesitate before pronouncing on the utility of these techniques for steady-state tokamak operation, because there is not yet experimental evidence of these effects in reactor regimes, because the eventual tokamak reactor design is itself still unclear, and because there is not even a guarantee that the tokamak reactor would be useful but for the problem of steady-state operation [see e.g., Lidsky, (1983), for a somber appraisal of tokamaks].

It does appear, however, that powerful techniques exist for producing continuous current in reactor plasmas. Several nicely crafted experiments have established the underpinnings of the theory of current generation by lower-hybrid waves. Other methods, too, enjoy favorable prospects. Research is underway in finding uses for these currents in addition to continuous operation and in exploiting the theoretical constructs that have been developed to quantify these effects.

Although it may be premature to pronounce on the future of steady-state tokamak operation based on noninductive means of current generation, it is timely to be enthusiastic that the now extensive scrutiny to which these methods have been subjected, as reviewed here, has failed to uncover fatal flaws. The continuance of this trend bodes well for the steady-state tokamak.

ACKNOWLEDGMENTS

It is a pleasure to acknowledge a long, fruitful, and most enjoyable collaboration with C.F.F. Karney that touched on many of the diverse topics reviewed here. Many helpful and appreciated comments on the manuscript were provided by V. Chan, D. Ehst, A. Kritz, F. Leuterer, M. Porkolab, and J. Stevens. This article might not have been written were it not for the encouragement of D. Baldwin.

This work was supported by the U.S. DoE under contract DE-AC02-76-CH03073. The author appreciates the warm hospitality of Courant Institute of Mathematical Sciences and the IBM T.J. Watson Research Center, where portions of this article were written. The author gratefully acknowledges fellowship support provided by the John Simon Guggenheim Memorial Foundation.

FIGURES

Fig. 1.1 Waves injected into a tokamak (schematic). Tokamak magnetic field has two components: a toroidal component encircling the torus hole and a poloidal component encircling the minor cross section. Wave energy is absorbed by resonant particles.

Fig. 1.2 Apparatus for injecting waves into tokamaks. The lower-hybrid grill, is a phased array of waveguides. The ion-cyclotron resonance heating (ICRF) apparatus is a phased array of current loops. The electron-cyclotron resonance heating (ECRH) horn is a flanged waveguide pointed tangentially into the torus.

Fig. 1.3 Schematic representation of the TFTR tokamak with neutral beam injector.

Fig. 1.4 Two regimes for current-drive: parallel acceleration of slow electrons with Alfvén waves and parallel acceleration of superthermal electrons with lower-hybrid waves.

Fig. 1.5 (a) Contours of steady-state electron velocity distribution f when lower-hybrid waves are injected with parallel phase velocities between three and five times thermal velocity v_T. (b) Surface of f (truncated at low speeds). (Karney and Fisch, 1979).

Fig. 1.6 Reported steady-state current by lower-hybrid waves vs. year. Initials correspond to various tokamak facilities. (Hooke, 1984).

Fig. 1.7 (a) Pushing electron along path $\vec{S}$ from velocity space location 1 to velocity space location 2. (b) Current carried by electron as function of time and initial coordinate.

Fig. 1.8 Schematic illustration of lower-hybrid wave coupling from a waveguide to the plasma, propagation through the plasma, and eventual absorption by the plasma. Plasma density n and plasma temperature T increase with distance into the plasma. Magnetic field B is perpendicular to density and temperature gradients. This wave, a mode of the plasma, cannot propagate in the free space region at the periphery; it may be scattered by a turbulent region; and it propagates through the plasma along characteristic "resonance cones," with well-defined boundaries, and with electric field E polarized in the direction of propagation.

Fig. 2.1 Normalized efficiency J/P_d as a function of average w^2 in a narrow spectrum for small $\vec{S}_w$. The waves exist only for $x < 1$. Open circles denote cyclotron damping and closed circles denote Landau damping. Lines show the theoretical prediction of Eq. (2.25), (Karney and Fisch, 1981).

Fig. 2.2 The parallel distribution function F(w), for the case shown in Fig. 5. In (b) the vertical scale has been magnified tenfold over that in (a). The dashed line in (b) shows the initial Maxwellian distribution, (Karney and Fisch, 1979).

Fig. 2.3 A plot of $\log_e J$ against $K \equiv w_1^2/2 - \log_e[\Delta(w_1-w_2)/(8\pi)^{1/2}]$. The dots give the numerical results. The line is the prediction of the 1-D theory given in Eq. (2.30), (Karney and Fisch, 1979).

Fig. 2.4a Comparison of the bremsstrahlung emission from numerically computed (solid lines) and analytically given (dashed lines) electron distribution function for the case $w_1 = 5$, $w_2 = 8$, $Z = 1$, and $T = 5$ keV (Fisch and Karney, 1985).

Fig. 2.4b Bremsstrahlung emission in the PLT experiment at $h\nu = 100$, 200, 300, and 400 keV in an approximately 1 keV plasma. Solid lines slow bremsstrahlung emissions from a distribution function that is a numerical solution of the Fokker-Planck equation. Parameters employed in the numerical solution are consistent with experimental observables (Stevens et al., 1986).

Fig. 2.5 Steady-state distribution functions for $\vec{D} \to \infty$ with $w_1 = 4$ and $w_2 = 5$. Figures (a) and (b) show the cases of electron-cyclotron waves and lower-hybrid waves, respectively (Karney and Fisch, 1981).

Fig. 2.6 The streamlines of the flux, $\vec{S}$, for the case shown in Fig. 5. Equal amounts of flux flow between adjacent contours (Karney and Fisch, 1979).

Fig. 2.7 The runaway probability $R(\hat{u} \equiv \hat{v}/v_R)$ for $Z = 1$. Parts (a) and (b) show R on two different scales. In (a), the contours are equally spaced at intervals of 0.05. In (b) the lowest 7 contours are geometrically spaced at intervals of $10^{1/3}$ between 10^{-3} and 10^{-1}; the remaining contours are equally spaced at intervals of 0.05 as in (a), (Karney and Fisch, 1986).

Fig. 2.8 The energy imparted to the electric field by the stopped electrons, $W_s(\vec{u} \equiv \vec{v}/v_R)$, for $Z = 1$. The innermost contours are equally spaced at intervals of 0.005 between -0.05 and 0.05. The remaining contours are equally spaced at intervals of 0.05 (Karney and Fisch, 1986).

Fig. 2.9 Efficiency for lower-hybrid current-drive (a) and for electron-cyclotron current-drive (b), (Karney and Fisch, 1986).

Fig. 2.10 Contour plots of $\chi(\tilde{p})$ for $Z = 1$ and (a) $\theta = 0$ and (b) $\theta = 0.01$. The contour levels are evenly spaced with increments of 50 qp_t^4/m^2r. The higher levels are on the right [i.e., $a\chi(p)/ap_{\|} > 0$], (Karney and Fisch, 1986).

Fig. 2.11 Efficiencies for localized excitation for (a) Landau-damped waves (parallel diffusion) and (b) cyclotron-damped waves (perpendicular diffusion). The different curves show the efficiencies for different temperatures as indicated by θ. In all cases $Z = 1$. The top scale gives the kinetic energy of the electrons. The right scale gives the efficiency for a plasma with $n = 10^{20}m^{-3}$, $\log\Lambda = 15$, and major radius $R = 1$ m. Here, $\nu_c \equiv r/m^2c^3$, (Karney and Fisch, 1986).

Fig. 2.12 *Efficiencies for a narrow Landau spectrum as a function of phase* velocity v_p. The curves correspond to the various values of θ. In all cases $Z = 1$. The top scale gives the parallel index of refraction $n_\parallel = c/v_p$. The right scale gives the efficiency for the same conditions as in Fig. 2.11.

Fig. 3.1 Normalized J/P_d vs average normalized parallel phase velocity w_a. The three cases considered are Landau damping (open circles), magnetic pumping (x's), and Alfvén waves (closed circles) in the limit $D_{QL} \to 0$. The solid lines are rough semianalytic fits to the data (Fisch and Karney, 1981).

Fig. 3.2 Schematic representation of current-drive by electron trapping and detrapping. Trapped electrons are located between slanted lines.

Fig. 3.3 Current-drive by perpendicular heating at mirror throats.

Fig. 3.4 Schematic representation of contours of response function g for (a) homogeneous plasma, and (b) in toroidal geometry (Antonsen and Hui, 1983).

Fig. 3.5 Wave-induced diffusion along nearly constant energy contours in velocity space. Diffusion is from low energy to high energy along the contours marked by arrows, but taking place only at the resonant regions denoted by vertical lines.

Fig. 3.6 Schematic representation of current-drive by counterstreaming ion populations in frame of reference of zero ion current. (a) One ion species (say hydrogen, $Z_i = 1$) with beam velocity v_b much greater than electron thermal velocity v_{Te}. (b) Counterstreaming ions with disparate ionic charge states.

Fig. 3.7 Ratio F of net current to fast ion current as a function of v_e^2/v_b^2 for $Z_{eff} = 2$ and several values of ε (Start et al., 1980).

Fig. 3.8 Net current times plasma major radius per megawatt of injected neutral power as a function of electron temperature for deuterons injected into a 1:1 deterium/tritium (D-T) plasma. The upper set of curves are for Z_{eff} = 1 and the lower set for Z_{eff} = 2. Curves are for beam energies of 40 and 160 keV and for ε = 0.03 and 0.1. The electron density is 1 × $10^{14}cm^{-3}$ (Start et al., 1980).

Fig. 3.9 Current-drive by asymmetric wave heating of minority species ions with ion charge state Z_α > 1 in hydrogen plasma. Hydrogen thermal velocity is denoted by v_{Ti}.

Fig. 3.10 Thermoelectric effect by plasma heating adjacent to pellets (Fisch, 1984).

Fig. 3.11 Phased pellet injection. Shadow effect is maximized for pellet spacing satisfying $\Delta x = \Delta z v_{Te}/v_p$ (Fisch, 1984).

Fig. 3.12 Asymmetric reflection of synchrotron radiation.

Fig. 4.1 Schematic diagram of the Synchromak device (Fukuda, 1978).

Fig. 4.2 Typical plasma shot with B = 14 kG and 90° phasing between waveguides. The solid lines show the shot with the rf power on (top frame) and the dotted lines show the typical shot with no rf power added. The third frame from the top exhibits the loop voltage drop; the bottom two frames show electron-cyclotron (I_c) and hard x-ray (H_x) emissions, (Yamamoto et al., 1980).

Fig. 4.3 (a) Superimposed signals with and without rf power: One-turn loop voltage (V_L) 0.8 V/div., total current (I_t) 8 kA/div., rf power 30 kW/div. (b) Loop voltage with dI/dt = 0 at high rf power: loop voltage 0.4 V/div., total current 4 kA/div. (baseline suppressed), rf power 30 kW/div. (c) Current increment ΔI_t normalized to rf power transmission coefficient T as a function of array; phase $\Delta\phi$ with a 4-msec rf pulse. Plasma parameters, I_t = 30 kA, n = 2 × $10^{12}cm^{-3}$, B = 8 kG. (Luckhardt et al., 1982).

Fig. 4.4 Steady-state current-drive efficiency at B = 8 Tesla. (a) Line-averaged density times current vs. power. (b) Efficiency vs. density. (Porkolab et al., 1984).

Fig. 4.5 Current vs. time at $n = 2.2 \times 10^{12} cm^{-3}$ at different rf powers. (Jobes et al., 1985).

Fig. 4.6 Efficiency W'/P_{rf} vs. injected rf power P_{rf} [where $W' \equiv (d/dt)(LI^2/2) - P_{ext}$] for I = 200 kA and a range of other parameters. (Jobes et al., 1985).

Fig. 4.7 Current ramp-up regions (schematic). Electrons accelerated by waves in collisional region A lose incremental energy to plasma heat. Electrons accelerated in collisionless region B are subsequently decelerated primarily by the dc toroidal electric field.

Fig. 4.8 Power flow (schematic) in rf ramp-up experiments.

Fig. 4.9 P_{el}/P_{rf} v_{ph}/v_R for 250 PLT shots. The rf power P_{rf} varied from 0 to 300 kW, the density n from 1.5×10^{12} to $6.0 \times 10^{12} cm^{-3}$, the plasma current I from 150 to 400 kA. Three waveguide phasings were used, 60°(*), 90°(+), and 135°(#). (Karney et al., 1985).

Fig. 4.10 Current vs. probe position. Inset: coil signals for rf input above and below the ring. (Start et al., 1982).

Fig. 4.11 Current per unit power times density (in units of $10^{16} m^{-3}$) vs. electron temperature. (Start et al., 1982).

Fig. 5.1 Cyclic oscillation of plasma parameters synchronous with injection of rf power P_{rf} or other external power source designed to drive nonohmic current.

Fig. 5.2 Current-drive by exploiting a periodic inversion of the distribution of α-particles are born at 3.5 MeV (a) and tend towards a monotonically decreasing energy distribution (b). For short times, the α-particles temporarily assume an inverted energy distribution (c).

REFERENCES

Abdou, M. et al., 1982, STARFIRE/DEMO - A Demonstration Tokamak Power Plant Study, Argonne National Laboratory Report ANL/FPP/TM-154.

Abe, H., 1984, in Proceedings Top. Conf. on Radiation in Plasma, Trieste, Italy, June 1983 (World Scientific Publishing Pte, Ltd., Singapore) Vol. 1, p. 177.

Akiyama, H., J. Gahl, K. Rathbun, M. Kristiansen, and M. Hagler, 1985, Rev. Sci. Instr. 56, 1151.

Alikaev, V.V. and V.L. Vdovin, 1983, Sov. J. Plasma Phys. 9, 538.

Alikaev, V.V. et al., 1983, in Proceedings of the Ninth Int. Conf. on Plasma Physics and Controlled Nucl. Fusion Research, Baltimore, MD, USA, 1982 (IAEA, Vienna) Vol. I, p. 239.

Alikaev, V.V., et al., 1985, Sov. J. Plasma Phys. 11, 31.

An, Z.G., C.S. Liu, D.A. Boyd, L. Muschietti, K. Appert, and J. Vaclavik, 1982, Phys. Fluids 25, 997.

An, Z.G., C.S. Liu, D.A. Boyd, L. Muschietti, K. Appert, and J. Vaclavik, 1983, Phys. Fluids 26, 345.

Ando, A. et al., 1986, Nucl. Fusion 26, 107.

Ando, A. et al., 1986, Phys. Rev. Lett. 56, 2180.

Andrews, P. and F.W. Perkins, 1983, Phys. Fluids 26, 2537.

Andrews, P.L., V.S. Chan and C.S. Liu, 1985, Phys. Fluids 28, 1148.

Andrews, P.L. and D.K. Bhadra, 1986, Nucl. Fusion 26, 897.

Antonsen, T.M., Jr. and K.R. Chu, 1982, Phys. Fluids 25, 1295.

Antonsen, T.M., Jr. and B. Hui, 1984, IEEE Trans. Plasma Sci. PS-12, 118.

Antonsen, T.M., Jr. and K. Yoshioka, 1986, Phys. Fluids 29, 2235.

Appert, K., A.H. Kritz, S. Succi and J. Vaclavik, 1983, in Proceedings Eleventh European Conf. on Controlled Fusion and Plasma Phys., Aachen, 1983 (European Physical Society, Petit Lancy, Switzerland) Vol. II, p. 329.

Badger, B. et al., 1973, University of Wisconsin Report No. UWFOM-68, (unpublished).

Bartiromo, R., F. Bombarda, and R. Giannelli, 1985, Phys. Rev. A. 32, 531.

Bartiromo, R., et al., 1986, Nucl. Fusion 26, 1106.

Belikov, V.S., Ya. I. Kolesnichenko, and I.S. Plotnik, 1982a, Sov. J. Plasma Phys. 8, 125.

Belikov, V.S., Ya. I. Kolesnichenko, and I.S. Plotnik, 1982b, Nucl. Fusion 22, 1559.

Belikov, V.S., Ya. I. Kolesnichenko, and I.S. Plotnik, 1984, Sov. J. Plasma Phys. 10, 388.

Bellan, P.M., 1984, Phys. Fluids 27, 2191.

Bellan, P.M., 1985, Phys. Rev. Lett. 54, 1381.

Bernabei, S. et al., 1982, Phys. Rev. Lett. 49, 1255.

Bernabei, S. et al., 1986, Nucl. Fusion 26, 111.

Bernstein, I.B., and M.D. Kruskal, 1962, Princeton University Plasma Physics Laboratory Report MATT-20.

Bernstein, I.B., and D.C. Baxter, 1981, Phys. Fluids 24, 108.

Bevir, M.K. and J.W. Gray, 1981, in Proceedings of Reversed Field Pinch Theory Workshop, ed. H. R. Lewis and R. A. Gerwin, Los Alamos Scientific Laboratory Report LA-8944-C, p. 176.

Bhadra, D.K., 1980, Nucl. Fusion 20, 619.

Bhadra, D.K. and C. Chu, 1982, Phys. Rev. Lett. 48, 1824.

Bhadra, D.K., C. Chu, R.W. Harvey, and R. Prater, 1983, Plasma Phys. 25, 361.

Bhadra, D.K., and C. Chu, 1985, J. Plasma Phys. 33, 237.

Bickerton, R.J., J.W. Connor and J.B. Taylor, 1971, Nature 229, 110.

Bickerton, R.J., 1972, Comments Plasma Phys. Controlled Fusion 1, 95.

Bolton, R.A., et al., 1978, in Proceedings Third Topical Meeting on Technology of Controlled Nuclear Fusion, CONF-780508, Vol. II, 824.

Bonoli, P.T., R.C. Englade and M. Porkolab, 1983, in Proceedings of the Fifth Topical Conf. on RF Plasma Heating (University of Wisconsin, Madison) p. 72.

Bonoli, P.T., R.C. Englade, and M. Porkolab, 1984, in Proceedings 4th Int. Symp. on Heating in Toroidal Plasmas, ed. H. Knoepfel and E. Sindoni (Monotypia Franchi, Perugia) Vol. II, p. 1311.

Bonoli, P.T., 1984, IEEE Trans. Plasma Sci. 12, 95.

Bonoli, P.T. and R.C. Englade, 1986, Phys. Fluids 29, 2931.

Borass, K., and A. Nocentini, 1984, Plasma Phys. and Contr. Fusion 26, 1299.

Borzunov, N.A., et al., 1964, Soviet Physics - Doklady 8, 914.

Brambilla, M., 1976, Nucl. Fusion 16, 47.

Budnikov, V.N. et al., 1984, Sov. J. Plasma Phys. 10 281.

Cairns, R.A., J. Owen, and C.N. Lashmore-Davies, 1983, Phys. Fluids 26, 3475.

Callen, J.D., R.J. Colchin, R.H. Fowler, D.G. McAlees, and J.A. Rome, 1975, in Proceedings Fifth International Conference on Plasma Physics and Controlled Nuclear Fusion Research, Tokyo, Japan, 1974, (IAEA, Vienna) Vol. I, 645.

Canobbio, E., and R. Croci, 1984, in Proceedings Fourth Int. Symp. on Heating in Toroidal Plasmas, Rome, Vol. I, p. 583.

Cavallo, A. et al., 1985, Bull. Amer. Phys. Soc. 30, 1572.

Chan, V.S., S.C. Chiu, J.Y. Hsu, and S.K. Wong, 1982, Nucl. Fusion 22, 787.

Chan, V.S., and F.W. McClain, 1983, Phys. Fluids 26, 154.

Chan, V.S., C.S. Liu, P.L. Andrews and F.W. McLain, 1984, in Proceedings Fourth Int. Symp. on Heating in Toroidal Plasmas, ed. H. Knoepfel and E. Sindoni (Monotypia Franchi, Perugia) Vol. II, p. 1334.

Chan, V.S. and S.C. Liu, 1985, Fusion Tech. 7, 288.

Chan, V.S., C.S. Liu and Y. C. Lee, 1986, Phys. Fluids 29, 1900.

Chandrasekhar, S., 1943, Rev. Mod. Phys. 15, 1.

Chapman, S., and T. G. Cowley, 1970, The Mathematical Theory of Non-uniform Gases 3rd edition (Cambridge University Press, Cambridge.)

Chiu, S.C., et al., 1983, Nucl. Fusion 23, 499.

Cho, T. et al., 1984, J. Phys. Soc. Japan. 53, 187.

Cho, T. et al., 1986, Nucl. Fusion 26, 349.

Chu, T.K. et al., 1986, Nucl. Fusion 26, 667.

Clark, W.H., et al., 1980, Phys. Rev. Lett. 45, 1101.

Cohen, R.S., L. Spitzer and R.M. Routley, 1950, Phys. Rev. 80, 230.

Conn, R.W., 1983, "The Engineering of Magnetic Fusion Reactors," Sci. Am. 249, 60.

Connor, J.W. and J.G. Cordey, 1974, Nucl. Fusion 14, 185.

Cordey, J.G. and W.G.F. Core, 1974, Phys. Fluids 17, 1626.

Cordey, J.G. and W.G.F. Core, 1975, Nucl. Fusion 15, 755.

Cordey, J.G., E.M. Jones, D.F.H. Start, A.R. Curtis, and I.F. Jones, 1979, Nucl. Fusion 19, 249.

Cordey, J.G., T. Edlington, and D.F.H. Start, 1982, Plasma Phys. 24, 73.

Cordey, J.G., 1983, Plasma Phys. 25, 361.

Cordey, J.G., 1984, Plasma Phys. and Controlled Fusion 26, 123.

Cox, M., and D.F.H. Start, 1984, Nucl. Fusion 24, 399.

Dawson, J.M., and P.K. Kaw, 1982, Phys. Rev. Lett. 48, 1930.

Decyk, V.K., 1984, J. Comput. Phys. 56, 461.

Decyk, V.K. and H. Abe, 1986, Phys. Fluids 29, 599.

de Groot, S.R., W.A. van Leeuwen and Ch. G. van Weert, 1980, Relativistic Kinetic Theory (North Holland, Amsterdam).

Demirkhanov, R.A., I. Ya. Kadysh, J.S. Fursa, and Yu. S. Khodyrov, 1965, Soviet Physics -Doklady Phys. 10, 174.

Demirkhanov, R. A. et al., 1983, in Proceedings of the Ninth Int. Conf. on Plasma Phys. and Controlled Nuclear Fusion Research, Baltimore, MD, USA, 1982 (IAEA, Vienna), Vol. II, p. 91.

Dnestrovskij, Yu. N., S.N. Krasheninnikov, V.V. Parail, and G.V. Pereverzev, 1983, in Proceedings of the Ninth Int. Conf. on Plasma Phys. and Controlled Nuclear Fusion Research, Baltimore, MD, USA, 1982 (IAEA, Vienna), Vol. II, p. 189.

Dnestrovskij, Yu. N., et al., 1985, in Proc. Twelfth European Physical Society Meeting on Controlled Fusion and Plasma Phys., Vol. II, p. 200.

Dreicer, H., 1960, Phys. Rev. 117, 329.

Dupree, T.H., 1966, Phys. Fluids 9, 1773.

Ehst, D.A., 1979, Nucl. Fusion 19, 1369.

Ehst, D.A., et al., 1982, J. Fusion Energy 2, 83.

Ehst, D.A., et al., 1985a, Nucl. Engrg. Des./Fusion 2, 305.

Ehst, D.A., et al., 1985b, Nucl. Engrg. Des./Fusion 2, 319.

Ehst, D.A., 1985, Nucl. Fusion 25, 629.

Ehst, D.A., K. Evans, Jr. and D.W. Ignat, 1986, Nucl. Fusion 26, 461.

Eldridge, O.C., 1980, Oak Ridge National Laboratory Report ORNL/M-7503.

Englade, R., P. Bonoli, and M. Porkolab, 1983, in Proceedings of the IAEA Tech. Committee Meeting on Noninductive Current Drive in Tokamaks, Culham, England.

Ferreira, A., M. R. O'Brien and D. F. H. Start, 1984, Plasma Phys. 26, 1585.

Fidone, I., G. Granata, and R.L. Meyer, 1982, Phys. Fluids 25, 2249.

Finn, J.M. and T.M. Antonsen, Jr., 1985, Comm. Plasma Phys. Controlled Fusion 9, 111.

Finn, J.M., 1986, Phys. Fluids 29, 2630.

Firestone, M., T.K. Mau and R.W. Conn, 1985, Comm. Plasma Phys. Controlled Nucl. Fusion 9, 149.

Fisch, N.J., 1978, Phys. Rev. Lett. 41, 873.

Fisch, N.J. and A. H. Boozer, 1980, Phys. Rev. Lett. 45, 720.

Fisch, N.J. and M. D. Kruskal, 1980, J. Math Phys. 21, 740.

Fisch, N.J., 1981a, Nucl. Fusion 21, 15.

Fisch, N.J., 1981b, in Proceedings Fourth Topical Conference on RF Plasma Heating ed. R. D. Bengtson and M. E. Oakes (University of Texas, Austin) paper B1.

Fisch, N.J., 1981c, Phys. Rev. A 24, 3245.

Fisch, N.J., and C.F.F. Karney, 1981, Phys. Fluids 24, 27.

Fisch, N.J., 1982, in Proceedings of the 3rd Joint Varenna-Grenable International Symposium, on Heating in Toroidal Plasmas: ed. C. Gormezano, G.G. Leotta, and E. Sindoni (Comm. European Communitres, Brussels), Vol. 3, p. 841.

Fisch, N.J. and T. Watanabe, 1982, Nucl. Fusion 22, 423.

Fisch, N.J., 1983, "Pushing Particles with Waves," American Scientist p. 27.

Fisch, N.J., 1984, Nucl. Fusion 24, 371.

Fisch, N.J., 1985a, Phys. Fluids 28, 245.

Fisch, N.J., 1985b, in Proceedings Course and Workshop on Applications of RF Waves to Tokamak Plasmas, ed S. Bernabei, U. Gasparino and E. Sindoni (Monotypia Franchi, Italy), Vol. I, p. 46.

Fisch, N.J. and C.F.F. Karney, 1985a, Phys. Rev. Lett. 54, 897.

Fisch, N.J. and C.F.F. Karney, 1985b, Phys. Fluids 28, 3107.

Fisch, N.J., 1986, Phys. Fluids 29, 172.

Fomenko, V.V., 1979. Nucl. Fusion 15, 1091.

Franz, M., unpublished (1986).

Fuchs, V., R.A. Cairns, M.M. Shoucri, K. Hizanidis, and A. Bers, 1985, Phys. Fluids 28, 3619.

Fuchs, V., R.A. Cairns, C.N. Lashmore-Davies and M.M. Shoucri, 1986, Phys. Fluids 29, 2931.

Fukuda, M. et al, 1976, J. Phys. Soc. Japan 41, 1376.

Fukuda, M., 1978, J. Phys. Soc. Japan 45, 283.

Fukuda, M. and K. Matsuura, 1978, J. Phys. Soc. Japan 44, 1344.

Furth, H.P., 1979, "Progress Toward a Tokamak Fusion Reactor," Sci. Am. 241, 51.

Fussman, G. et al., 1981, Phys. Rev. Lett. 47, 1004.

Gahl, J., O. Ishihara, K. Wong, M. Hagler, and M. Kristiansen, 1985, Bull. Am. Phys. Soc. 30, 1622.

Gell, Y. and R. Nakach, 1984, Phys. Rev. A 29, 1520.

Gell, Y. and R. Nakach, 1985, Phys. Rev. A 31, 3846.

Goree, J. et al., 1985, Phys. Rev. Lett. 55, 1669.

Gormezano, C. et al., 1983, in Proceedings of the Eleventh European Conference on Controlled Fusion and Plasma Physics (European Physical Society, Petit-Lancy, Switzerland) Vol. 1, p.325.

Gormezano, C. et al., 1985, in Proceedings of the Sixth Topical Conf. on RF Plasma Heating, Pine Mountain, Georgia.

Grad, H., 1963, Phys. Fluids 6, 47.

Grisham, L.R., D.E. Post, D.R. Mikkelsen, and H.P. Eubank, 1982, Nucl. Technol./Fusion 2, 199.

Harvey, R.W., and J.M. Rawls, 1973, Nucl. Fusion 19, 1529.

Harvey, R.W., J.C. Riordan, J.L. Luxon and K.D. Marx, 1981, in Proceedings Fourth Topical Conf. on Radio Frequency Plasma Heating, Austin, Texas, Paper C9.

Harvey, R.W., K.D. Marx and M.G. McCoy, 1981, Nuclear Fusion 21, 153.

Hasegawa, A., 1980, Nucl. Fusion 20, 1158.

Hayes, M.A. and J.S. DeGroot, 1981, Phys. Letters 86A, 161

Hayes, M. A. and M. R. Brown, 1986, Phys. Fluids 29, 247.

Hazeltine, R.D. and A.A. Ware, 1986, Phys. Fluids 19, 1163.

Hewitt, D., K. Hizandis, V. Krapchev, and A. Bers, 1983, Proceedings IAEA Tech. Comm. Meeting on Noninductive Current Drive in Tokamaks Culham, England.

Hinton, F. and R.D. Hazeltine, 1976, Rev. Mod. Phys. 42, 239

Hirano, K., K. Matsuura and A. Mohri, 1971, Phys. Letters 36A, 215.

Hogan, J.T., 1981, Nucl. Fusion 21, 365.

Hooke, W., et al., 1983, in Proceedings of the Ninth International Conference on Plasma Phys. and Controlled Nucl. Fusion Research, Baltimore, MD, USA, 1982 (IAEA, Vienna). Vol. ?] p 239.

Hooke, W., 1984, Plasma Physics and Controlled Fusion 26, 133.

Hugrass, W.N., et al., 1980, Phys. Rev. Lett. 44, 1676.

Ignat, D.W., P.H. Rutherford, and H. Hsuan, 1985, in Proceedings Course and Workshop on Application of RF Waves to Tokamak Devices, ed. S. Bernabei, V. Gasparino and E. Sindoni (Monotypia Franchi, Italy) Vol. II, p. 525.

Jensen, T.H. and M.S. Chu, 1984, Phys. Fluids 27, 2881.

Jobes, F.C. et al., 1984, Phys. Rev. Lett. 52, 1005.

Jobes, F.C., et al., 1985, Phys. Rev. Lett. 55, 1295.

Karney, C.F.F., and N.J. Fisch, 1979, Phys. Fluids 22,.

Karney, C.F.F., and N.J. Fisch, 1981, Nucl. Fusion 21, 1549.

Karney, C.F.F., and N.J. Fisch, 1985, Phys. Fluids 28, 116.

Karney, C.F.F., N.J. Fisch, and F.C. Jobes, 1985, Phys. Rev. A 32, 2554.

Karney, C.F.F., 1988, Computer Physics Reports 4, 183.

Karney, C.F.F., and N.J. Fisch, 1986, Phys. Fluids 29, 180.

Kato, K., 1980, Phys. Rev. Lett. 44, 779.

Kerbel, G.D. and M.G. McCoy, 1985, Phys. Fluids 28, 3629.

Killeen, J., and K.D. Marx, 1970, Methods of Computational Physics, edited by P. Adler, S. Fernbach, and M. Rotenberg (Academic Press), Vol. 9, p. 422.

Klima, R., 1973a, Plasma Phys. 15, 215.

Klima, R., 1973b, Plasma Phys. 15, 1031.

Klima, R., 1974, Czech. J. Phys. B 21, 864.

Klima, R., and V.L. Sizonenko, 1975, Plasma Phys. 17, 463.

Klima, R. et al., 1978, Phys. Lett 65A, 23.

Klima, R., and A. V. Longinov, 1979, Fiz. Plamy 5, 496, [Sov. J. Plasma Phys. 5 (3), 277 (1980)].

Klima, R., 1980, Czech J. Phys. B 30, 874.

Knowlton, S., et al., 1986, Phys. Rev. Lett. 57, 587.

Kojima, T., S. Takamura, and T. Okuda, 1981, Phys. Letters 83A, 172.

Kolesnichenko, Ya. I., S.V. Putvinskii, S.N. Reznik, V.A. Chuyanov, and V.A. Yavorskii, 1981, Sov. J. Plasma Phys. 7, 441.

Krapchev, V.B., D.W. Hewett and A. Bers, 1985, Phys. Fluids 28, 522.

Krasheninnikov, S.I., 1983, Fizika Plazmi 9, 1201 (in Russian).

Krasheninnikov, S. I., et al., 1985, "Optimization of OH Coil Recharging by Means of Lower-Hybrid Waves" (INTOR Workshop, unpublished).

Kritz, A.H., N.J. Fisch, and C.F.F. Karney, 1981, Phys. Fluids 24, 504.

Krivenski, V., et al., 1985, Nucl. Fusion 25, 127.

Kubo, S. et al., 1983, Phys. Rev. Lett. 50, 1994.

Kubo, S. et al., 1984, J. Phys. Soc. Japan 53, 1047.

Kuo, S.P. and M.C. Lee, 1986, Phys. Fluids 29, 1024.

Kulsrud, R.M., Y.-C. Sun, N.K. Winsor, and H.A. Fallon, 1973, Phys. Rev. Lett. 31, 690.

LaHaye, R.J., et al., 1980, Nucl. Fusion 20, 218.

Lallia, P., 1974, in Proceedings of 2nd Topical Conference on RF Plasma Heating, Lubbock, Texas, paper C3.

Landau, L., 1936, Physik. Z. Sowjetunion, 10, 154.

Landau, L., 1949, Phys. Rev. 77, 567.

Leuterer, F., et al., 1985, in Proceedings of Tenth International Conf. Plasma Phys. and Controlled Nuclear Fusion, London, UK, 1984 (IAEA, Vienna) Vol. I, p. 597.

Leuterer, F., et al., 1985, Phys. Rev. Lett. 55, 95.

Leuterer, F., et al., 1985, Plasma Phys. and Controlled Nucl. Fusion 27, 1399.

Liewer, P.C., R.W. Gould and P.M. Bellan, 1986, "One-dimensional Modelling of D. C. Current Drive by AC Helicity Injection in a Tokamak," (submitted to Phys. Fluids).

Lidsky, L., 1983, "The Trouble with Fusion," MIT Technology Review, p. 32.

Liu, C.S., Z.G. An, D.A. Boyd, Y.C. Lee, L. Muschietti, K. Appert, and J. Vaclavik, 1982, Comments Plasma Phys. Contr. Fusion 7, 21.

Liu, C.S., V.S. Chan, D.K. Bhadra, and R.W. Harvey, 1982, Phys. Rev. Lett. 48, 1479.

Liu, C.S., et al., 1984, Phys. Fluids 27, 1709.

Liu, C.S., V. S. Chan, and Y. C. Lee, 1985, Phys. Rev. Lett. 55, 583.

Lloyd, B. et al., 1983, in Proceedings IAEA Workshop on Non-Inductive Current Drive in Tokamaks, Culham, U.K., Culham Laboratory Report CLM-CD, Vol. I, p. 250.

Longinov, A.V., S.S. Pavlov and K.N. Stephanov, 1986, in Proceedings of the Thirteenth European Conf. on Controlled Nuclear Fusion and Plasma Physics

Luckhardt, S.D., et al., 1982, Phys. Rev. Lett. 48, 152.

Luckhardt, S.C. et al., 1986, Phys. Fluids 29, 1985.

McCormick, K. et al., 1985, in Proceedings of Twelfth European Conf. on Controlled Fusion and Plasma Physics, Budapest.

McNally, J.R., Jr., 1978, Oak Ridge National Laboratory Report ORNL/TM-6492.

McWilliams, R., E.J. Valeo, R.W. Motley, W.M. Hooke, and L. Olsen, 1980, Phys. Rev. Lett. 44, 245.

McWilliams, R. and R.W. Motley, 1981, Phys. Fluids 24, 2022.

McWilliams, R. and R.C. Platt, 1986, Phys. Rev. Lett. 56, 835.

Maekawa, T., et al., 1981, Phys. Lett. 85A, 339.

Maekawa, T., et al., 1983, Nucl. Fusion 23, 242.

Mayberry, M.J., et al., 1985, Phys. Rev. Lett. 55, 829.

Midzuno, Y.,J. 1973, Phys. Soc. Japan 34, 801.

Midzuno, Y.,J. 1975, Phys. Soc. Japan 38, 553.

Mikkelsen, D.R., and C.E. Singer, 1983, Nuclear Technology/Fusion 4, 237.

Mitarai, O., and A. Hirose, 1984, Nucl. Fusion 24, 481.

Montgomery, D., and D. Tidman, 1964, Plasma Kinetic Theory, (McGraw-Hill, NY)

Motley, R.W., W.M. Hooke, and G. Annania, 1979, Phys. Rev. Lett. 24 1799.

Motley, R.W., 1980, Phys. Fluids 23, 2050.

Motley, R.W. et al., 1985, in Proceedings Tenth Int. Conf. on Plasma Physics and Controlled Nuclear Fusion Research, London, 1984 (IAEA, Vienna) Vol. I, p. 473.

Muschietti, L., J. Vaclavik, and K. Appert, 1982, Plasma Phys. 24, 987.

Nakamura, M. et al., 1981, Phys. Rev. Lett. 47, 1902.

Nakamura, M. et al., 1984, J. Phys. Soc. Japan 53, 3399.

Nishio, S. and M. Sugihara, 1985, Nuclear Eng./Design Fusion 3, 59.

O'Brien, M.R., M. Cox, and D.H.F. Start, 1986, Comput. Phys. 40, 131.

Ohkawa, T., 1970, Nucl. Fusion 10, 185.

Ohkawa, T., 1976, General Atomic Company Report GA-A13847.

Okano, K., N. Inoue, and T. Uchida, 1983, Nucl. Fusion 23, 235.

Okazaki, T., M. Sugihara, S. Nishio and N. Fujisawa, 1985, Nucl. Eng./Design Fusion 3, 73.

Okazaki, T., M. Sugihara and N. Fujisawa, 1986, Nucl. Fusion 26, 1029.

Okazaki, T., M. Sugihara and N. Fujisawa, 1986, Comput. Phys. 40, 131.

Okuda, H., R. Horton, M. Ono, and K.-L. Wong, 1985, Phys. Fluids 26, 3365.

Osovets, S. M., and I. A. Popov, 1972, in Proceedings of Fifth European Conference on Controlled Fusion and Plasma Physics Grenoble, France, Vol. I, p. 8.

Ott, E., 1979, Phys. Fluids 22, 1732.

Parail, V.V., and O.P. Pogutse, 1976, Sov. J. Plasma Phys. 2, 125.

Parail, V.V., and G.V. Pereverzev, 1982, Sov. J. Plasma Phys. 8, 25.

Parail, V.V., and G.V. Pereverzev, 1983, Sov. J. Plasma Phys. 9, 341.

Parail, V.V., G.V. Pereverzev, and I.A. Vojksekhovich, 1985, in Proceedings of the Tenth Int. Conf. on Plasma Phys. and Controlled Nuclear Fusion Research, London, UK, 1984 (IAEA, Vienna) Vol. 1, p. 605.

Parks, P.B. and F.B. Marcus, 1981, Nucl. Fusion 21, 1207.

Parlange, F. et al., 1985, in Proceedings of Twelfth European Conf. on Controlled Fusion and Plasma Physics, Budapest, Vol. II, p. 172,.

Perkins, F.W., 1982, Bull. Amer. Phys. Soc. Vol. 27, No. 8, Part II, p. 1101

Porkolab, M., et al., 1977, Phys. Rev. Lett. 38, 230.

Porkolab, M., 1977, Phys. Fluids 20, 2058.

Porkolab, M., et al., 1983, in Proceedings of the Nineth International Conference on Plasma Physics and Controlled Fusion Research, Baltimore, MD, USA 1982 (IAEA, Vienna) Vol. I, p. 227.

Porkolab, M., 1984a, IEEE Trans. Plasma Sci. 12, 107.

Porkolab, M., et al., 1984b, Phys. Rev. Lett. 53, 450.

Porkolab, M., 1985a, in Wave Heating and Current Drive in Plasmas, V.L. Granatstein and P.L. Colestock, eds. (Gordon and Breach, NY) p. 219-280.

Porkolab, M., 1985b, in Proceedings Course and Workshop on the Application of RF Waves to Tokamak Devices, ed. S. Benabei, V. Gasparino and E. Sindoni (Monotypa Franchi, Italy) Vol. I, p 288.

Reiman, A.H., 1983, Phys. Fluids 26, 1338 .

Robinson, B.B. and I.B. Bernstein, 1962, Ann. Phys. (NY) 18, 110.

Robinson, D.C., M.W. Alcock, N.R. Ainsworth, B. Lloyd, and A.W. Morris, 1982, in Proceedings 3rd Varenna-Grenoble Symp. on Heating in Toroidal Plasmas (Euratom 7979 EN) Vol. II, p. 647.

Rose, D.J., and M. Clark, 1961, Plasmas and Controlled Fusion (MIT Press, Cambridge).

Rosenbluth, M.N., R.D. Hazeltine, and F.L. Hinton, 1972, Phys. Fluids 15, 116.

Rutherford, P. H., 1985, "Resistive Instabilities in Tokamaks," in Proceedings Course and Workshop on Basic Physical Processes of Toroidal Fusion Plasmas, Varenna, Italy.

Santini, F., E. Barbato, F. DeMarco, S. Podda, and A. Tucillo, 1984, Phys. Rev. Lett. 52, 1300.

Santini, F., 1985, in Proceedings of Course and Workshop on the Application of RF Waves to Tokamak Devices, ed. S. Bernabei, U. Gasparino and E. Sindoni, (Monotypia Francha, Italy) Vol. I, p. 251.

Sheffield, J., 1985, Nucl. Fusion 25, 1733.

Shimozuma, T. et al., 1985, J. Phys. Soc. Japan 54, 1360.

Singer, C.E. and D.R. Mikkelsen, 1983, J. Fusion Energy 3, 13.

Slusher, R.E. and C.M. Surko, 1978, Phys. Rev. Lett. 40, 400.

Soldner, F.X. et al., 1986, Phys. Rev. Lett. 57, 1137.

Sperling, J.L., 1978, Phys. Fluids 21, 221.

Spitzer, L. and R. Härm, 1953, Phys. Rev. 89, 977.

Start, D.F.H., P.R. Collins, E.M. Jones, A.C. Riviere, and D.R. Sweetman, 1978, Phys. Rev. Lett. 40, 1497.

Start, D.F.H., and J.G. Cordey, 1980, Phys. Fluids 23, 1477.

Start, D.F.H., J.G. Cordey, and E. M. Jones, 1980, Plasma Phys. 22, 303.

Start, D.F.H., et al., 1982, Phys. Rev. Lett. 48, 624.

Start, D.F.H., 1983, Plasma Phys. 25, 793.

Start, D.F.H., M. R. O'Brien, and P.M.V. Grace, 1983, Plasma Phys. 25, 1431.

Stevens, J. E. et al., 1982, in Proceedings of the 3rd Joint Varenna-Grenoble Int. Symp. Heating in Toroidal Plasmas: (Comm. European Communities, Brussels), ed. C. Gormezano, G. G. Leotta and E. Sindoni Vol. 2, p. 455.

Stevens, J.E. et al., 1985, Nucl. Fusion 25, 1529.

Stix, T.H., 1962, The Theory of Plasma Waves (McGraw-Hill, NY)

Stix, T.H., 1972, Plasma Phys. 14, 367.

Stringer, T.E., 1963, Plasma Phys. (Jo[illegible] of Nuclear Energy C) 5, 89.

Succi, S., K. Appert, L. Muschiett[illegible]vaclarik, and J.M. Wersinger, 1984, Phys. Lett. A 106, 137.

Sugihara, R., Y. Midzuno, and M. Fukuda, 1981, J. Phys. Soc. Jpn. 50, 2442.

Taguchi, M., 1982, J. Phys. Soc. Japan 51, 1975.

Taguchi, M., 1983, J. Phys. Soc. Japan 52, 2035.

Taylor, J.B. 1974, Phys. Rev. Lett. 33, 1139.

Thonemann, P.C., W.T. Co[illegible]hig, and D.P. Davenport, 1952, Nature 5, 34.

Toi, K., et al., 1984, Phys. Rev. Lett. 52, 2144.

Tonon, G., 1984, Plasma Phys. 26, 145.

Trubnikov, B.A., 1965, in Reviews of Plasma Physics, edited by M.A. Leontovich (Consultants Bureau, NY) Vol. I, p. 105.

Uckan, N.A., 1985, "Noninductive Current Drive in Tokamaks," Oak Ridge National Laboratory Report ORNL/TM-9296.

Uesugi, Y. et al., 1985, Nucl. Fusion 25, 1623.

Vaclavik, J., K. Appert, A.H. Kritz and L. Muschietti, 1983, Plasma Phys. 25, 1283.

Valeo, E J. and D.C. Eder, 1985 in Proceedings Course and Workshop on Applications of RF Waves to Tokamak Plasmas, ed. S. Bernabei, U. Gasparino and E. Sindoni (Monotypia Francha, Perugia, Italy) Vol. II, p. 493.

van Houtte, D. et al., 1984, Nucl. Fusion 24, 1485.

van Houtte, D. et al., 1984, in Proceedings Fourth Int. Symp. on Heating in Toroidal Plasmas, Rome Vol. I, p. 554.

Vedenov., A.A., 1967, in Reviews of Plasma Physics, edited by M.A. Leontovich, (Consultants Bureau, NY) Vol. 3, p. 229.

von Goeler, S. et al., 1985, Nucl. Fusion 25, 1515.

Wang, M.C. and G.E. Uhlenbeck, 1945, Rev. Mod. Phys. 17, 323.

Ware, A.A., 1970, Phys. Rev. Lett. 25, 15.

Ware, A.A., 1973, Nucl. Fusion 13, 793.

Wegrove, J.-G. and F. Engelmann, 1984, Comments Plasma Phys. Controlled Fusion 8, 211.

Wong, K.-L., 1979, Phys. Rev. Lett. 43, 438.

Wong, K.-L., R. Horton, and M. Ono, 1980, Phys. Rev. Lett. 45, 117.

Wong, K.-L. and M. Ono, 1983, Nucl. Fusion 23, 805.

Wong, K.-L. and M. Ono, 1984, Nucl. Fusion 24, 615.

Wort, D.J.M., 1971, Plasma Phys. 13, 258.

Yamamoto, T. et al., 1980, Phys. Rev. Lett. 45, 716.

Yoshikawa, S., and M. Yamato, 1966, Phys. Fluids 9, 1814.

Yoshioka, K. and T.M. Antonsen, Jr., 1986, Nucl. Fusion 26, 839.

Yoshioka, K., T.M. Antonsen, Jr., and E. Ott, 1986, Nucl. Fusion 26, 439.

Yuen, S.Y., D. Kaplan, and D.R. Cohn, 1980, Nucl. Fusion 20, 159.

Zhang, Z.X. and C.X. Chen, 1985, Fusion Tech. 7, 236.

#8510389

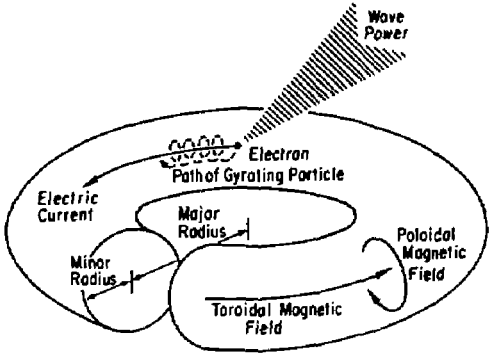

Fig. 1.1

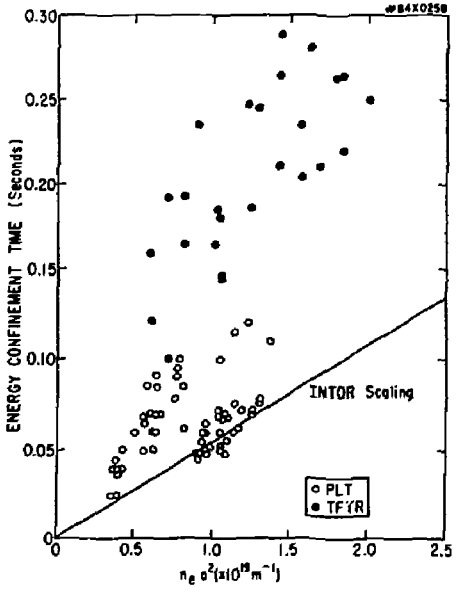

Fig. 1.2

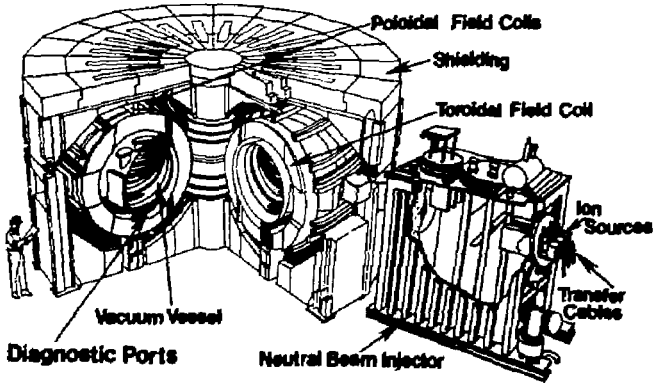

Fig. 1.3

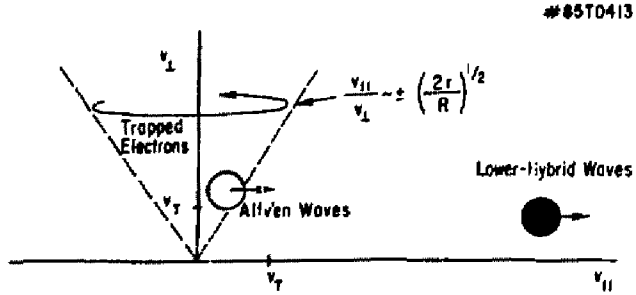
#85T0413
$v_\perp$
$\frac{v_{\parallel}}{v_\perp} \sim \pm \left(\frac{2r}{R}\right)^{1/2}$
Trapped Electrons
v_T
Alfvén Waves
Lower-Hybrid Waves
v_T
$v_\parallel$

Fig. 1.4

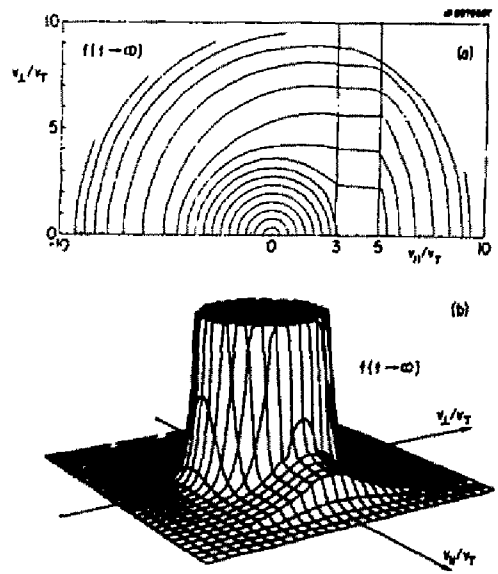
10
5
0
$f(t=0)$
$v_\perp/v_T$
(a)
-10
0
3
5
10
$v_\parallel/v_T$
(b)
$f(t=0)$
$v_\perp/v_T$
$v_\parallel/v_T$

Fig. 1.5

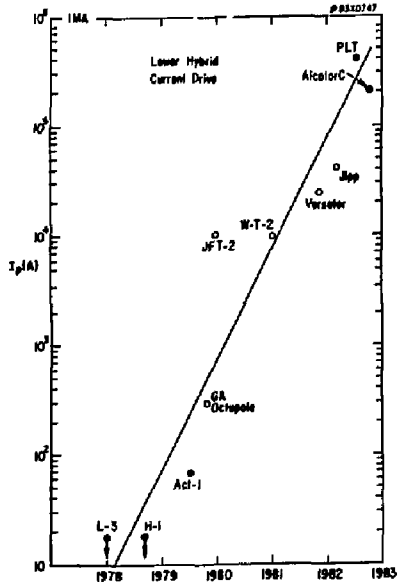

Fig. 1.6

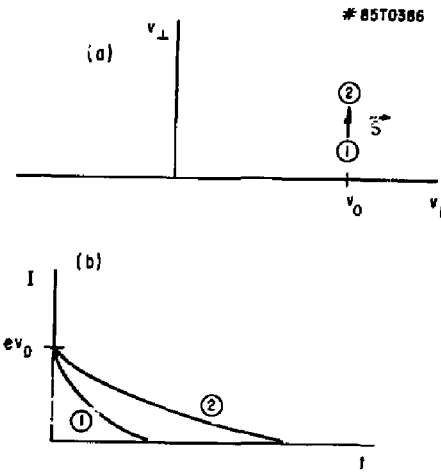

Fig. 1.7

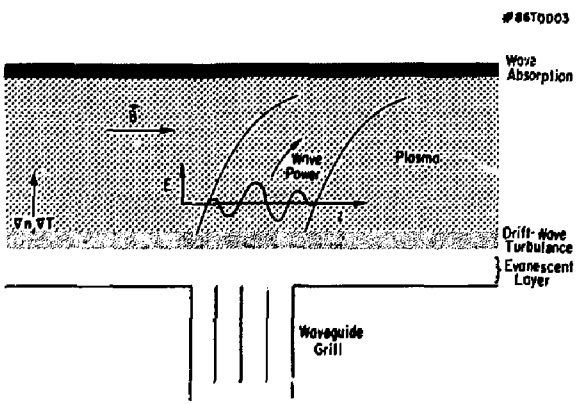

Fig. 1.8

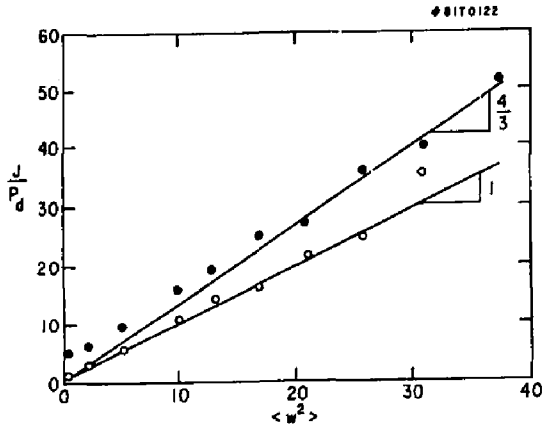

Fig. 2.i

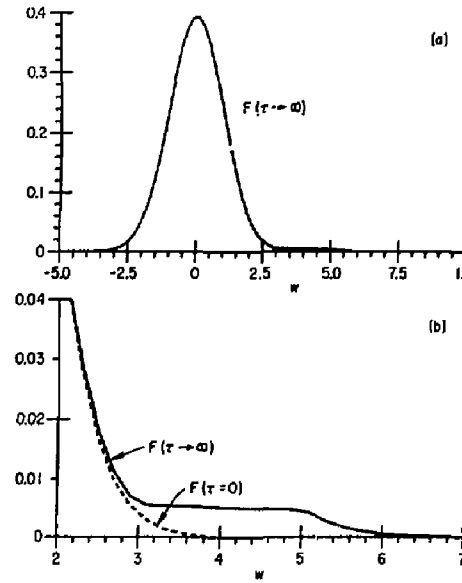

Fig. 2.2

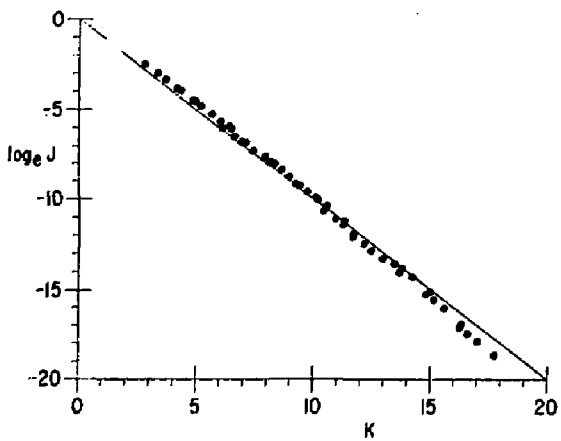

Fig. 2.3

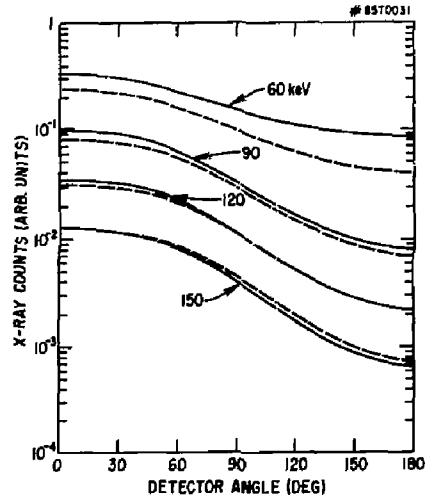

Fig. 2.4(a)

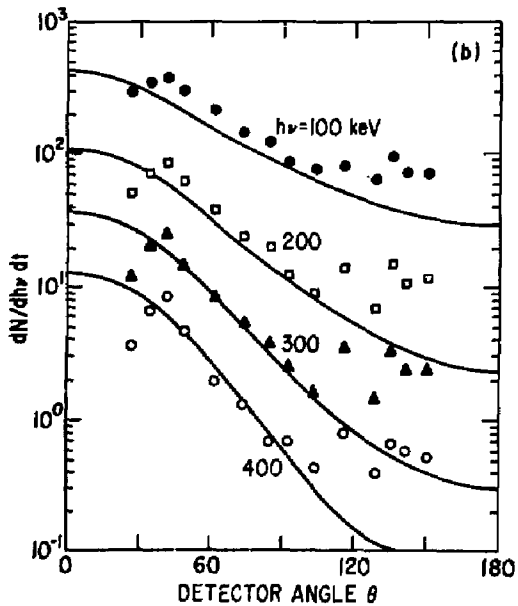

Fig. 2.4(b)

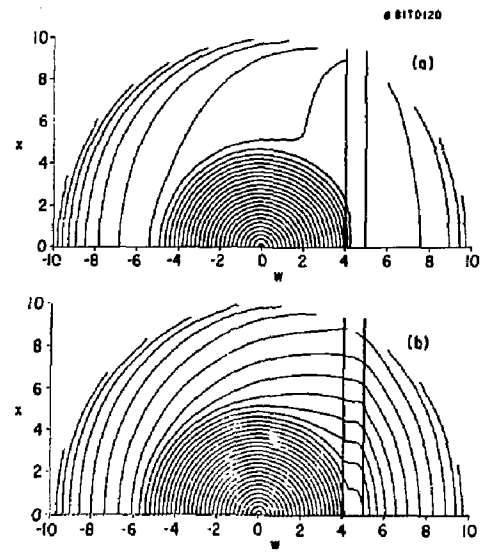

Fig. 2.5

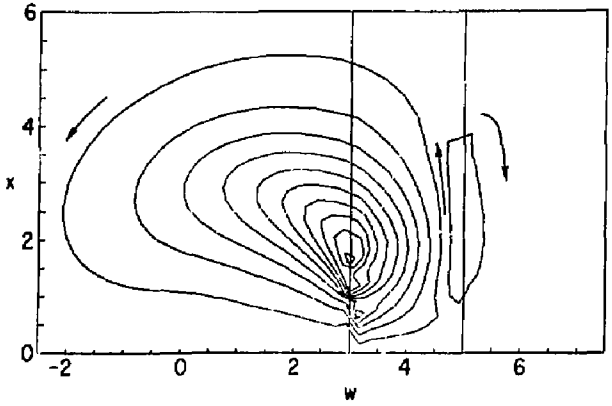

Fig. 2.6

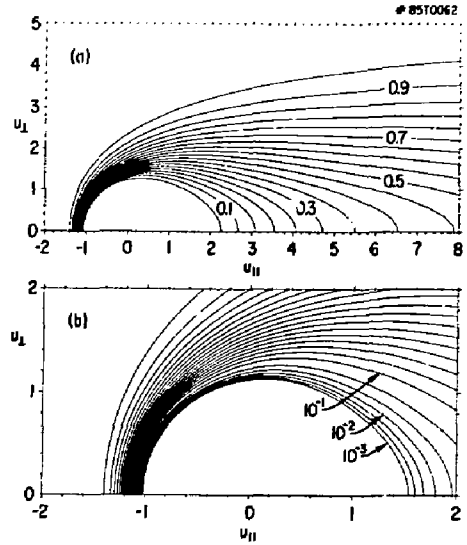

Fig. 2.7

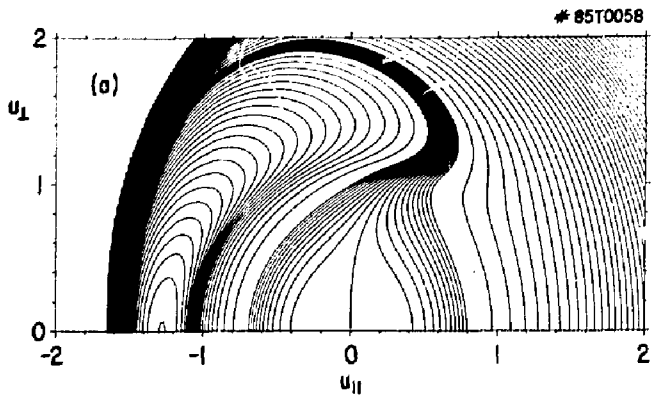

Fig. 2.8

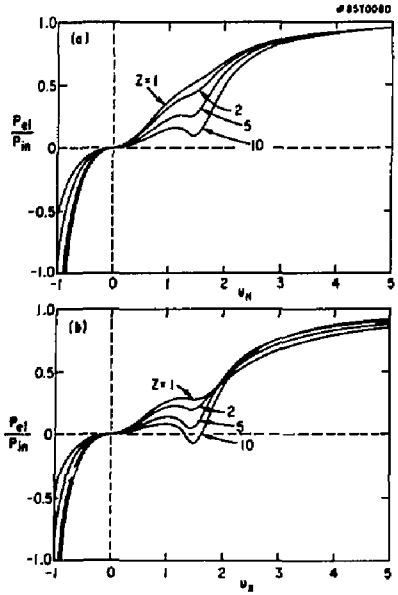

Fig. 2.9

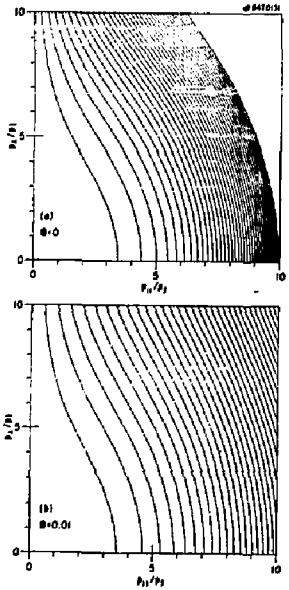

Fig. 2.10

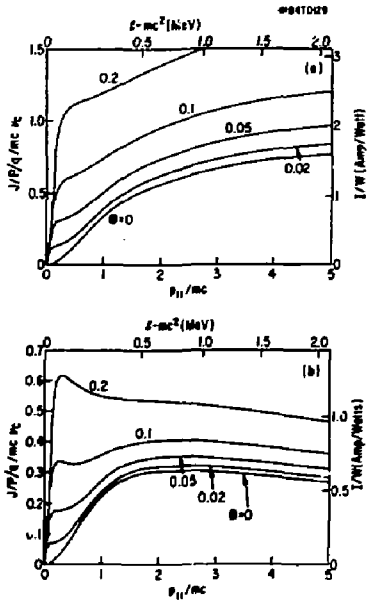

Fig. 2.11

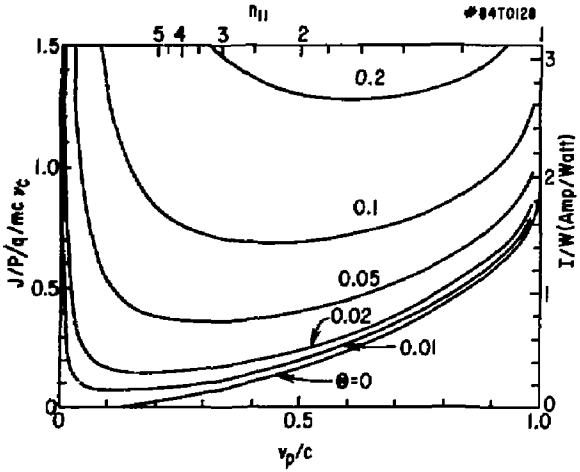

Fig. 2.12

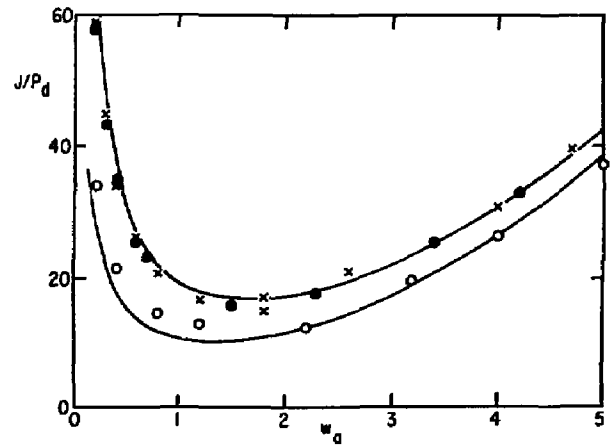

Fig. 3.1

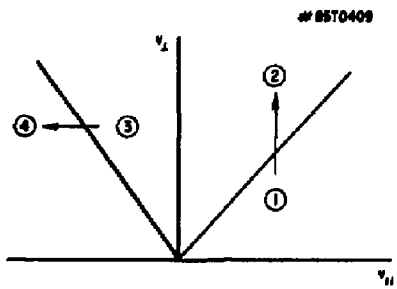

Fig. 3.2

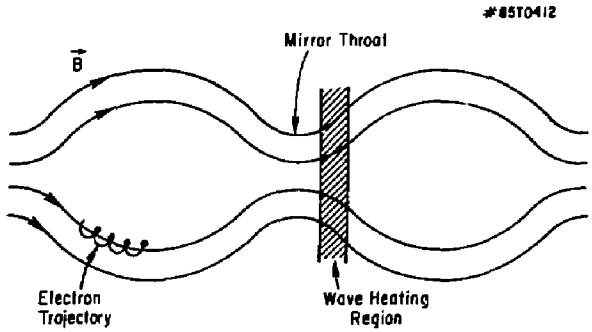

Fig. 3.3

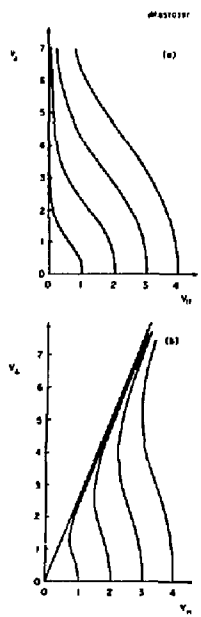

Fig. 3.4

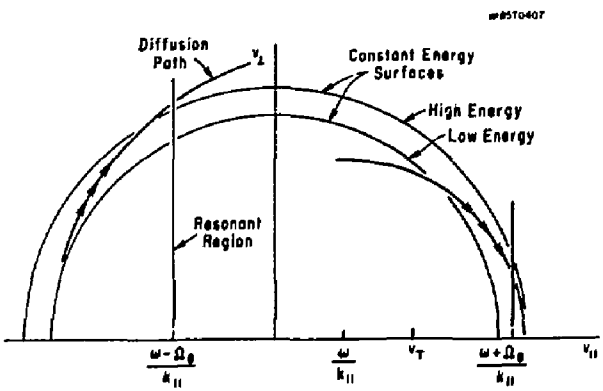

Fig. 3.5

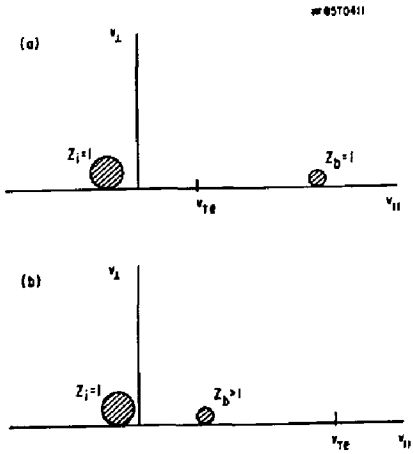

Fig. 3.6

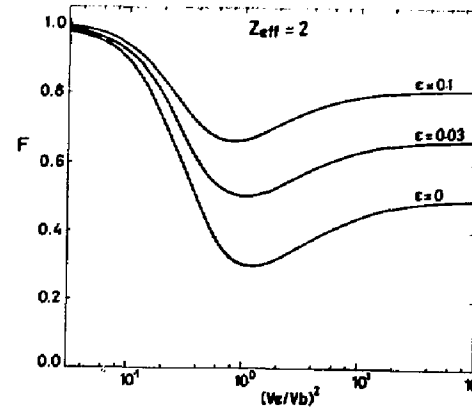

Fig. 3.7

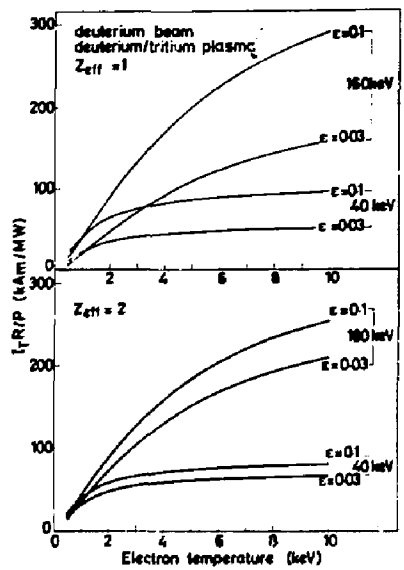

Fig. 3.8

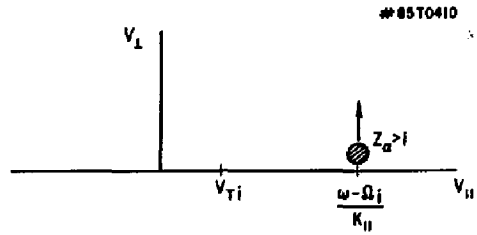

Fig. 3.9

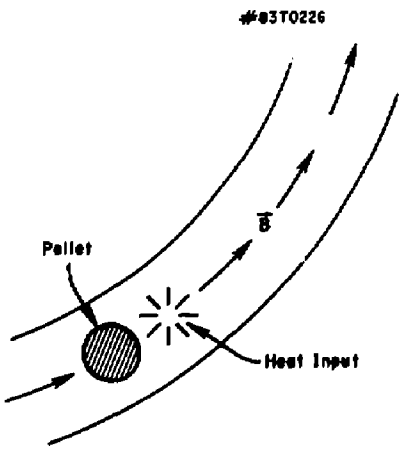

Fig. 3.10

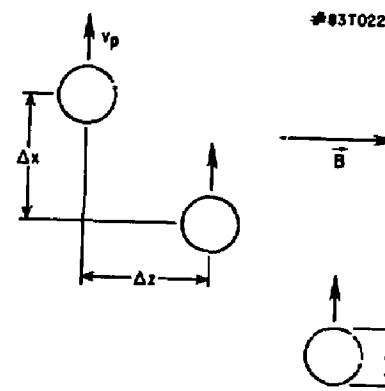

Fig. 3.11

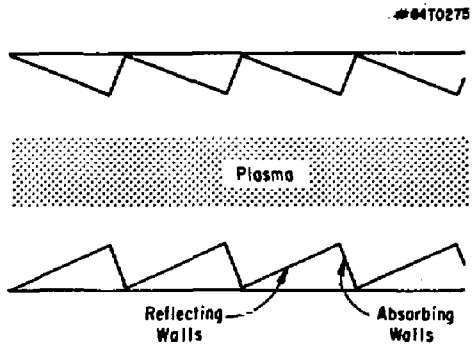

Asymmetrical Reflection of Radiation

Fig. 3.12

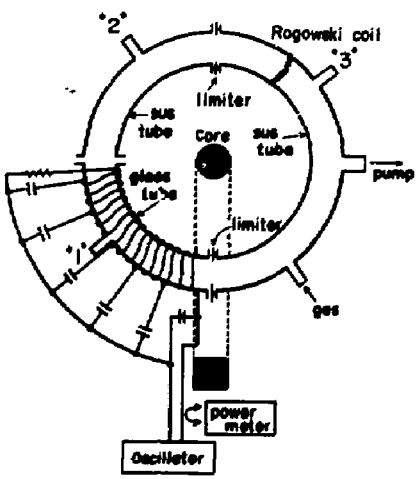

Fig. 4.1

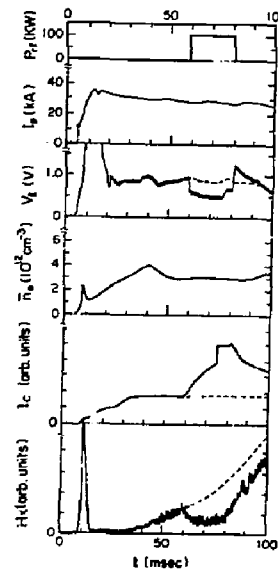

Fig. 4.2

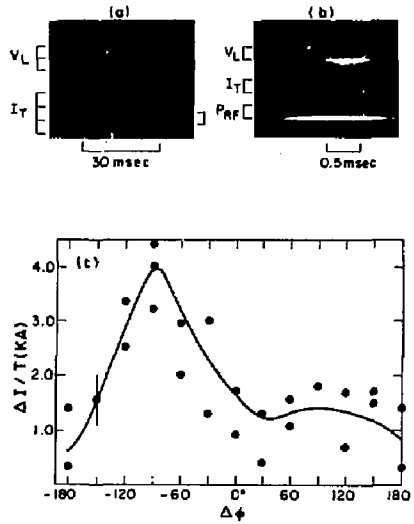
(a)
(b)
V_L
I_T
P_{RF}
30 msec
0.5msec
(c)
ΔI_T (KA)
$\Delta\phi$

Fig. 4.3

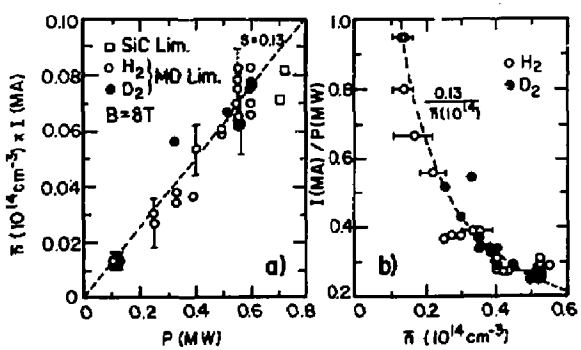
SiC Lim.
H_2
D_2
MO Lim.
B=8T
s=0.13
a)
b)
P (MW)
$\bar{n}$ (10^{14}cm^{-3}) x I (MA)
I (MA) / P (MW)
$\bar{n}$ (10^{14}cm^{-3})
0.13 / $\bar{n}$(10^{14})

Fig. 4.4

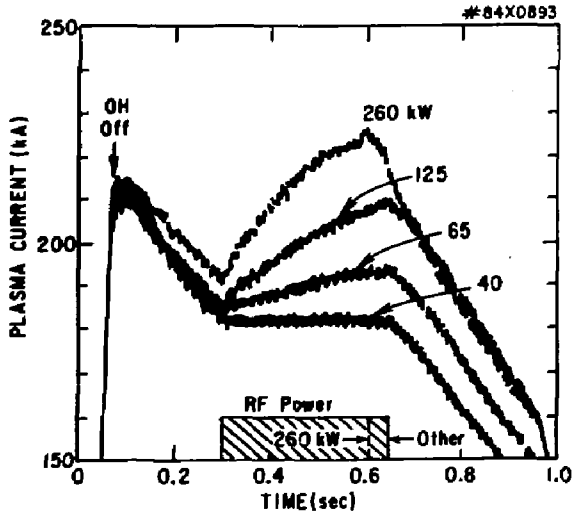

Fig. 4.5

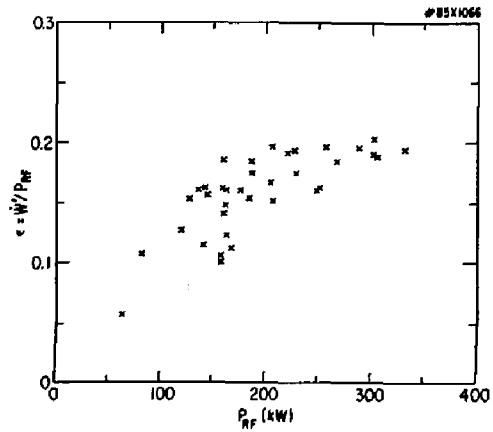

Fig. 4.6

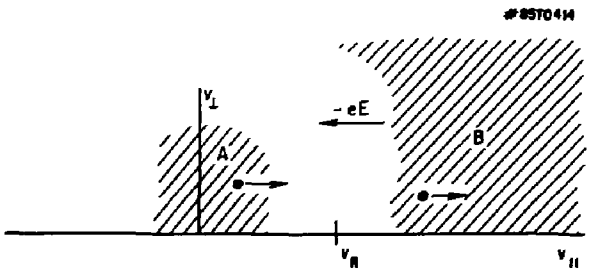

Fig. 4.7

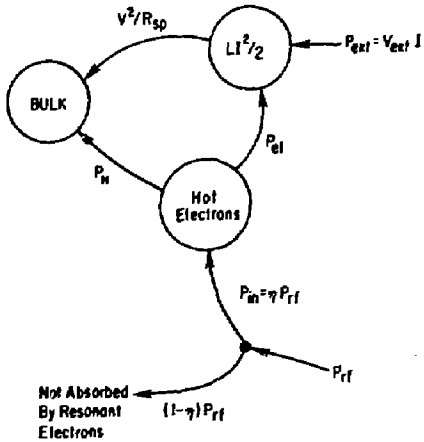

Fig. 4.8

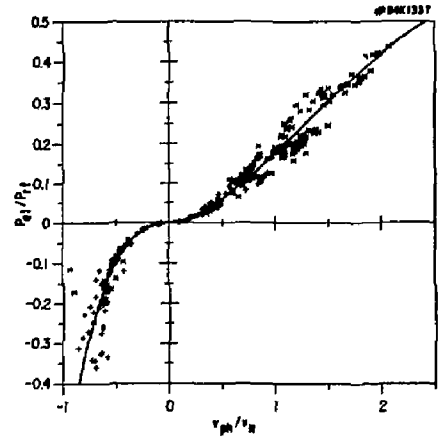

Fig. 4.9

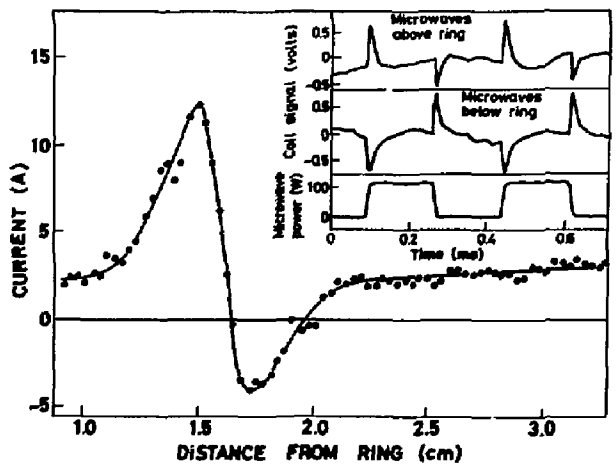

Fig. 4.10

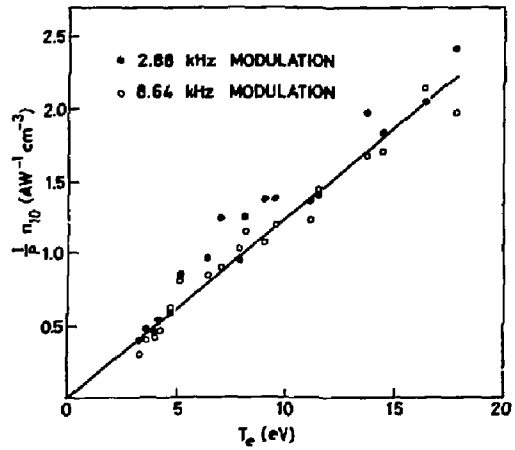

Fig. 4.11

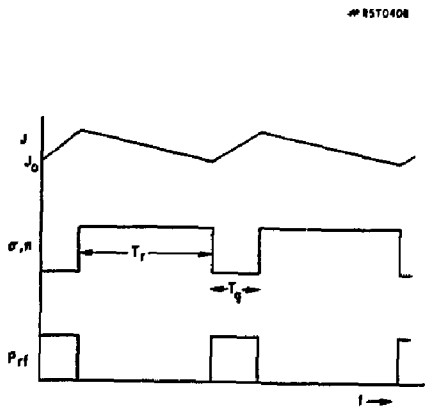

Fig. 5.1

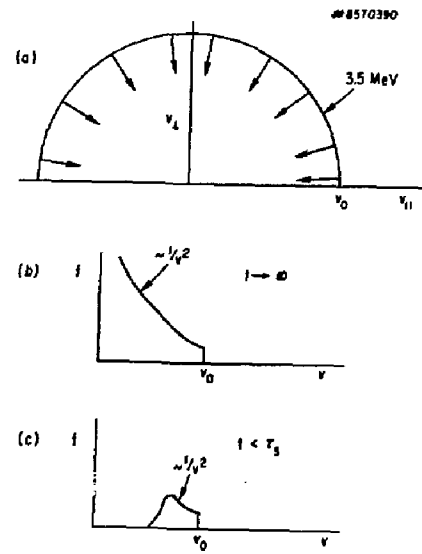

Fig. 5.2

EXTERNAL DISTRIBUTION IN ADDITION TO UC-20

Dr. Frank J. Paoloni, Univ of Wollongong, AUSTRALIA
Prof. M.H. Brennan, Univ Sydney, AUSTRALIA
Plasma Research Lab., Australian Nat. Univ., AUSTRALIA
Prof. I.R. Jones, Flinders Univ., AUSTRALIA
Prof. F. Cap, Inst Theo Phys, AUSTRIA
Prof. M. Heindler, Institut fur Theoretische Physik, AUSTRIA
M. Goossens, Astronomisch Instituut, BELGIUM
Ecole Royale Militaire, Lab de Phys Plasmas, BELGIUM
Com. of European, Dg XII Fusion Prog, BELGIUM
Prof. R. Boucique, Laboratorium voor Natuurkunde, BELGIUM
Dr. P.H. Sakanaka, Univ Estadual, BRAZIL
Instituto De Pesquisas Espaciais-INPE, BRAZIL
Library, Atomic Energy of Canada Limited, CANADA
Dr. M.P. Bachynski, MPB Technologies, Inc., CANADA
Dr. A.M. Skarsgard, Univ of Saskatchewan, CANADA
Dr. H. Barnard, University of British Columbia, CANADA
Prof. J. Teichmann, Univ. of Montreal, CANADA
Prof. S.R. Sreenivasan, University of Calgary, CANADA
Prof. Tudor W. Johnston, INRS-Energie, CANADA
Dr. C.R. James, Univ. of Alberta, CANADA
Dr. Peter Lukac, Komenskeho Univ, CZECHOSLOVAKIA
The Librarian, Culham Laboratory, ENGLAND
Mrs. S.A. Hutchinson, JET Library, ENGLAND
C. Mouttet, Lab. de Physique des Milieux Ionises, FRANCE
J. Radet, CEN/CADARACHE - Bat 506, FRANCE
Dr. Tom Mual, Academy Bibliographic, HONG KONG
Preprint Library, Cent Res Inst Phys, HUNGARY
Dr. B. Dasgupta, Saha Inst, INDIA
Dr. R.K. Chhajlani, Vikram Univ. INDIA
Dr. P. Kaw, Institute for Plasma Research, INDIA
Dr. Phillip Rosenau, Israel Inst Tech, ISRAEL
Prof. S. Cuperman, Tel Aviv University, ISRAEL
Librarian, Int'l Ctr Theo Phys, ITALY
Prof. G. Rostagni, Univ Di Padova, ITALY
Miss Clelia De Palo, Assoc EURATOM-ENEA, ITALY
Biblioteca, del CNR EURATOM, ITALY
Dr. H. Yamato, Toshiba Res & Dev, JAPAN
Prof. I. Kawakami, Atomic Energy Res. Institute, JAPAN
Prof. Kyoji Nishikawa, Univ of Hiroshima, JAPAN
Direc. Dept. Lg. Tokamak Res. JAERI, JAPAN
Prof. Satoshi Itoh, Kyushu University, JAPAN
Research Info Center, Nagoya University, JAPAN
Prof. S. Tanaka, Kyoto University, JAPAN
Library, Kyoto University, JAPAN
Prof. Nobuyuki Inoue, University of Tokyo, JAPAN
S. Mori, JAERI, JAPAN
M.H. Kim, Korea Advanced Energy Research Institute, KOREA
Prof. D.I. Choi, Adv. Inst Sci & Tech, KOREA
Prof. B.S. Liley, University of Waikato, NEW ZEALAND
Institute of Plasma Physics, PEOPLE'S REPUBLIC OF CHINA
Librarian, Institute of Phys., PEOPLE'S REPUBLIC OF CHINA
Library, Tsing Hua University, PEOPLE'S REPUBLIC OF CHINA
Z. Li, Southwest Inst. Physics, PEOPLE'S REPUBLIC OF CHINA
Prof. J.A.C. Cabral, Inst Superior Tecn, PORTUGAL
Dr. Octavian Petrus, AL I CUZA University, ROMANIA
Dr. Johan de Villiers, Plasma Physics, AEC, SO AFRICA
Prof. M.A. Hellberg, University of Natal, SO AFRICA
Fusion Div. Library, JEN, SPAIN
Dr. Lennart Stenflo, University of UMEA, SWEDEN
Library, Royal Inst Tech, SWEDEN
Prof. Hans Wilhelmson, Chalmers Univ Tech, SWEDEN
Centre Phys des Plasmas, Ecole Polytech Fed, SWITZERLAND
Bibliotheek, Fom-Inst Voor Plasma-Fysica, THE NETHERLANDS
Dr. D.D. Ryutov, Siberian Acad Sci, USSR
Dr. G.A. Eliseev, Kurchatov Institute, USSR
Dr. V.A. Glukhikh, Inst Electro-Physical, USSR
Dr. V.T. Telok, Inst. Phys. Tech. USSR
Dr. L.M. Kovrizhnykh, Institute Gen. Physics, USSR
Prof. T.J.M. Boyd, Univ College N Wales, WALES
Nuclear Res. Establishment, Julich Ltd., W. GERMANY
Bibliothek, Inst. Fur Plasmaforschung, W. GERMANY
Dr. K. Schindler, Ruhr Universitat, W. GERMANY
ASDEX Reading Rm, IPP/Max-Planck-Institut fur Plasmaphysik, W. GERMANY
Librarian, Max-Planck Institut, W. GERMANY
Prof. R.K. Janev, Inst Phys, YUGOSLAVIA